Dissertation

The role of platelet-derived factors on extravillous trophoblasts

submitted by

Freya Adda LYSSY

MSc, BSc

for the Academic Degree of

Doctor of Philosophy

(PhD)

at the

Medical University of Graz

Division of Cell Biology, Histology and Embryology

Gottfried Schatz Research Center for Cell Signaling, Metabolism and Aging

under the supervision of

Univ. Prof. Priv.-Doz. Mag.rer.nat. Dr.scient.med. Martin GAUSTER

2025

Declaration of Academic Integrity

I hereby declare that this thesis is my own original work and that I have fully acknowledged by name all of those individuals and organizations that have contributed to the research for this thesis. Due acknowledgement has been made in the text to all other material used. Throughout this thesis and in all related publications I followed the guidelines of “Good Scientific Practice and Ombuds Committee at the Medical University of Graz”.

Furthermore, I hereby declare that if artificial intelligence (AI) tools were used for the generation and/or correction of certain text passages in the creation of this work, such employment was conducted in compliance with ethical principles, academic integrity, and the regulations of my university. Additionally, it was ensured that this usage was transparently disclosed and appropriately attributed.

Graz, March 2025 Freya Lyssy

Disclosures

This cumulative dissertation is based on the following original publications:

Lyssy, F., Guettler, J., Brugger, B. A., Stern, C., Forstner, D., Nonn, O., Fischer, C., Herse, F., Wernitznig, S., Hirschmugl, B., Wadsack, C., & Gauster, M. (2023). **Platelet-derived factors dysregulate placental sphingosine-1-phosphate receptor 2 in human trophoblasts.** *Reproductive biomedicine online*, *47*(2), 103215. https://doi.org/10.1016/j.rbmo.2023.04.006

Lyssy, F., Forstner, D., Brugger, B. A., Ujčič, K., Guettler, J., Kupper, N., Wernitznig, S., Daxboeck, C., Neuper, L., El-Heliebi, A., Kloimboeck, T., Kargl, J., Huppertz, B., Ghaffari-Tabrizi-Wizsy, N., & Gauster, M. (2024). **The chicken chorioallantoic membrane assay revisited - A face-lifted approach for new perspectives in placenta research.** *Placenta*, S0143-4004(24)00113-9. https://doi.org/10.1016/j.placenta.2024.04.013

Lyssy, F., Forstner, D., Guettler, J., Kupper, N., Ujčič, K., Neuper, L., Daxboeck, C., El-Heliebi, A., Kummer, D., Krappinger, J.C., Vejzovic, D., Rinner, B., Cvirn, G., Wernitznig, S., Moser, G., Valdes, D.S., Herse, F., Höbler, A.-L., Pollheimer, J., James, J.L., Feichtinger, J., Gauster, M. (2025). **Maternal platelet-derived factors induce trophoblastic LAIR2 expression to promote trophoblast invasion and inhibit platelet activation at the fetal-maternal interface.** *Journal of Thrombosis and Haemostasis,* ISSN 1538-7836, https://doi.org/10.1016/j.jtha.2025.03.020

Co-authors who contributed to the thesis and the publications and agreed to the use of their data in the thesis:

From the Division of Cell Biology, Histology and Embryology, Gottfried Schatz Research Center, Medical University of Graz, Austria
Désirée Forstner, Jacqueline Güttler, Stefan Wernitznig, Kaja Ujčič, Nadja Kupper, Christine Daxböck, Lena Neuper, Amin El-Heliebi, Daniel Kummer, Gerit Moser, Julian C. Krappinger, Julia Feichtinger, Berthold Huppertz, Martin Gauster

From the Department of Obstetrics and Gynecology, Medical University of Graz, Austria
Christian Wadsack, Christina Stern, Birgit Hirschmugl

From the Division of Physiological Chemistry, Otto Loewi Research Center, Medical University of Graz, Austria
Gerhard Cvirn

From the Division of Pharmacology, Otto Loewi Research Center, Medical University of Graz, Austria
Julia Kargl, Teresa Kloimböck

From the Division of Biomedical Research, Core Facility Alternative Biomodels and Preclinical Imaging, Medical University of Graz,
Djenana Vejzovic, Beate Rinner

Charité-Universitätsmedizin Berlin, Corporate Member of Freie Universität Berlin and Humboldt-Universität zu Berlin, Berlin, Germany
Olivia Nonn, Florian Herse, Cornelius Fischer, Daniela S. Valdés

Particles-Biology Interactions Laboratory, Department of Materials Meet Life, Swiss Federal Laboratories for Materials Science and Technology (Empa), Switzerland.
Beatrice A. Brugger

Division of Immunology, Research Unit CAM Lab, Otto Loewi Research Center, Medical University of Graz, Austria
Nassim Ghaffari-Trabizi-Wizsy

Maternal-Fetal Immunology Group, Reproductive Biology Unit, Medical University of Vienna, Austria
Anna-Lena Höbler, Jürgen Pollheimer

Department of Obstetrics and Gynaecology, Faculty of Medical and Health Sciences, The University of Auckland, Auckland, New Zealand
Joanna L. James

During my PhD studies I contributed to the following publications:

Forstner, D., Guettler, J., Brugger, B. A., **Lyssy, F.,** Neuper, L., Daxboeck, C., Cvirn, G., Fuchs, J., Kraeker, K., Frolova, A., Valdes, D. S., Stern, C., Hirschmugl, B., Fluhr, H., Wadsack, C., Huppertz, B., Nonn, O., Herse, F., & Gauster, M. (2023). **CD39 abrogates platelet-derived factors induced IL-1β expression in the human placenta**. Frontiers in cell and developmental biology, 11, 1183793. https://doi.org/10.3389/fcell.2023.1183793

Brugger, B. A., Neuper, L., Guettler, J., Forstner, D., Wernitznig, S., Kummer, D., **Lyssy, F.,** Feichtinger, J., Krappinger, J., El-Heliebi, A., Bonstingl, L., Moser, G., Rodriguez-Blanco, G., Bachkönig, O. A., Gottschalk, B., Gruber, M., Nonn, O., Herse, F., Verlohren, S., Frank, H. G., … Gauster, M. (2023). **Fluid shear stress induces a shift from glycolytic to amino acid pathway in human trophoblasts**. *Cell & bioscience*, *13*(1), 163. https://doi.org/10.1186/s13578-023-01114-3

Acknowledgements

PhD student Freya Lyssy received funding from the Austrian Science Fund (FWF, 10.55776/P35118 to Martin Gauster), the Medical University of Graz through the PhD program Molecular Medicine (MolMed) and was recipient of the Marietta Blau-Grant from the Oesterreichischer Austauschdienst (OeAD-GmbH).

Completing this doctoral journey has been a challenging yet rewarding experience, and it would not have been possible without the immeasurable endeavor of many individuals. Therefore, I would like to thank everybody who contributed to this project and helped me throughout my PhD studies.

First and foremost, I would like to express my deepest gratitude to my supervisor, Professor Martin Gauster. Thank you for your unwavering support, insightful guidance and patience throughout the years. Your encouragement and constructive criticism have been invaluable in shaping this project and helped me grow as a researcher.

Many thanks to the members of my thesis committee Associate Professor Juergen Pollheimer and Research Professor Axel Schlagenhauf for their indispensable feedback, perceptive discussions and helpful collaborations.

My sincerest appreciation goes out to every current and former member of the AG Gauster. Thank you for every possible help I can think of; for providing your active help in the lab but also for your encouraging words and moral support along the way.

Many thanks to all my colleagues from the Division of Cell Biology, Histology and Embryology, Medical University of Graz for their assistance and advice during my everyday work.

I would like to express my profound gratefulness to Associate Professor Jo James, who graciously welcomed me as a guest researcher at the University of Auckland in 2024. Additionally, I would like to acknowledge her entire lab, where I had the privilege to gain so much knowledge and meet many incredible new colleagues.

Last but definitely not least, I would like to thank my whole family as well as my best friends. Your unconditional love and support are what brought me this far in life.

Thank you! ♥

Table of contents

Abbreviations 1
Zusammenfassung 3
Abstract 4
1. Introduction 5
1.1. The human placenta 5
1.1.1. Embryo implantation and early placentation 5
1.1.2. Trophoblast differentiation and villi formation 6
1.1.3. Remodeling of the uterine spiral arteries 7
1.1.4. Nutrient transport and gas exchange 8
1.1.5. Endocrine function 9
1.1.6. Immunological function 9
1.2. Human Platelets 10
1.2.1. Platelet Formation 10
1.2.2. Platelet Function 11
1.2.2.1. Platelet Adhesion 11
1.2.2.2. Platelet Secretion 12
1.2.2.3. Platelet Aggregation 12
1.2.3. Platelet-derived factors 13
1.3. Role of platelets during pregnancy 13
1.3.1. Maternal platelets at the fetal-maternal interface 13
2. Aims and Objectives 15
3. Publications and Results 17
4. Discussion 21
4.1. Platelet-derived factors deregulate S1PR2 in human trophoblasts 21
4.2. The chorioallantoic membrane assay revisited – A facelifted approach for new perspectives in placenta research 23
4.3. Maternal platelet-derived factors induce trophoblastic LAIR2 expression to promote trophoblast invasion and inhibit platelet activation at the fetal-maternal interface 26
4.4. Combining maternal platelet- and trophoblast research 28
5. Conclusion 31
6. References 32

Abbreviations

ACTB	Actin beta
ADP	Adenosine diphosphate
AIP	Abnormal Invasive Placenta
ATP	Adenosine triphosphate
CAM	Chorioallantoic membrane
cAMP	Cyclic adenosine monophosphate
CCT	Cell column trophoblast
CK7	Cytokeratin 7
CRH	Corticotrophin-releasing hormone
CTB	Cytotrophoblast
dNK	Decidual natural killer cell
ECM	Extracellular matrix
eEVT	Endovascular EVT
EV	Extracellular vesicle
EVT	Extravillous trophoblast
FBS	Fetal bovine serum
FFPE	Formalin-fixed paraffin-embedded
GA	Gestational age
GO	Gene ontology
GPCR	G-protein coupled receptor
GPIb/V/IX	Glycoprotein Ib-V-IX complex
GPVI	Platelet glycoprotein VI
h	Hour
H&E	Hematoxylin & eosin
HAND1	Heart- and neural crest derivatives-expressed protein 1
hCG	Human chorionic gonadotropin
HELLP	Hemolysis, elevated liver enzyme syndrome
HLA-G	Human leukocyte antigen G

hPL	Human placental lactogen
HSC	Hematopoietic stem cell
iEVT	Interstitial EVT
IgG	Immunoglobulin G
IL	Interleukin
IVS	Intervillous space
LAIR2	Leukocyte-associated immunoglobulin-like receptor 2
mRNA	Messenger RNA
OCS	Open canalicular system
p.c.	Post conception
PE	Preeclampsia
PR	Platelet releasate
PRP	Platelet rich plasma
S1P	Sphingosine-1-phosphate
S1PR	S1P receptor
SNARE	Soluble N-ethylmaleimide-sensitive-factor attachment receptor
STB	Syncytiotrophoblast
TEM	Transmission electron microscopy
TGF-β	Transforming growth factor beta
THR	Thrombin
t-SNARE	Target SNARE
TXA_2	Thromboxane A_2
VEGF	Vascular endothelial growth factor
v-SNARE	Vesicle SNARE
vWF	Von Willebrand factor

Zusammenfassung

Während der menschlichen Plazentation wandern extravillöse Trophoblasten (EVT) ins Endometrium ein und bilden Pfropfen in Spiralarterien, um den intervillösen Raum (IVS) zunächst vom mütterlichen Blut abzuschirmen. Mitte des ersten Trimesters lösen sich diese Pfropfen und bilden kapillargroße Kanäle. Aufgrund ihrer geringen Größe könnten Thrombozyten die ersten mütterlichen Blutzellen im IVS sein. Aktivierte Blutplättchen wurden dort nachgewiesen, was die Hypothese bildet, dass diese umliegende Trophoblasten beeinflussen.

Eine meiner Studien definiert die Sphingosin-1-Phosphat Rezeptoren S1PR1-S1PR3 in der Plazenta. S1PR2 Expression war im ersten Trimester überwiegend, nahm aber gegen Ende der Schwangerschaft ab, während S1PR1 und S1PR3 anstiegen. S1PR1 war primär in Endothelzellen, S1PR2 und S1PR3 in Trophoblasten lokalisiert. BeWo-Zellexperimente zeigten, dass thrombozytäre Faktoren S1PR2 herunterregulieren, was auf einen Zusammenhang mit zunehmender Präsenz von Blutplättchen in der Plazenta hindeutete.

Um ethische und experimentelle Einschränkungen in der Plazentaforschung zu umgehen, etablierte ich in einer weiteren Studie den Chorioallantoismembran (CAM) Assay neu. ACH-3P-Sphäroide drangen in die Membran ein, erodierten Blutgefäße und imitierten so die IVS-Perfusion. Das Modell ermöglichte Immunfluoreszenzfärbungen und *in situ* Hybridisierung und eignet sich somit zur Untersuchung von Trophoblastinvasion unter Blutflussbedingungen.

In einer weiteren Studie zeigte ich, dass thrombozytäre Faktoren das Genexpressionsprofil von ACH-3P-Sphäroiden verändern. Unter anderem wurde LAIR2, nachweisbar in Zellsäultrophoblasten (CCTs) und EVTs in Ersttrimester-Plazenten, signifikant hochreguliert. Funktionelle Analysen ergaben, dass LAIR2 die Thrombozytenaktivierung hemmt und gleichzeitig die Trophoblastinvasivität erhöht - ein Hinweis auf seine Rolle bei der Regulierung mütterlicher Blutgerinnung und EVT-Invasion.

Die Ergebnisse weisen darauf hin, dass mütterliche Thrombozyten während der frühen Plazentation eine wichtige Rolle spielen und ein fein abgestimmter regulatorischer Rückkopplungsmechanismus zwischen Trophoblasten und Blutplättchen besteht, der für die korrekte Etablierung des uteroplazentaren Blutflusses wesentlich sein könnte.

Abstract

During human placentation extravillous trophoblasts (EVTs) migrate into the maternal endometrium and form plugs in uterine spiral arteries to prevent maternal blood from entering the intervillous space (IVS). By mid-first trimester, these plugs loosen and form capillary-sized channels. Given their small size, platelets might be the first maternal blood cells to enter the IVS. Activated platelets have been found within these intercellular gaps, supporting the hypothesis that activation of maternal platelets affects surrounding trophoblasts.

One of my studies investigated sphingosine-1-phosphate receptors S1PR1–S1PR3 in the placenta across gestation. S1PR2 was dominantly expressed in the first trimester but decreased towards term, while S1PR1 and S1PR3 increased. S1PR1 was mainly in endothelial cells, whereas S1PR2 and S1PR3 were in villous trophoblasts. BeWo cell experiments showed that platelet-derived factors significantly downregulated S1PR2, suggesting a link between increasing platelet presence and S1PR2 decline in the placenta over gestation.

Furthermore, to address challenges of studying early human placentation due to ethical and experimental limitations, I revisited the chicken chorioallantoic membrane (CAM) assay. ACH-3P spheroids invaded the CAM, and eroded its blood vessels, mimicking early IVS perfusion. The model is compatible with advanced analysis techniques, rendering it a promising tool for studying trophoblast invasion under blood flow conditions.

Another study of mine demonstrated that the gene expression profile of ACH-3P spheroids significantly changed when exposed to platelet-derived factors. *LAIR2* was significantly upregulated and found in cell column trophoblasts (CCTs) and invasive EVTs in first trimester placentas. Functional analysis revealed that LAIR2 inhibits platelet activation while enhancing trophoblast invasiveness, suggesting a role in regulating maternal blood coagulation and EVT invasion into the decidua.

In conclusion, results from my studies suggest that maternal platelets play a significant role during early human placentation. We theorize about a fine-tuned regulatory feedback mechanism between trophoblasts and maternal platelets which might be essential for proper establishment of uteroplacental blood flow.

1.Introduction

1.1. The human placenta

The human placenta is a vital organ that plays a pivotal role in the health of both mother and fetus, with the potential to influence their future lives even beyond the time of pregnancy (1). A series of complex and tightly regulated processes ensures the development of the placenta and hence a healthy development of the embryo (2). Any abnormalities in placental development during the first trimester can lead to various complications during pregnancy including preeclampsia (PE), fetal growth restriction, stillbirth, placental abruption and preterm labor (1).The placenta at term has a discoid shape with a diameter of 15 – 25 cm, an average thickness of 3 cm, and an average weight of about 500 – 600 g (3). Human placentation is classified as hemochorial placentation, meaning that maternal blood has direct contact with the trophoblast layer of the villous placenta (4). On the fetal side, the placenta is defined by the chorionic plate and on the maternal side by the basal plate, representing the decidua. The space between these plates is filled with placental villi, which are bathed in maternal blood that perfuses the so-called intervillous space (IVS). During the initial phase of pregnancy this space is mainly filled with endometrial gland secretion and maternal blood plasma. However, by the end of the first trimester, uterine spiral arteries will be remodeled to enable maternal blood flow into the IVS. Placental villi, which are tree-like structures comprising multiple cell layers and enclose the fetal blood vessels, regulate crosstalk and bi-directional transport between maternal and fetal blood circulation, without them being in direct contact (5,6).

1.1.1. Embryo implantation and early placentation

After successful fertilization the zygote migrates toward the uterine cavity by ciliary motility of the fallopian tube epithelium. At the same time the zygote undergoes a series of cell divisions resulting in a multicellular structure called the blastocyst. The blastocyst consists of an inner cell mass, which will later form the embryo, and an outer cell mass - the trophectoderm - responsible for the establishment of the placenta (7).

Embryo implantation is a tightly regulated process, that involves a coordinated sequence of events and interactions between a competent blastocyst and a receptive uterus, to successfully establish a pregnancy (8). It marks the first cell-to-cell interaction between the mother and the developing embryo. Three sequential steps are relevant for successful implantation: apposition, adhesion and invasion (9,10). The orientated apposition allows interaction of the trophectoderm with microvilli protrusions on the apical surface of

endometrial luminal epithelium. The blastocyst then adheres tightly to the endometrium, followed by invasion and penetration into the deeper stroma anchoring the embryo tightly in the endometrium. During this process, extensive crosstalk between maternal decidua and the trophoblasts takes place at the maternal-fetal interface, which serves as the primary site for physical and functional interaction between mother and fetus and is also the site for placentation (9). On the maternal side endometrial glands and decidual stromal cells regulate the implantation activity through secretory products like cytokines and growth factors which are relevant for attachment and adhesion (9). Furthermore, decidualized stromal cells regulate the invasion of trophoblasts, which produce both pro-invasive factors (e.g. IL1b, IL-6, IL-11) and anti-invasive factors (e.g. IL-10, VEGF) which together maintain the invasion of trophoblasts at a balanced state. Additionally, maternal immune cells (e.g. dNK, macrophages, leukocytes) with function to prevent immune rejection of the fetus also contribute to the organization of the maternal-fetal interface in early pregnancy (9).

1.1.2. Trophoblast differentiation and villi formation

After successful implantation and initiation of placentation, stem cells of the trophectoderm differentiate into the first trophoblast lineages: early mononuclear cytotrophoblasts (CTBs) and a primitive syncytium (11). These trophoblast cells undergo extensive proliferation and differentiation and eventually follow two different pathways: villous or extravillous (6,12). Villous CTBs proliferate, differentiate, and fuse to form an initially oligonucleated and later on multinucleated syncytium, called the syncytiotrophoblast (STB) (6,13). However, these CTBs can also differentiate into a migratory and invasive phenotype to become extravillous trophoblasts (EVTs). The composition of these cell types may vary during pregnancy to adapt to the growing needs of the developing fetus. Defective placentation compromises gestational well-being, possibly resulting in pregnancy pathologies. Therefor defined subtypes of trophoblasts and their functions as well as a sophisticated regulation is needed to support normal development of the placenta (14). Approximately 10 days post conception (p.c.) placental villi start to develop by rows of proliferative CTBs breaking through the expanding syncytial mass. These primary villi extend into the underlying maternal decidua and EVTs emerging from these villi then erode uterine blood vessels and glands. Secondary villi are established during the following days by migration of extraembryonic mesoderm into these primary structures. At the same time the epithelial surface branches and expands enormously by continuous proliferation and fusion of villous CTBs (12). The STB is thought to arise from asymmetrical cell division, differentiation and fusion of villous CTBs with the pre-existing syncytium. The STB layer provides the interface between mother and fetus for

nutrient transport and gas exchange in floating villi and secretes critical pregnancy hormones such as human chorionic gonadotropin (hCG) and placental lactogen (12,15).
Around 17 days p.c. secondary villi develop into tertiary villi containing placental vessels. The placental vasculature continues to undergo extensive expansion in the late-first and second trimester as a result of branching angiogenesis. Towards the end of pregnancy the placental capillaries elongate and form loops that are pushed up against the STB layer of terminal villi, decreasing the exchange distance between maternal and fetal circulations and thereby maximizing oxygen and nutrient transport to the fetus (12).
Apart from developing chorionic villi, proliferating CTBs at distal parts also expand laterally at about 15 days p.c. to form the trophoblastic shell, representing the outermost site of the placenta encircling the embryo. During early phases of placentation this trophoblastic shell gives rise to the second differentiated trophoblast cell types, the invasive EVTs. Once matured placental villi have formed, EVTs originate from the differentiation of CTBs in the tips of anchoring villi. In these villi, rows of proliferative proximal cell column trophoblasts (CCTs) develop and represent the progenitor cells of differentiated EVTs. Upon building the distal cell column, cells stop mitosis but do not exit the cell cycle to reach a quiescent state (12).
Furthermore, EVTs can be divided into two distinct EVT populations: interstitial (iEVT) or endovascular (eEVT). iEVTs invade the decidual stroma and provoke numerous effects during early pregnancy. They interact with decidual stromal cell, macrophages and decidual natural killer cells (dNKs) in order to regulate immunological acceptance of the placental allograft and control EVT function (12). As iEVTs reach the underlying myometrium, they undergo a final differentiation step into multinucleated trophoblast giant cells losing their invasive capacity. iEVTs that are recruited to maternal spiral arteries differentiate into eEVTs that migrate along their lumen and adopt a vascular adhesion phenotype (14,16).

1.1.3. Remodeling of the uterine spiral arteries

One key event in human placentation is vascular remodeling, mediated by EVTs, to ensure a constant supply of maternal blood. Inadequate or incomplete remodeling is characterized by shallow trophoblast invasion, decreased population of invasive trophoblasts and narrow bore arteries retaining muscular walls, and is associated with second trimester miscarriages, PE, pre-term birth and some cases of fetal growth restriction (17). These pathologies increase the risk of morbidity and mortality in pregnancy and above all can have long term consequences for the health of both mother and child, e.g. development of cardiovascular disease, increased risk of elevated serum cholesterol, stroke, type II diabetes, adiposity, osteoporosis and insulin resistance (18–20).

As mentioned before EVTs detach from the cell columns of distal regions of villi and migrate into the decidual stroma as iEVTs to communicate with different decidual cell types. Furthermore, they invade the maternal spiral arteries of the decidua up to the first third of the myometrium (21). In the first weeks of pregnancy, EVTs plug the spiral arteries, thus preventing precocious onset of blood flow to the developing placenta and therefore protecting it against damage through oxidative stress and fetal loss (22). However, by the middle of the first trimester these trophoblast plugs become loosely cohesive forming capillary sized channels allowing maternal blood plasma to pass through (2). By the 10th week of gestation, these plugs dissolve, and the endothelial layer of the spiral arteries is replaced by eEVTs (22). Moreover, iEVTs approach them from the outside by accumulating in the muscular vessel wall promoting its elastosis and degradation, where decidual macrophages and dNKs contribute considerably to the process. This results in an increase in diameter of the spiral arteries establishing low-pressure blood flow to the placenta (21,23).

1.1.4. Nutrient transport and gas exchange

The placenta acts to provide oxygen, water, carbohydrates, amino acids, lipids, vitamins, minerals and other nutrients to the fetus (6). During the initial phase of placental development nutrient supply is solely histiotrophic, meaning a mix of cellular secretions, cell debris and transudation is released from endometrial glands into the space between the maternal and fetal surface and finally taken up by the trophoblast (24). From week 10-12 of gestation onwards transfer of nutrients happens through the placental barrier as then maternal blood flow into the IVS is established and villi of the placenta are in contact with maternal blood (6). Depending on the type of substance that needs to cross the placental barrier there are several mechanisms in place: passive/simple diffusion, facilitated diffusion or carrier-mediated transport (13,25,26). Several factors influence the transport across the placenta such as uteroplacental and umbilical blood flow, area available for exchange, placental metabolism, and activity/expression of specific transporter proteins in the placental barrier (26).

Since fetal lungs do not participate in gas exchange while *in utero*, the placenta is the responsible organ for transfer of respiratory gases. Oxygen is a small molecule and therefore has no problem crossing the placenta by passive diffusion (25). Its transfer mainly depends on oxygen partial pressure gradient between maternal blood in the IVS and the fetal blood in villous- and umbilical cord vessels. The concentration gradient is influenced partly by maternal and environmental factors but also by the blood flow rate across the membrane and referred to as flow-limited. Impairment of the uterine or fetal-placental circulations can have

an enormous impact on the rate of fetal growth (27). It is worth mentioning that the placenta itself consumes about 40% of the oxygen supplied to the fetal-placental unit to utilize it for protein synthesis and active transport and ionic pumping (28). Similar to oxygen, carbon dioxide can also pass by passive diffusion and is regulated by the partial pressure gradient for carbon dioxide between the fetal blood in the umbilical arteries and maternal blood in the IVS (25).

1.1.5. Endocrine function

The placenta is a major endocrine organ as placental hormones can have very diverse but profound effects on maternal physiology and behavior (27). The hormones are mainly produced in the STB and CTBs of the placental villi, however, also to some extend in the EVTs and can generally be divided into groups according to their biochemical structure. Steroid hormones like progesterone, estrogens and glucocorticoids are synthesized or modified from maternal cholesterol and fetal pre-cursor hormones (13). Progesterone is the main pregnancy-maintaining hormone, necessary for the nidation and implantation of the embryo (29). In addition to a number of other functions during pregnancy, estrogens have been discussed to play a role in short- as well as long-term endothelial adaptation during pregnancy (30). hCG, an essential peptide hormone during pregnancy, is mainly produced by the STB and secreted into maternal circulation. It is a commonly used marker for diagnosis of pregnancy, as hCG levels rise significantly during the initial phase of pregnancy (31). It is a multifaceted hormone, which is important for the implantation process, and preservation of the pregnancy. Moreover, it is essential for placental growth and development and the adaption of the maternal immune system (32,33). Moreover, the placenta produces large amounts of numerous other hormones like leptin, corticotrophin releasing hormone (CRH) or human placental lactogen (hPL) just to mention a few here.

1.1.6. Immunological function

The hemochorial placentation is the most invasive type amongst Eutherians (placental mammals), in which intimate contact of fetal tissue to the maternal immune system is established. Therefore, it is of utmost importance that the maternal immune system is adapted during pregnancy in order to tolerate the semiallogeneic fetus. Changes in the immune system occur both systemically as well as locally (34). Following implantation local immune cells like dNKs, macrophages and regulatory T cells in the endometrium are immediately adapted to establish a balance between tolerance of fetal trophoblasts and limitation of their invasion (34,35).

As soon as placental circulation is established, peripheral blood comes into close contact with fetal cells in the IVS, which might also impact the systemic immune response (34). It has indeed been shown that passage of maternal blood through the placenta triggers activation of inflammatory cells such as leukocytes (36). Furthermore, villous trophoblasts have been shown to produce and secrete various factors, like cytokines or pregnancy hormones which might affect the immune system (34). Since neonates lack a mature immune system, they rely heavily on sources of immunity derived from the mother to recognize pathogens. The placenta is one of the sources from which antibodies, such as immunoglobulin G (IgG) can be transferred directly into the serum establishing a passive immunity for the baby (37).

1.2. Human Platelets

Platelets are the smallest of human blood cells, nevertheless they play essential roles in processes of hemostasis and thrombosis. Additionally, platelets are part of the innate immune defense, modulators of the immune response, and involved in wound healing and hematogenic metastasis (38). Platelets are anucleate cell fragments derived from megakaryocytes in the bone marrow (39). The elimination of platelets from the blood stream happens via macrophages from the liver and spleen by recognition of several sugar residues platelets feature upon aging (40). Because of their short lifespan of only 8-10 days new platelets have to be produced every day to maintain a normal blood count (41). With a range from 1.5-4.0 x 10^5/µL in healthy individuals, platelets are the second most abundant cells in the circulation and well situated to rapidly respond to vascular damage (39). It is essential for the function of platelets that they are capable of undergoing cell-cell (aggregation) as well as cell-matrix (adhesion) interactions using a broad palette of surface receptors. Moreover, platelets can produce and store diverse granule contents and rapidly secrete these upon activation (42). Platelets significantly contribute to innate immunity to affect adaptive immune responses by expressing a broad range of functional immune receptors (39).

1.2.1. Platelet Formation

Megakaryocytes develop from hematopoietic stem cells (HSC) in the bone marrow, however, they are also present in the yolk sac, fetal liver, and spleen during early development (43). During hematopoietic differentiation, HSC divide asymmetrically and give rise to multipotent progenitor cells that progressively lose their capacity for self-renewal and multipotency, leading to bipotent megakaryocytic/erythroid progenitors that can ultimately differentiate into unipotent megakaryocyte progenitors and later on megakaryocyte precursor cells (44). The key regulator of megakaryopoiesis is thrombopoietin, a cytokine mainly produced by the liver

(45). During their maturation process megakaryocytes increase in size and are filled with platelet-specific granules. They expand their cytoplasmic content of cytoskeletal proteins, and develop a highly tortuous invaginated membrane system (43).

Mature megakaryocytes extend long branching processes, so-called proplatelets, into blood sinusoids of the bone marrow. Proplatelets consist of platelet-sized swellings in tandem arrays, which are connected via thin cytoplasmic bridges (43). The multi-lobed nucleus remains in the megakaryocyte body and is afterwards extruded and degraded (46). For the final step of platelet biogenesis, proplatelets are detached, remodeled and fragmented into individual platelets. Released platelets are swept away rapidly and need further remodeling in the downstream circulation to finally represent bona fide platelets (44).

1.2.2. Platelet Function

Under normal circumstances platelets remain in the bloodstream without interacting with the intact vessel wall. However, as soon as trauma on the tissue appears, platelets tend to adhere to the extracellular matrix (ECM) in a process involving the action of several different receptors, leading to initial tethering, rolling of the platelets over the damaged area, and ultimately adhering firmly to the vessel wall to stop further hemorrhage (47). The function of platelets is comprised of a series of complex and carefully coordinated procedures. However, these processes can be divided into three broad categories: adhesion, secretion and aggregation (38).

1.2.2.1. Platelet Adhesion

The initial step of hemostasis is the interaction of platelets with the exposed subendothelial ECM, which contains several different adhesive macromolecules, such as laminin, fibronectin, collagens or von Willebrand Factor (vWF) to mention a few (48). The numerous binding sites of vWF multimers initiate first contacts to the platelet receptor glycoprotein GPIb/V/IX complex on platelets which causes the formation of strong bonds and platelet capture (38). However, this binding is insufficient to mediate a stable adhesion but rather keeps the platelet in close contact to the surface, while platelets themselves establish contacts with collagen in the ECM through immunoglobulin superfamily receptor GPVI. This binding process then triggers intracellular signals, shifting the platelet integrins to a high-affinity state which causes the release of adenosine diphosphate (ADP) and thromboxane A_2 (TXA_2). Together with locally synthesized thrombin (THR) these agonists stimulate receptors coupled to heterotrimeric G proteins (G_q, $G_{12/13}$, G_i), which induce further signaling events and act synergistically to induce full platelet activation (48).

1.2.2.2. Platelet Secretion

Platelet secretion is a critical process during platelet activation, which involves the release of over 300 active molecules from intracellular granules. Platelets carry three main types of intracellular secretory granules, α granules, dense granules and lysosomes. Platelets consist of a complex system of internal membrane invaginations, which are essential routes for platelet releasates (49). Although there are still gaps in the knowledge of how exactly platelet secretion is regulated, it is known that like other endocrine cells calcium dependent exocytosis occurs. This exocytosis process is mediated by soluble N-ethylmaleimide-sensitive-factor attachment protein receptors (SNAREs) that are present on the membranes of granules or vesicles (v-SNAREs) and on the plasma or target membrane (t-SNAREs) (50). Cognate v- and t-SNAREs interact to form a trans-bilayer complex which places vesicles and target membranes next to each other, thereby providing the driving force for membrane fusion and finally leading to the release of granule contents (49,50).

1.2.2.3. Platelet Aggregation

During platelet aggregation platelets adhere to each other at the site of vascular injury, eventually forming a hemostatic plug to finally arrest bleeding (51). It is considered a complex and dynamic process involving several ligands, receptors and platelets in different states of activation (47). Depending on shear rates, platelet aggregation can be divided into three different mechanisms. Under shear rates <1.000 s^{-1}, platelet aggregation is mediated by agonist induced activation of integrin αIIbβ3 which undergoes conformational changes allowing interaction with fibrinogen. Platelets are then bridged through fibrinogen and aggregates are formed (47,52). Considering shear rates between 1.000 s^{-1} to 10.000 s^{-1}, aggregation occurs in two steps. First, discoid, non-activated platelets can form adhesive contacts with other adherent, discoid platelets through tethers originating from shear stress. These tethers are established through interactions of GPIb/IX/V and integrin αIIbβ3 with vWF and fibrinogen. During the second step, soluble agonists like ADP, THR, and TXA_2 are accumulated, which induce platelet activation followed by shape change, and degranulation. Moreover, these agonists are ligands for GPCRs which induce a fast increase in calcium concentrations. These activation processes lead to the irreversible activation of integrin αIIbβ3, which is then interacting with fibrinogen, vWF and fibronectin to form stable platelet aggregates (47,53). When the shear stress is >10.000 s^{-1} platelet aggregation occurs exclusively via vWF-GPIbα interactions and does not need αIIbβ3 or actual activation of platelets (51).

1.2.3. Platelet-derived factors

Platelets play a pivotal role in numerous processes including hemostasis, thrombosis, allergic inflammation, non-allergic responses and even tumor progression. Various studies discussed the particular importance of exocytosis from the three different main types of secretory granules in these processes (54). α-granules are the most abundant granules in platelets, with about 50-80 α-granules per platelet. They are round or oval shaped and have a size of about 200-500 nm, therefor comprising roughly 10% of the platelet volume (55). α-granules contain soluble as well as membrane-bound proteins. Following platelet activation, soluble granule proteins are released into the extracellular compartment, while membrane-associated granule proteins are expressed on the platelet surface. Although most membrane-bound proteins are already present on the surface of resting platelets (e.g. intergins), some are exclusively expressed in activated platelets (e.g. P-selectin) (56). Dense granules are smaller (200-300 nm), fewer in number (3-8 per platelet) and have a high morphological variability (57,58). Dense granules are a subtype of lysosome-related organelles, originating from the endosomal system (56). These granules carry serotonin, nonmetabolic adenine nucleotide pool of ADP and ATP, calcium and pyrophosphate (54). Platelets contain very few primary and secondary lysosomes (no more than 3 per platelet). These organelles are slightly smaller than α-granules and are spherical in form. Despite the fact that platelet lysosomes carry at least 13 different acid hydrolases (e.g. cathepsin), their physiological function in hemostasis remains to be elucidated (57).

1.3. Role of platelets during pregnancy

During pregnancy platelet counts decrease gradually from first to second to the third trimester, with an estimated reduction of 10% at term in uncomplicated cases. The recovery to the level of the non-pregnant state usually occurs within a few weeks postpartum (57,59). Several physiological changes during pregnancy are responsible for this phenomenon, such as hemodilution, as well as accelerated platelet sequestration and consumption in the placental circulation (60).

1.3.1. Maternal platelets at the fetal-maternal interface

In the human hemochorial term placenta maternal blood has direct contact with the trophoblast layer (5). However, before uteroplacental blood flow is fully established, during invasion processes EVTs form trophoblast plugs within the lumen of maternal spiral arteries to prevent maternal blood cells from entering the IVS (2). Nevertheless, it has been shown

that by the middle of the first trimester these trophoblast plugs become loosely cohesive forming capillary-sized channels. Maternal platelets might be the first among maternal blood cells that can enter these trophoblast cell gaps and further the IVS. In fact, several studies observed maternal platelets in fragmentary trophoblast plugs of uterine blood vessels, and in vessel-like channels and adjacent intercellular spaces of EVTs in distal parts of cell columns (4,61,62). In fact, studies have shown the appearance of maternal platelets at these distal trophoblast column interstices from six weeks of gestation onwards in 80% of all cases (63). Altogether these observations suggest the capability of small maternal plasma components like platelets or multivesicular cargos to pass such narrow intercellular gaps of weak trophoblast plugs and to enter the IVS even before uteroplacental blood flow is fully established (62). Transmission electron microscopy (TEM) imaging of platelets in these areas showed the appearance of filopodia and fine-grained material in the open canalicular system (OCS) and cell surface invaginations, indicating the activation of these platelets and the release of their granule content into the trophoblast interstices (62). Recent studies have reported that the EVT marker HLA-G does neither inhibit nor induce platelet activation, yet other substrates for platelet adhesion like collagen type IV, laminin and fibronectin are present in these intercellular gaps (62,64). Although it has been suggested that platelet-derived soluble factors might enhance invasive capacities of trophoblasts and could therefore potentially contribute to uterine vascular remodeling, the exact physiological role of activated platelets in distal parts of trophoblast columns remains to be elucidated (61,62).

On the one hand maternal platelets contribute to perivillous fibrin deposition, which could help the shaping of placental villi and the IVS (62,65). One the other hand excessive platelet activation at the fetal-maternal interface might provoke inflammasome activation in the placental trophoblast and trigger enhanced formation of circulating platelet-monocyte aggregates which subsequently leads to a sterile inflammation of the placenta and a systemic inflammatory response in the mother (4). It has been hypothesized that these systemic effects include renal and endothelial dysfunction, which can lead to gestational vascular disease, such as PE and hemolysis, elevated liver enzymes, and low platelet count (HELLP) syndrome (4,66). The debate of the role of maternal platelets during the development of the human placenta remains ongoing. Nonetheless, emerging evidence indicates that the extent of platelet activation plays a pivotal role in this regard (4,62).

2. Aims and Objectives

In light of previous research and preliminary data, we propose that maternal platelets engage with both the early villous and extravillous trophoblast, influencing the development of the placenta. Platelets can beneficially contribute to the shaping of the early human placenta, however, platelets may have a pathological effect during oxidative and inflammatory stress. Increased platelet activation at the maternal-fetal interface has been shown to trigger inflammation in the trophoblast, with possible tremendous effects on mother and baby. The aims and objectives of this study were as follows:

I. Platelet-derived factors dysregulate placental sphingosine-1-phosphate receptor 2 in human trophoblasts

Sphingosine-1-phosphate (S1P) is a crucial bioactive sphingolipid that plays a key role in regulating diverse cellular processes, including apoptosis, cell motility, differentiation, proliferation, and calcium signaling. It can be produced and stored in platelets, and upon platelet activation also be released. S1P can bind to five different receptors (S1PR1-5), all of which are part of the seven-transmembrane G protein-coupled receptor family. Three of these receptors have been identified on human placental cells. Moreover, previous studies have implied that pregnant women with PE show increased levels of plasma S1P compared to healthy controls. In this study, receptors S1PR1-3 were localized in the human placenta and changes in expression levels were analyzed over gestation. Furthermore, the influence of different flow rates, various oxygen concentrations and platelet-derived factors on the expression profile of these receptors was determined.

II. The chicken chorioallantoic membrane assay revisited – A face-lifted approach for new perspectives in placenta research

The study of human placentation is significantly constrained by ethical restrictions on the use of embryonic tissue and anatomical differences between the human placenta and those of commonly used laboratory animals. Although the development of models such as trophoblast stem-cell derived organoids has offered valuable insights into key processes, the consideration of maternal blood flow during trophoblast invasion still seems to be neglected in most models. In this study we aimed to establish a proper model to investigate the behavior of trophoblast cells during invasion and initial contact with circulating blood cells.

III. Maternal platelet-derived factors induce trophoblastic LAIR2 expression to promote trophoblast invasion and inhibit platelet activation at the fetal-maternal interface

During the process of human placentation, EVTs, which emerge from trophoblast cell columns of anchoring villi invade the uterine mucosa, where they erode blood vessels and replace vascular endothelial cells. Maternal platelets have been detected in the intercellular gaps of CCTs; however, their physiological role remains to be elucidated. The objective of this study was to examine the effect of platelet-derived factors on trophoblasts which are exposed to maternal platelets as a result of the erosion of decidual blood vessels.

3. Publications and Results

The results of this thesis are published in the following scientific papers and are briefly summarized here:

Lyssy, F., Guettler, J., Brugger, B. A., Stern, C., Forstner, D., Nonn, O., Fischer, C., Herse, F., Wernitznig, S., Hirschmugl, B., Wadsack, C., & Gauster, M. (2023). **Platelet-derived factors dysregulate placental sphingosine-1-phosphate receptor 2 in human trophoblasts.** *Reproductive biomedicine online*, *47*(2), 103215. https://doi.org/10.1016/j.rbmo.2023.04.006

Lyssy, F., Forstner, D., Brugger, B. A., Ujčič, K., Guettler, J., Kupper, N., Wernitznig, S., Daxboeck, C., Neuper, L., El-Heliebi, A., Kloimboeck, T., Kargl, J., Huppertz, B., Ghaffari-Tabrizi-Wizsy, N., & Gauster, M. (2024). **The chicken chorioallantoic membrane assay revisited - A face-lifted approach for new perspectives in placenta research.** *Placenta*, S0143-4004(24)00113-9. https://doi.org/10.1016/j.placenta.2024.04.013

Lyssy, F., Forstner, D., Guettler, J., Kupper, N., Ujčič, K., Neuper, L., Daxboeck, C., El-Heliebi, A., Kummer, D., Krappinger, J.C., Vejzovic, D., Rinner, B., Cvirn, G., Wernitznig, S., Moser, G., Valdes, D.S., Herse, F., Höbler, A.-L., Pollheimer, J., James, J.L., Feichtinger, J., Gauster, M. (2025). **Maternal platelet-derived factors induce trophoblastic LAIR2 expression to promote trophoblast invasion and inhibit platelet activation at the fetal-maternal interface.** *Journal of Thrombosis and Haemostasis,* ISSN 1538-7836, https://doi.org/10.1016/j.jtha.2025.03.020

I. Platelet-derived factors dysregulate placental sphingosine-1-phosphate receptor 2 in human trophoblasts

This study investigated the expression dynamics of S1P receptors in human placentas across different gestational stages and further assessed effects of oxygen level, shear stress and platelet-derived factors on the expression of these receptors. S1PR2 was identified as the predominant receptor during the first trimester, with a significant decline towards term. In contrast, S1PR1 and S1PR3 increased with GA. S1PR1 was localized in endothelial cells, while S1PR2 could mainly be found in the STB and S1PR3 in CTBs in distal parts of anchoring villi. Co-incubation experiments revealed that S1PR2 was significantly downregulated in differentiated BeWo cells, a human trophoblast cell line originating from a choriocarcinoma, when exposed to platelet-derived factors. This finding suggests a potential negative impact of platelet-derived factors on S1PR2 expression, which may contribute to its diminished levels throughout gestation. Moreover, the study established that fluid flow rates (1 ml/min and 3 ml/min) did not have a significant effect on the expression of S1PR2 and S1PR3 in BeWo cells. Furthermore, the investigation revealed that fluctuations in oxygen concentrations (2.5%, 12% and 21%) did not elicit substantial alterations in placental S1PR2 expression. However, a notable decline in S1PR3 expression was observed at high oxygen levels.

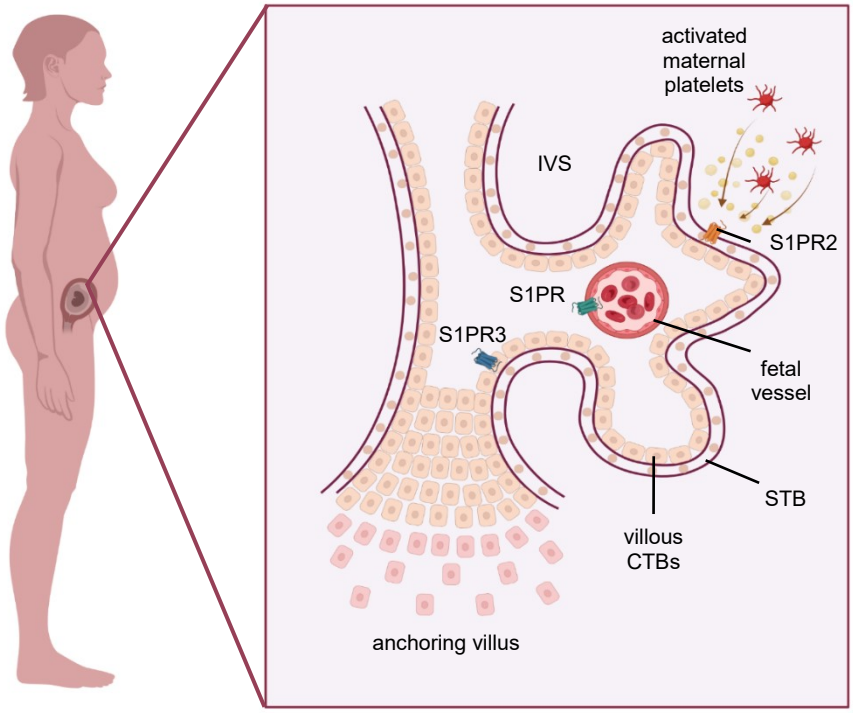

Figure 1 Schematic representation of the S1P receptors in the human placenta. S1PR2 is the predominant receptor during the first trimester and is expressed in the STB. S1PR2 is downregulated in response to platelet-derived factors. The expression levels of S1PR1 and S1PR3 rise with GA, while expression level of S1PR2 decreases. S1PR1 can be found mainly in endothelial cells and S1PR3 mainly in CTBs of distal parts of anchoring villi. Created with BioRender.com.

II. The chicken chorioallantoic membrane assay revisited – A face-lifted approach for new perspectives in placenta research

In this study a 3D cell culture model was introduced using the human first trimester trophoblast cell line ACH-3P. 24 h after seeding these cells in non-adhesive U-bottom 96-well plates, a single spheroid per well was formed. Interestingly, morphological analysis of these spheroids showed that they have an average diameter of about 750 µm and a cavity in the middle. Further ultrastructural analysis revealed high compactness of the spheroid walls, with some intercellular channels in more loosely cohesive areas on the inside of the spheroids.

ACH-3P spheroids successfully penetrated the CAM, a highly vascularized extraembryonic membrane of the chicken egg, with visible macroscopic changes happening within 20-24 h. Notably, some of the spheroids' cavities were filled with chicken blood, indicating an interaction between the trophoblast cells and the CAM's vascular network.

In addition, the employment of a padlock probe-based *in situ* hybridization technique led to the specific detection of human *ACTB* mRNA in invaded ACH-3P cells. This finding signifies the feasibility of this methodology for the analysis of CAM invasion in the absence of suitable antibodies. Overall, the study proposes that the CAM assay can effectively model trophoblast invasion and blood vessel interaction. This provides researchers with a new perspective on placenta research.

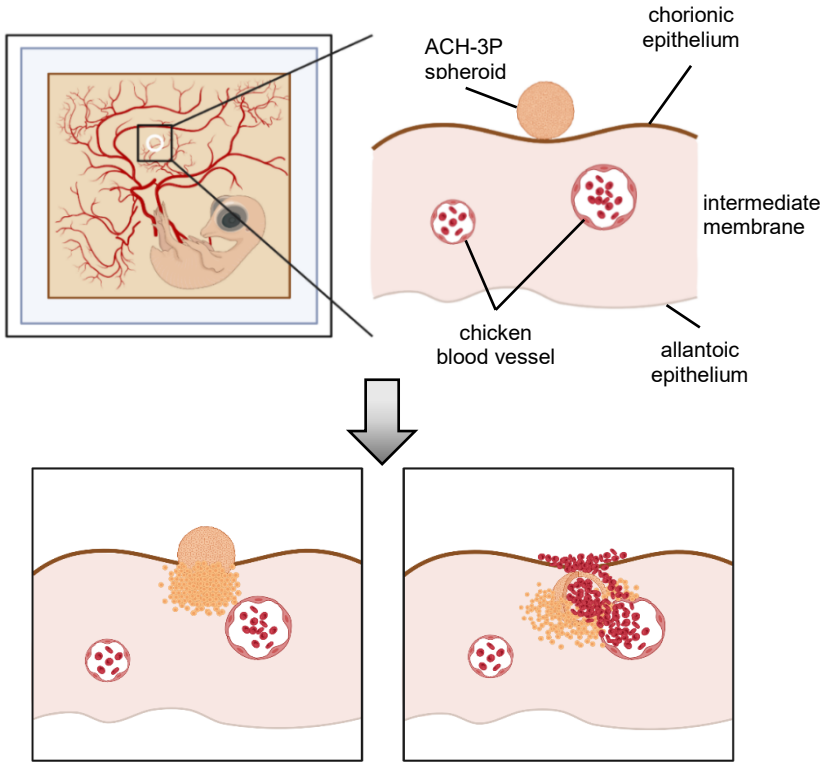

Figure 2 Schematic representation of the CAM assay with ACH-3P spheroids. Small silicone rings are placed on the chorioallantoic membrane of chicken eggs. Within these silicone rings several spheroids were planted and incubated. After 20-24 h the spheroids penetrated the membrane and eventually infiltrated chicken blood vessels leading to heavy bleedings of the chicken embryo. Created with BioRender.com.

III. Maternal platelet-derived factors induce trophoblastic LAIR2 expression to promote trophoblast invasion and inhibit platelet activation at the fetal-maternal interface

In this study the effect of platelets and platelet-derived factors on trophoblasts was investigated, in particular those of CCTs, which differentiate into EVTs. Platelet-derived factors altered the transcription profile of ACH-3P spheroids significantly. Out of these genes, further investigations looked into genes that are linked to embryonic development, e.g. *LAIR2*. LAIR2 was exclusively detected in CCTs and invaded EVTs in first trimester villous placenta and decidua samples. Moreover, morphological analysis revealed a co-location of extravasated maternal erythrocytes within interstitial gaps of invaded decidua samples together with LAIR2 positive EVTs. Furthermore, it was proven that LAIR2 was able to enhance the invasiveness of trophoblasts on the one hand, but on the other hand it was inhibiting type 1 collagen-induced platelet activation. Since LAIR2 was significantly upregulated in trophoblasts upon incubation with platelet-released factors, one can speculate about a fine-tuned regulatory feedback mechanism between invading trophoblasts and maternal platelets, which might be essential for the establishment of uteroplacental blood flow.

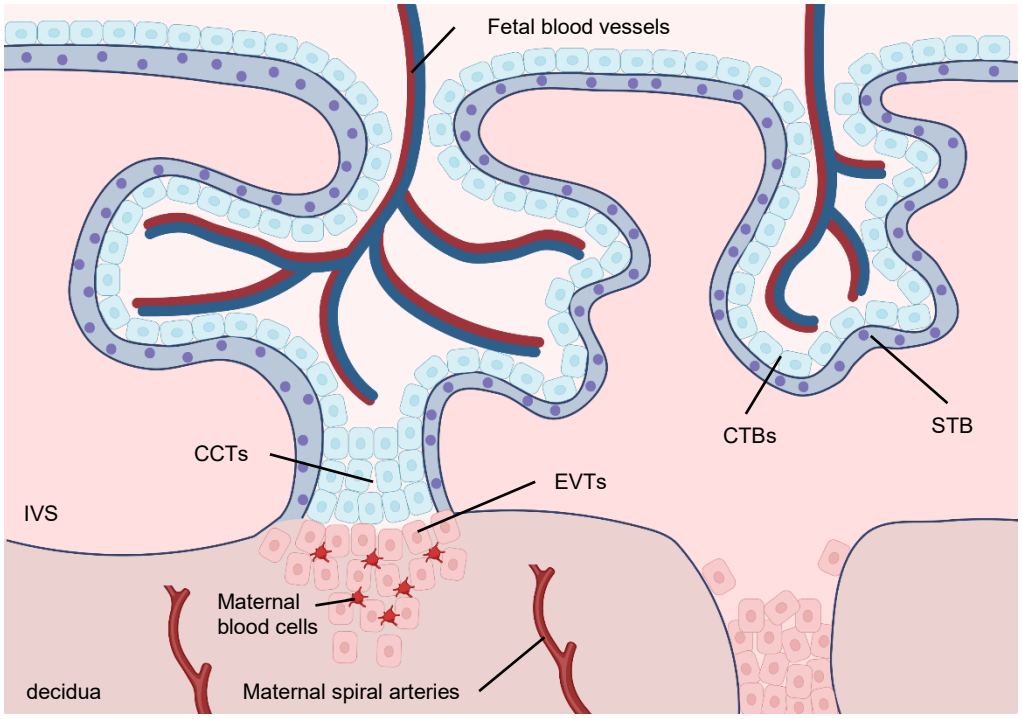

Figure 3 Schematic representation of an early human placenta. During human placentation EVTs from the distal part of anchoring villi migrate into the maternal endometrium to form trophoblast plugs within the lumen of uterine spiral arteries to prevent maternal blood cells from entering the IVS. By the middle of the first trimester these trophoblast plugs become loosely cohesive, forming capillary-shaped channels and maternal platelets may be the first of maternal blood cells that can these intercellular gaps. When these platelets are activated the transcription profile of the surrounding trophoblasts can be altered. Created with BioRender.com.

4. Discussion

4.1. Platelet-derived factors deregulate S1PR2 in human trophoblasts

This research paper provides a comprehensive analysis of the spatiotemporal expression patterns of various S1PR subtypes in the human placenta throughout gestation. Placental S1PR1 and S1PR3 levels increase with advancing GA, whereas S1PR2 is predominantly expressed in the villous trophoblast compartment during the first trimester and decline significantly towards term. In human trophoblasts, S1P is believed to inhibit differentiation by interacting with G_i-coupled S1P receptors, which suppress the adenylate cyclase activity and reduce intercellular cyclic adenosine monophosphate (cAMP) production (67,68). However, it still needs to be elucidated if this inhibitory effect is mediated through a particular S1PR (e.g. S1PR2) in the first trimester placenta. Noteworthy, S1P has been discussed as a potential inhibitor for EVT migration, predominantly through S1PR2 (69). Furthermore, S1PR2 is supposedly involved in S1P-induced expression of IL-6 in BeWo cells (70). It is tempting to speculate that, based on these facts and our own studies, the predominant S1PR2 expression in the first trimester placenta plays a role in regulating trophoblast differentiation and migration as well as invasion processes. As the needs shift from fast cell mass expansion and invasion during the initial phase of pregnancy to more precise metabolic processes later on, the expression pattern of the S1PR might also shift in order to adapt to the current demands. The aforementioned hypotheses are in accordance with the findings from other studies, which suggest that S1PR1 and S1PR3 are reduced in cases of PE. This reduction of expression level may be the cause of impaired vasculogenesis and angiogenesis observed in this syndrome (71).

Besides the changes in expression levels, the location of these receptors is also interesting. We found S1PR1 to be mainly expressed in the endothelium of placental villi, which aligns with other studies confirming S1PR1 expression in endothelial cells of other organs (72,73). We found S1PR2 and S1PR3 mainly to be expressed in trophoblasts, which seems plausible with their potential role in trophoblast development and remodeling of the spiral arteries. When uteroplacental blood flow is fully established with the start of the second trimester, fluid shear stress is produced which introduces hemodynamic forces to the different trophoblast subtypes (74). Interestingly, S1PR1 in vascular endothelial cells is described to be a predominant mechanosensor, which is upregulated by laminar shear stress itself (75). The hypothesis that the onset of maternal blood flow triggers the observed upregulation of placental S1PR towards term remains speculative. However, the results of the present study, which were obtained from experiments involving flow culture, appear to contradict this

hypothesis. Indeed, the data demonstrate that neither S1PR2 nor S1PR3 showed upregulation in differentiated BeWo cells in response to fluid flow.

Before complete remodeling of the spiral arteries, the early placenta has low oxygen levels of 2-3%, which rise with ongoing placentation to about 8-10% (76). Here, we found no significant difference in the expression level of S1PR2 or S1PR3 when cells were cultured under 2.5% or 12% oxygen. We therefore postulate that the difference in the expression pattern throughout gestation is not linked to the rise in oxygen concentrations. When cells were incubated at atmospheric oxygen levels (21%) a significant difference of S1PR3 expression could be detected. However, since placental cells will not be surrounded by such oxygen levels, this effect can be seen as non-physiological and therefore be neglected.

Our observations, in accordance with those of others have revealed the presence of platelets within trophoblast columns, indicating their capacity to pass these channels given their small diameter (61,63). Since these platelets were also found in an active state, speculations were made whether their released factors might influence the expression of S1P receptors (64). In light of substantial evidence connecting S1P to inflammatory processes and prior deliberations on the association between an impairment of the sphingolipid signature and PE, it is crucial to investigate which receptor is affected by dysregulation in response to platelet-derived factors (71,77,78). In this study, a unique approach was utilized to treat trophoblasts with platelet-derived factors. Specifically, activated platelets from pregnant women were incubated in culture inserts above the cells. This method enabled the investigation of the effect of factors released from platelets without the potential for bias, as platelets themselves express S1PRs.

The impact of THR itself on the expression of some genes, here S1PR2 and S1PR3, needs to be taken under consideration. THR is a multifaceted enzyme, that is able to bind to a variety of substrates, thereby influencing the molecular basis of cells in numerous ways (79). However, since the difference in expression level of S1PR2 is even more pronounced upon treatment with platelet-released factors, it can be assumed that a substantial part of the effect is due to the treatment with these factors. Interestingly, we observed a divergent impact on S1PR2 and S1PR3. The significant downregulation of S1PR2 and the propensity for upregulation of S1PR3 exhibited in this study may be indicative of the opening of the spiral arteries and the influx of maternal blood into the IVS at the end of the first trimester. In this case, it can be hypothesized that an earlier inflow of maternal blood, and thus potential activation of platelets and release of their cargo, would dysregulate the expression pattern of the S1PR too early. This, in turn, could contribute to pregnancy complications characterized by inadequate infiltration and migration of EVTs into the maternal decidua. Further research

needs to be conducted to evaluate the exact timeline of changes in S1PR patterns and the influence this could have on the ongoing development of the placenta. Previous studies have demonstrated that S1PR1 expression on the cell surface is indeed downregulated by its activation of agonists, such as small molecule FTY720-P, HDL-S1P or albumin-S1P (80). Despite the absence of extensive discourse on the underlying mechanisms of S1PR2 and S1PR3 dysregulation in the existing literature, we hypothesize that a comparable response is exhibited by S1PR2 due to its regulation through excessive release of platelet cargo, which encompasses S1P.

4.2. The chorioallantoic membrane assay revisited – A facelifted approach for new perspectives in placenta research

This research paper provides an insight into the innovation of methods that have already been established in other research areas and offers an overview of how the advantages of these methods can be best utilized for placenta research. Initially, a fast and straightforward technique is presented for the establishment of a 3D cell culture model using the human trophoblast cell line ACH-3P. The benefit of this simple, high-throughput approach is the consistent, reproducible spheroid generation of uniform size that was observed across different cell passages. To date, a variety of methodologies have been devised for the growth and cultivation of spheroids, which can be classified into two distinct categories: scaffold-based and scaffold-free approaches (81). Scaffold-based methods employ the use of biomaterial, including hydrogels, biofilms, and particles. These materials favor the self-assembly of cells, thereby resulting in the formation of 3D structures (82). Scaffold-free or also so-called technical methods include for example pellet formation, hanging drop, liquid overlay, spinner culture or rotating vessel wall and are frequently regarded as the optimal approach due to their cost-effectiveness, simplicity, and high yield (83). Nonetheless, some of these methods are characterized by a considerable investment of time and are consequently suboptimal with respect to efficiency. Furthermore, these methods may give rise to variations in spheroid size and shape and carry the risk of cell damage due to fluidic shear stress (84).

While this method might not be universally applicable to all types of cells, the ACH-3P cell line has demonstrated a high degree of compatibility with this approach, showing no discernible challenges in terms of viability and functionality. So far, a definite explanation remains elusive concerning the formation of cavities by the spheroids and the potential to close during extended cultivation periods. It is noteworthy that we developed a method for the co-incubation of ACH-3P cells with isolated platelets from pregnant women. This

approach was employed to study the interaction between these two different types of cells during spheroid formation. Our findings revealed that platelets were predominantly present in the spheroid cavity, a phenomenon that may be attributed to the influence of gravitational forces and cell size and density during the formation process. Additionally, platelets were observed within capillary-sized channels of the spheroids, thereby mimicking *in vivo* like situations during the early human placental development. These small intercellular gaps and channels may also enable nutrient and oxygen supply all the way to the center of the spheroids, which would explain that the spheroids were negative for caspase 3, even after several days in culture. Given that other protocols have noted, insufficient nutrient supply and hypoxic cores in the cultivation of large spheroids, we want to highlight the benefit of the proposed approach, particularly in the context of subsequent experiments and downstream analysis (81).

The first concept of the CAM assay was supposedly introduced in 1911 by Rous and Murphy. Initially, the assay was used to study implantation and avian tumors. However, over the years a progressive refinement of the assay to meet the evolving demands of researchers, thereby unveiling its multifaceted applications across diverse research areas was witnessed (85). The conventional method of performing the CAM assay entailed an *in ovo* approach, wherein a small window was incised into the shell of the chicken egg to administer the test material. Yet, this setup proved to be rather impractical for assessing and visualizing the CAM and soon the *ex ovo* technique was introduced (86). But even this method came with some flaws, e.g. lower survival rate of the embryos because of small ruptures in the yolk membrane. This problem is nowadays reduced by gently cracking the egg and incubating the embryos in confined curved spaces (e.g. weighing boats) to minimize the total impact on the yolk sac (86,87). Another fundamental step in the execution of the CAM assay is the transfer of silicone rings onto the membrane. This will subsequently serve as the area of incubation for the test material. It is of utmost importance to ensure that the designated area of invasion does not come into contact with large blood vessels. This precautionary measure is crucial to avoid excessive bleedings too early during the experimental procedure. Ideally, the silicone rings should be carefully placed between bigger blood vessels with caution to also leave out areas directly above the embryo and too close to the rim of the dish. Furthermore, it is vital to take the test material into account, which must be transferred onto the membrane in advance. It may be necessary to adjust the dimension of the silicone rings, in case the intention is to incubate tumor tissue for example. Depending on the specific types of cells one wants to incubate it might also be relevant to test out and eventually modify the quantity of cells. In this study, we found that the incubation of 5 spheroids in each of three silicone rings

on the same egg is the optimal setup to introduce enough cells without immediately exhausting the embryo with too much xenograft mass. From the moment of transfer of the test material onto the CAM onwards the spheroids were in direct contact with the membrane. This is another huge advantage of this method, as there is no need for additional culture media or the use of biomaterials like Matrigel® to improve the environment for the cells. The environment appears to be favorable for the promotion of attachment and consequent invasion of the cells into the membrane.

In contrast to the reports of other labs, where an incubation period for tumor cells lasted several days, our experiments had to be terminated after a maximum of 48 h. Already 20-24 h after the transfer of the ACH-3P spheroids, visible changes in the membrane became apparent. The formation of small petechiae was observed, which soon led to bleedings. The experiments were stopped, and the CAM tissues were subsequently subjected to histological analysis. Following the staining of multiple sections for H&E, we could confirm that the spheroids had completely penetrated the membrane, extending all the way to the allantoic membrane. Interestingly, the ACH-3P cell mass seemed to have kept some of their features as for example the original cavities of the spheroids could still be observed in numerous cases. It is particularly noteworthy that these cavities were found to be filled with blood cells from the chicken embryo. This is highly intriguing, as it potentially mimics the occurrence of certain events during early placental development, such as invasion and remodeling of the spiral arteries. The blood filling of the spheroids can eventually be compared with initial steps of early blood leakage through trophoblast plugs and into the developing IVS. However, it should be mentioned that no blood clotting could be detected at any point which finally led to the death of the chicken embryos due to excessive bleeding. To date, we have not found an explanation for the apparent complete lack of blood coagulation during these stages of chicken egg development. However, it needs to be stressed that the red blood cells and thrombocytes of chickens (e.g. presence of nuclei) differ from those of humans. Furthermore, it is important to note that the ACH-3P spheroids do not fully resemble the IVS. This is due to their fact that their cavities are lined with mononucleated cells rather than a syncytium, which is a characteristic of the IVS.

Via immunohistochemical as well as immunofluorescense staining for human CK7 and HLA-G we could confirm that the invaded cells in the CAM were in fact ACH-3P cells. Moreover, we could visualize the endothelium (vWF) of the chicken embryo vessels, which was in very close proximity to the trophoblast cells further reinforcing parallels to happenings in the first trimester of pregnancy. It should be acknowledged that the vWF antibody was of anti-human origin and it is therefore challenging to specifically stain only the endothelium.

Furthermore, we tested the feasibility of implementing a padlock-probe based *in situ* hybridization on CAMs that had been invaded by ACH-3P spheroids. When targeting for *ACTB* mRNA, which encodes for human beta actin, clear punctual signals could be detected exclusively in areas where we confirmed ACH-3P cells via histological methods. We therefore propose this method can be used as an alternative approach for analysis in cases antibodies are not specific or available.

4.3. Maternal platelet-derived factors induce trophoblastic LAIR2 expression to promote trophoblast invasion and inhibit platelet activation at the fetal-maternal interface

This research paper suggests that activated maternal platelets and their released factors affect the transcription profile of invasive trophoblasts at the fetal-maternal interface. Results of our transcriptomic study revealed that trophoblast cells shift towards an expression pattern associated with migration and adhesion, thereby possibly contributing to tissue and vascular development. From the list of deregulated genes, we further investigated the ones which according to literature seemed to be involved in embryonic development or platelet function. Of particular interest seemed *LAIR2*, a gene exclusively expressed in EVTs and significantly upregulated by platelet-derived factors. It is noteworthy that bioinformatic pseudotime analysis of a publicly available single nuclei RNA-sequencing dataset from the first-trimester placenta (88) has successfully mapped LAIR2 expression to the CCT trajectory. This finding is further corroborated *in situ* on both the mRNA and protein levels. Finally, these discoveries could also be substantiated *in vitro*, when primary trophoblast organoids were triggered to undergo EVT differentiation. It is noteworthy that the presence of resting platelets within trophoblast spheroids did not stimulate additional LAIR2 expression, whereas THR-activated platelets did. This observation indicates that the regulatory function is not exerted by the platelets themselves, but rather by platelet-derived factors. In this regard, we propose a newly conceptualized 3D model to investigate the interaction of human platelets with trophoblasts *in vitro*, thereby simulating the presence of platelets within the intercellular space of distal chorionic villi (CCTs) in the first trimester of pregnancy. Previous TEM studies have found platelets in these locations to be activated *in vivo*, which leads to the hypothesis that factors released from these platelets may have an impact on the fate of the CCTs and potentially induce the expression of specific genes, such as *LAIR2*, in this particular trophoblast lineage (64). Platelets contain a huge amount of transforming growth factor beta (TGF-β), which is why it needs to be considered as one of the key components of the released factors upon

platelet activation (89). Interestingly, TGF-β has recently been discussed as a potentially fundamental trigger in the differentiation of placental EVTs into decidual EVTs (90). However, further investigations need to be conducted to draw conclusions on the exact factors that influence differentiation pathways of trophoblasts.

In recent years, there has been an increasing focus on the search for alternatives to animal products in research. One of the proposed alternatives is human platelet-rich plasma (PRP), which due to its ability to promote cell viability, might act as an alternative to fetal bovine serum (FBS) in cell culture experiments (91). The present study lends further support to this claim, as it was found that spheroids treated with platelet releasate (PR) exhibited a significantly increased viability. Furthermore, the platelet-released factors did not induce caspase-dependent apoptosis.

Our morphological analysis confirmed the invasion of EVTs from distal parts of the trophoblast cell columns into tissue of the decidua basalis. However, we also found maternal erythrocytes within intercellular gaps of these highly invaded decidua areas. Typically heightened vascular permeability or compromised vessel wall integrity are reasons for blood cell leakage. This phenomenon has been discussed in several pathological circumstances such as tissue trauma or within tissue shadowed by leaky or immature blood vessels (e.g. atherosclerotic plugs or tumors) (92). However, here we found extravasation of maternal blood vessels in areas of invasion in several samples suggesting this might be a naturally occurring process at least to some extent during placentation. Of note, decidual tissue contains collagen, produced by decidual stromal cells, as well as laminin and fibronectin, derived from EVTs (93). All of these substrates can bind to platelet receptors and cause activation suggesting to trigger coagulation of these extravasated maternal blood (94–96). Coagulation and accompanying deposition of fibrin have been hypothesized to develop a layer of fibrinoid located deeper in the basal plate that embeds maternal and fetal cells, the so called Nitabuch stria (65). LAIR2 is a soluble receptor which can bind to collagen to initiate immune responses. It can act as a decoy receptor by preventing the binding of LAIR1 to collagen, which might affect immune cell behavior and tumor microenvironments (97). LAIR2 has been discussed in tumor research suggesting its association to immune infiltration and its function to serve as a biomarker for exhausted T cells in the tumor microenvironment (98). In consideration of the available evidence, it is tempting to hypothesize that EVT-derived LAIR2 may play a modulating role in the immune interactions of maternal immune cells with invading trophoblasts. An additional function of LAIR2 could be fine-tuning of the coagulation of leaked maternal blood in perivascular regions of the Nitabuch stria.

In this study we were able to verify findings of previous research, which indicated that LAIR2 is mainly expressed in CCTs and EVTs of the first trimester placenta (99,100). Furthermore, LAIR2 contributed to higher invasiveness of the ACH-3P cells, implying that increased LAIR2 levels might also enhance trophoblast invasiveness in an autocrine manner and therefore positively influencing placental development and function (101). However, these processes are referred to as being highly regulated, with the potential to be significantly impacted by even minor alterations in the molecular profile, here particularly in the context of trophoblasts differentiating towards the EVT phenotype. These adverse effects might potentially result in pregnancy pathologies like Abnormal Invasive Placenta (AIP) (102). It is worth noting that the potential correlation between diminished LAIR2 expression in placental tissue and the development of PE has been subject to prior discussion. Indeed, the potential for impaired conversion of uterine spiral arteries due to downregulation of this gene has been discussed. A study of samples obtained from chorionic villus biopsies revealed a contrast in expression levels of LAIR2 in placental tissue between women who developed PE and those who remained healthy throughout gestation. This observation even suggests the potential for a biomarker that could assist in predicting the risk of developing PE (99,100,103).

4.4. Combining maternal platelet- and trophoblast research

Despite the significant progress made in our understanding of placental development, numerous questions concerning this process remain unresolved. Due to legal and ethical considerations it is still challenging to find out more about specific mechanisms and factors involved during the development of the embryo and the placenta, particularly in the initial phase of pregnancy. Since placentation is highly variable in mammals there is still a lack of appropriate animal models to answer certain research questions (104,105). A notable strength of this dissertation is the integration of multiple models to analyze the phenomena of early human placentation. In addition, we were able to apply several models to study maternal platelets and their possible effect on the human placenta.

Here we used two different cell lines to study trophoblast cells. The BeWo cell line is a choriocarcinoma cell line extensively used to study villous trophoblast fusion as they have the potential to form syncytia when adding forskolin (106). The ACH-3P cell line is a hybridoma cell line established by fusing primary human first trimester trophoblasts (GA 12 weeks) with the human choriocarcinoma cell line AC1-1. It is an excellent tool to study interaction of syngeneic trophoblast subpopulations (107). The use of carcinoma cell lines for trophoblast research has been heavily criticized in the last years. This is due to the fact that carcinoma cell lines may be highly malignant, contain aberrant numbers of chromosomes, or

consist of a heterogeneous population of trophoblasts mixed with mesenchymal cells (104,108,109). However, obtaining tissue from first trimester placenta still remains challenging for reasons outlined above. Therefor trophoblast cell lines continue to be a valuable tool to pursue knowledge of trophoblast cell biology, immunology, endocrine function and placental development (108). Recently, the use of 3D cell culture models has become increasingly popular. This type of cultivation can mimic cellular communication i.e. cell-cell and cell-matrix interactions and is therefore believed to be more analogous to *in vivo* situations than conventional 2D cultures (81). In this thesis we could establish a 3D cell culture model with the use of the ACH-3P cell line. We confirmed that the cultivation of ACH-3P spheroids is a relatively straightforward process which is also relatively cost-effective. Moreover, the spheroids can be easily handled and are suitable for further experiments (e.g. CAM assay) or downstream analysis (e.g. RNA and protein isolation, histological processing). These protocols could as well be applied to other trophoblast cell lines (e.g. BeWo, JEG-3) without any major changes (data not shown here), demonstrating their proof of concept.

In addition to the traditional *in vitro* cell line models, parts of this thesis also incorporate the use of primary cell culture. Various types of primary (trophoblast) cells can be isolated from placental tissue via digestion procedures (110,111). Furthermore, in recent years human trophoblast stem cell models have been developed. Human trophoblast stem cells and primary trophoblasts have the capacity to give rise to the three major trophoblast lineages and are therefore a powerful tool to study human trophoblast lineage development (112,113). In the course of this project, we were able to isolate CTBs from first trimester placenta samples and went even one step further and cultivated them as organoids in an *in vitro* 3D model. As mentioned above 3D cell culture models come closer to *in vivo* situations as the cells have more possibilities for communication with one another as well as their environment (81). The development of placental organoids has been a huge leap forward for this research niche as these organoids can self-aggregate to form “mini organs” which reflect *in vivo* placental structure and function (110). They can either be generated from cell mixtures that contain stem cell populations as shown here, or they can be generated from pure stem cell preparations and can subsequently be differentiated into mature cell types (114,115). Despite the before mentioned restrictions due to legal and ethical considerations, placenta research has undergone significant advancements over the years. The availability of numerous diverse models enables the investigation of events throughout the entire period of gestation.

Here, we also want to highlight the great variety of ways we used to treat trophoblast cells and tissue with platelets and their derived factors. In recent years, our lab has utilized a

diversity of methods for the treatment of trophoblasts and placental tissue with platelet-derived factors. Human platelets can be isolated from whole blood by separating plasma containing the platelets, called platelet-rich plasma (PRP), from red blood cells and leukocytes. However, this isolation procedure is rather critical since it can have an impact on the platelet response (116,117). During the so-called platelet washing method repeated centrifugation at different speed and resuspension of the buffered solution is used to separate platelets from other blood cells as well as plasma components and anticoagulant factors used during blood withdrawal (117). After this procedure we were able to resuspend the platelet pellet in culture medium. From this step onwards one can decide to either use platelets themselves in culture or by activating them and isolating their derived factors. We co-incubated the platelets with the ACH-3P cell line in specially coated U-bottom 96-well plates. Through the spheroid forming process platelets were encapsulated within the spheroids. Since platelets were in direct contact with several layers of trophoblast cells, this is an excellent model for us to mimic *in vivo* like situations of the first trimester, when uteroplacental blood flow is not yet fully established, but some platelets can be found within gaps of trophoblast cell columns. One major advantage in the use of PR to treat cells or tissue with platelet-derived factors is to study the effect of platelet-released factors without having to deal with the bias that platelets themselves might contain certain transcripts of interest. Moreover, we propose the use of a pool of PR from 10 or more different pregnant donors, which is intended to compensate for any potential biological inequalities. Another option is to use transwell inserts to incubate platelets in near proximity of cells, so they are exposed to the platelet factors without directly interfering with each other.

In this thesis we could explain the importance of studying platelets during early human placental development. In this context we want to emphasize the importance of studying different aspects of platelets. As mentioned before it is established that platelets can be either useful or harmful to placental development, which highly depends on the degree of activation (4). We also want to accentuate that the location of the platelets is of great relevance, as they might be in contact with different types of cells or ECM. Furthermore, shear stress should not be neglected when studying platelets as they are also exposed to different flow rates *in vivo*. Altogether we want to highlight that platelets and their derived factors have an impact on surrounding trophoblasts. We found several genes related to embryonic or placental development, to be deregulated in the presence of platelet-derived factors. Interestingly, several of these genes are then also connected to platelet function like *LAIR2*, which can inhibit collagen type I-induced platelet activation. But also S1PRs, which indirectly relate to platelet function since platelets can release their substrate S1P when activated.

5. Conclusion

In conclusion, our study found that platelets and their derived factors can impact the gene expression profile of trophoblasts. Here for example, we discovered that expression levels of S1P receptors, which are differentially expressed across gestation, can be influenced by platelet-derived factors.

Furthermore, we found an overall change in the transcription profile of trophoblasts treated with platelet-derived factors. This includes several genes that are involved in embryonic- and placental development like *LAIR2*, which in return can impact platelet activation.

In this work we also want to highlight the use of several state-of-the-art techniques that combine trophoblast and platelet research. The use of several different cell lines and primary cells in conventional 2D as well as 3D culture makes this work original. In addition, we used different ways to expose trophoblasts to platelet-derived factors. The application of the CAM assay in combination with trophoblast spheroids is a unique approach, which we believe needs to be reconsidered more, when investigating trophoblast invasion and differentiation processes in the context of blood flow.

Altogether, we believe that dysregulation of certain genes in response to platelet-derived factors may potentially impact trophoblast differentiation and migration processes, which are essential for the development of a healthy placenta. We propose that platelets play a huge role in early placentation and that several fine-tuned feedback mechanisms regulate the interplay between trophoblasts and maternal platelets. We would like to highlight the importance of further research on the role of maternal platelets to clarify their potential effects on placentation and pregnancy outcomes.

6. References

1. Turco MY, Moffett A. Development of the human placenta. Development. 2019 Nov 15;146(22):dev163428.

2. Roberts VHJ, Morgan TK, Bednarek P, Morita M, Burton GJ, Lo JO, et al. Early first trimester uteroplacental flow and the progressive disintegration of spiral artery plugs: new insights from contrast-enhanced ultrasound and tissue histopathology. Hum Reprod. 2017 Dec 1;32(12):2382–93.

3. Sadler TW, Langman J, Drews U, Sadler TW. Medizinische Embryologie: die normale menschliche Entwicklung und ihre Fehlbildungen. 11., aktualisierte und erw. Aufl. Stuttgart: Thieme; 2008. 530 p.

4. Moser G, Guettler J, Forstner D, Gauster M. Maternal Platelets—Friend or Foe of the Human Placenta? Int J Mol Sci. 2019 Nov 11;20(22):5639.

5. Benirschke K. Pathology of the Human Placenta. 3rd ed. New York, NY: Springer New York; 1995. 1 p.

6. Gude NM, Roberts CT, Kalionis B, King RG. Growth and function of the normal human placenta. Thromb Res. 2004 Jan;114(5–6):397–407.

7. Ochoa-Bernal MA, Fazleabas AT. Physiologic Events of Embryo Implantation and Decidualization in Human and Non-Human Primates. Int J Mol Sci. 2020 Mar 13;21(6):1973.

8. Oghbaei F, Zarezadeh R, Jafari-Gharabaghlou D, Ranjbar M, Nouri M, Fattahi A, et al. Epithelial-mesenchymal transition process during embryo implantation. Cell Tissue Res. 2022 Apr;388(1):1–17.

9. Li X, Kodithuwakku SP, Chan RWS, Yeung WSB, Yao Y, Ng EHY, et al. Three-dimensional culture models of human endometrium for studying trophoblast-endometrium interaction during implantation. Reprod Biol Endocrinol. 2022 Aug 13;20(1):120.

10. Idelevich A, Vilella F. Mother and Embryo Cross-Communication. Genes. 2020 Mar 31;11(4):376.

11. Gamage TK, Chamley LW, James JL. Stem cell insights into human trophoblast lineage differentiation. Hum Reprod Update. 2016 Dec;23(1):77–103.

12. Knöfler M, Haider S, Saleh L, Pollheimer J, Gamage TKJB, James J. Human placenta and trophoblast development: key molecular mechanisms and model systems. Cell Mol Life Sci. 2019 Sep;76(18):3479–96.

13. Huppertz B. The Placenta: Basics and Clinical Significance. 1st ed. Berlin, Heidelberg: Springer Berlin / Heidelberg; 2023. 1 p.

14. Xiao Z, Yan L, Liang X, Wang H. Progress in deciphering trophoblast cell differentiation during human placentation. Curr Opin Cell Biol. 2020 Dec;67:86–91.

15. Aplin JD. Developmental cell biology of human villous trophoblast: current research problems. Int J Dev Biol. 2010;54(2–3):323–9.

16. Gauster M, Moser G, Wernitznig S, Kupper N, Huppertz B. Early human trophoblast development: from morphology to function. Cell Mol Life Sci CMLS. 2022 Jun 5;79(6):345.

17. Harris LK. Review: Trophoblast-Vascular Cell Interactions in Early Pregnancy: How to Remodel a Vessel. Placenta. 2010 Mar;31:S93–8.

18. Funai EF, Friedlander Y, Paltiel O, Tiram E, Xue X, Deutsch L, et al. Long-Term Mortality After Preeclampsia: Epidemiology. 2005 Mar;16(2):206–15.

19. Barker DJ, Martyn CN, Osmond C, Hales CN, Fall CH. Growth in utero and serum cholesterol concentrations in adult life. BMJ. 1993 Dec 11;307(6918):1524–7.

20. Moster D, Lie RT, Markestad T. Long-Term Medical and Social Consequences of Preterm Birth. N Engl J Med. 2008 Jul 17;359(3):262–73.

21. Dietrich B, Haider S, Meinhardt G, Pollheimer J, Knöfler M. WNT and NOTCH signaling in human trophoblast development and differentiation. Cell Mol Life Sci. 2022 Jun;79(6):292.

22. Pollheimer J, Vondra S, Baltayeva J, Beristain AG, Knöfler M. Regulation of Placental Extravillous Trophoblasts by the Maternal Uterine Environment. Front Immunol. 2018 Nov 13;9:2597.

23. Harris LK. IFPA Gabor Than Award lecture: Transformation of the spiral arteries in human pregnancy: Key events in the remodelling timeline. Placenta. 2011 Mar;32:S154–8.

24. Burton GJ, Jauniaux E. The human placenta: new perspectives on its formation and function during early pregnancy. Proc Biol Sci. 2023 Apr 26;290(1997):20230191.

25. Griffiths SK, Campbell JP. Placental structure, function and drug transfer. Contin Educ Anaesth Crit Care Pain. 2015 Apr;15(2):84–9.

26. Lager S, Powell TL. Regulation of nutrient transport across the placenta. J Pregnancy. 2012;2012:179827.

27. Burton GJ, Fowden AL. The placenta: a multifaceted, transient organ. Philos Trans R Soc Lond B Biol Sci. 2015 Mar 5;370(1663):20140066.

28. Carter AM. Placental Oxygen Consumption. Part I: In Vivo Studies—A Review. Placenta. 2000 Mar;21:S31–7.

29. Lai TJ, Teng SW, Chang CK, Huang CY. Progesterone in Pregnancy: Evidence-Based Strategies to Reduce Miscarriage and Enhance Assisted Reproductive Technology. Med Sci Monit Int Med J Exp Clin Res. 2024 Mar 8;30:e943400.

30. Pastore M, Jobe S, Ramadoss J, Magness R. Estrogen Receptor-α and Estrogen Receptor-β in the Uterine Vascular Endothelium during Pregnancy: Functional Implications for Regulating Uterine Blood Flow. Semin Reprod Med. 2012 Jan;30(01):46–61.

31. Nwabuobi C, Arlier S, Schatz F, Guzeloglu-Kayisli O, Lockwood CJ, Kayisli UA. hCG: Biological Functions and Clinical Applications. Int J Mol Sci. 2017 Sep 22;18(10):2037.

32. Heidegger H, Jeschke U. Human Chorionic Gonadotropin (hCG)-An Endocrine, Regulator of Gestation and Cancer. Int J Mol Sci. 2018 May 17;19(5):1502.

33. Schumacher A, Heinze K, Witte J, Poloski E, Linzke N, Woidacki K, et al. Human Chorionic Gonadotropin as a Central Regulator of Pregnancy Immune Tolerance. J Immunol. 2013 Mar 15;190(6):2650–8.

34. Svensson-Arvelund J, Ernerudh J, Buse E, Cline JM, Haeger JD, Dixon D, et al. The Placenta in Toxicology. Part II: Systemic and Local Immune Adaptations in Pregnancy. Toxicol Pathol. 2014 Feb;42(2):327–38.

35. Trundley A, Moffett A. Human uterine leukocytes and pregnancy. Tissue Antigens. 2004 Jan;63(1):1–12.

36. Mellembakken JR, Aukrust P, Olafsen MK, Ueland T, Hestdal K, Videm V. Activation of Leukocytes During the Uteroplacental Passage in Preeclampsia. Hypertension. 2002 Jan;39(1):155–60.

37. Atyeo C, Alter G. The multifaceted roles of breast milk antibodies. Cell. 2021 Mar;184(6):1486–99.

38. Jurk K, Kehrel BE. Platelets: Physiology and Biochemistry. Semin Thromb Hemost. 2024 Jul;50(05):794–803.

39. Maouia A, Rebetz J, Kapur R, Semple JW. The Immune Nature of Platelets Revisited. Transfus Med Rev. 2020 Oct;34(4):209–20.

40. Reusswig F, An O, Deppermann C. Platelet life cycle during aging: function, production and clearance. Platelets. 2024 Dec 31;35(1):2433750.

41. Burnouf T, Strunk D, Koh MBC, Schallmoser K. Human platelet lysate: Replacing fetal bovine serum as a gold standard for human cell propagation? Biomaterials. 2016 Jan;76:371–87.

42. Koenen RR. The prowess of platelets in immunity and inflammation. Thromb Haemost. 2016;116(10):605–12.

43. Machlus KR, Italiano JE. The incredible journey: From megakaryocyte development to platelet formation. J Cell Biol. 2013 Jun 10;201(6):785–96.

44. Boscher J, Guinard I, Eckly A, Lanza F, Léon C. Blood platelet formation at a glance. J Cell Sci. 2020 Oct 15;133(20):jcs244731.

45. Hitchcock IS, Kaushansky K. Thrombopoietin from beginning to end. Br J Haematol. 2014 Apr;165(2):259–68.

46. Machlus KR, Thon JN, Italiano JE. Interpreting the developmental dance of the megakaryocyte: a review of the cellular and molecular processes mediating platelet formation. Br J Haematol. 2014 Apr;165(2):227–36.

47. Broos K, Feys HB, De Meyer SF, Vanhoorelbeke K, Deckmyn H. Platelets at work in primary hemostasis. Blood Rev. 2011 Jul;25(4):155–67.

48. Varga-Szabo D, Pleines I, Nieswandt B. Cell Adhesion Mechanisms in Platelets. Arterioscler Thromb Vasc Biol. 2008 Mar;28(3):403–12.

49. Golebiewska EM, Poole AW. Secrets of platelet exocytosis – what do we really know about platelet secretion mechanisms? Br J Haematol. 2014 Apr;165(2):204–16.

50. Ren Q, Wimmer C, Chicka MC, Ye S, Ren Y, Hughson FM, et al. Munc13-4 is a limiting factor in the pathway required for platelet granule release and hemostasis. Blood. 2010 Aug 12;116(6):869–77.

51. Jackson SP. The growing complexity of platelet aggregation. Blood. 2007 Jun 15;109(12):5087–95.

52. Ruggeri ZM. Mechanisms Initiating Platelet Thrombus Formation. Thromb Haemost. 1997;78(01):611–6.

53. Maxwell MJ, Westein E, Nesbitt WS, Giuliano S, Dopheide SM, Jackson SP. Identification of a 2-stage platelet aggregation process mediating shear-dependent thrombus formation. Blood. 2007 Jan 15;109(2):566–76.

54. McNicol A, Israels SJ. Platelet Dense Granules. Thromb Res. 1999 Jul;95(1):1–18.

55. Blair P, Flaumenhaft R. Platelet alpha-granules: basic biology and clinical correlates. Blood Rev. 2009 Jul;23(4):177–89.

56. Gremmel T, Frelinger AL, Michelson AD. Platelet Physiology. Semin Thromb Hemost. 2024 Nov;50(08):1173–86.

57. Michelson AD, editor. Platelets. 3rd ed. London ; Waltham, MA: Academic Press; 2013. 1353 p.

58. Chen Y, Yuan Y, Li W. Sorting machineries: how platelet-dense granules differ from α-granules. Biosci Rep. 2018 Oct 31;38(5):BSR20180458.

59. Reese JA, Peck JD, McIntosh JJ, Vesely SK, George JN. Platelet counts in women with normal pregnancies: A systematic review. Am J Hematol. 2017 Nov;92(11):1224–32.

60. Reese JA, Peck JD, Yu Z, Scordino TA, Deschamps DR, McIntosh JJ, et al. Platelet sequestration and consumption in the placental intervillous space contribute to lower platelet counts during pregnancy. Am J Hematol. 2019 Jan;94(1):E8–11.

61. Sato Y, Fujiwara H, Zeng BX, Higuchi T, Yoshioka S, Fujii S. Platelet-derived soluble factors induce human extravillous trophoblast migration and differentiation: platelets are a possible regulator of trophoblast infiltration into maternal spiral arteries. Blood. 2005 Jul 15;106(2):428–35.

62. Guettler J, Forstner D, Gauster M. Maternal platelets at the first trimester maternal-placental interface – Small players with great impact on placenta development. Placenta. 2022 Jul;125:61–7.

63. Forstner D, Maninger S, Nonn O, Guettler J, Moser G, Leitinger G, et al. Platelet-derived factors impair placental chorionic gonadotropin beta-subunit synthesis. J Mol Med. 2020 Feb;98(2):193–207.

64. Guettler J, Forstner D, Cvirn G, Maninger S, Brugger BA, Nonn O, et al. Maternal platelets pass interstices of trophoblast columns and are not activated by HLA-G in early human pregnancy. J Reprod Immunol. 2021 Apr;144:103280.

65. Kaufmann P, Huppertz B, Frank HG. The fibrinoids of the human placenta: origin, composition and functional relevance. Ann Anat - Anat Anz. 1996 Dec;178(6):485–501.

66. Kohli S, Ranjan S, Hoffmann J, Kashif M, Daniel EA, Al-Dabet MM, et al. Maternal extracellular vesicles and platelets promote preeclampsia via inflammasome activation in trophoblasts. Blood. 2016 Oct 27;128(17):2153–64.

67. Johnstone ED, Chan G, Sibley CP, Davidge ST, Lowen B, Guilbert LJ. Sphingosine-1-phosphate inhibition of placental trophoblast differentiation through a Gi-coupled receptor response. J Lipid Res. 2005 Sep;46(9):1833–9.

68. Singh AT, Dharmarajan A, Aye ILMH, Keelan JA. Sphingosine–sphingosine-1-phosphate pathway regulates trophoblast differentiation and syncytialization. Reprod Biomed Online. 2012 Feb;24(2):224–34.

69. Westwood M, Al-Saghir K, Finn-Sell S, Tan C, Cowley E, Berneau S, et al. Vitamin D attenuates sphingosine-1-phosphate (S1P)-mediated inhibition of extravillous trophoblast migration. Placenta. 2017 Dec;60:1–8.

70. Goyal P, Brunnert D, Ehrhardt J, Bredow M, Piccenini S, Zygmunt M. Cytokine IL-6 secretion by trophoblasts regulated via sphingosine-1-phosphate receptor 2 involving Rho/Rho-kinase and Rac1 signaling pathways. Mol Hum Reprod. 2013 Aug 1;19(8):528–38.

71. Dobierzewska A, Palominos M, Sanchez M, Dyhr M, Helgert K, Venegas-Araneda P, et al. Impairment of Angiogenic Sphingosine Kinase-1/Sphingosine-1-Phosphate Receptors Pathway in Preeclampsia. Oudejans C, editor. PLOS ONE. 2016 Jun 10;11(6):e0157221.

72. Wang F, Van Brocklyn JR, Hobson JP, Movafagh S, Zukowska-Grojec Z, Milstien S, et al. Sphingosine 1-Phosphate Stimulates Cell Migration through a Gi-coupled Cell Surface Receptor. J Biol Chem. 1999 Dec;274(50):35343–50.

73. Panetti T. Differential effects of sphingosine 1-phosphate and lysophosphatidic acid on endothelial cells. Biochim Biophys Acta BBA - Mol Cell Biol Lipids. 2002 May 23;1582(1–3):190–6.

74. Brugger BA, Guettler J, Gauster M. Go with the Flow—Trophoblasts in Flow Culture. Int J Mol Sci. 2020 Jun 30;21(13):4666.

75. Aoki S, Osada M, Kaneko M, Ozaki Y, Yatomi Y. Fluid shear stress enhances the sphingosine 1-phosphate responses in cell–cell interactions between platelets and endothelial cells. Biochem Biophys Res Commun. 2007 Jul;358(4):1054–7.

76. Zhao H, Wong RJ, Stevenson DK. The Impact of Hypoxia in Early Pregnancy on Placental Cells. Int J Mol Sci. 2021 Sep 7;22(18):9675.

77. Del Gaudio I, Sasset L, Di Lorenzo A, Wadsack C. Sphingolipid Signature of Human Feto-Placental Vasculature in Preeclampsia. Int J Mol Sci. 2020 Feb 4;21(3):1019.

78. Spiegel S, Milstien S. The outs and the ins of sphingosine-1-phosphate in immunity. Nat Rev Immunol. 2011 Jun;11(6):403–15.

79. Davie E, Kulman J. An Overview of the Structure and Function of Thrombin. Semin Thromb Hemost. 2006 Feb;32(S 1):003–15.

80. Cartier A, Hla T. Sphingosine 1-phosphate: Lipid signaling in pathology and therapy. Science. 2019 Oct 18;366(6463):eaar5551.

81. Habanjar O, Diab-Assaf M, Caldefie-Chezet F, Delort L. 3D Cell Culture Systems: Tumor Application, Advantages, and Disadvantages. Int J Mol Sci. 2021 Nov 11;22(22):12200.

82. Ryu NE, Lee SH, Park H. Spheroid Culture System Methods and Applications for Mesenchymal Stem Cells. Cells. 2019 Dec 12;8(12):1620.

83. Gunti S, Hoke ATK, Vu KP, London NR. Organoid and Spheroid Tumor Models: Techniques and Applications. Cancers. 2021 Feb 19;13(4):874.

84. Tseng T, Wong C, Hsieh F, Hsu S. Biomaterial Substrate-Mediated Multicellular Spheroid Formation and Their Applications in Tissue Engineering. Biotechnol J. 2017 Dec;12(12):1700064.

85. Marshall KM, Kanczler JM, Oreffo RO. Evolving applications of the egg: chorioallantoic membrane assay and ex vivo organotypic culture of materials for bone tissue engineering. J Tissue Eng. 2020;11:2041731420942734.

86. Naik M, Brahma P, Dixit M. A Cost-Effective and Efficient Chick Ex-Ovo CAM Assay Protocol to Assess Angiogenesis. Methods Protoc. 2018 May 31;1(2):19.

87. Nowak-Sliwinska P, Segura T, Iruela-Arispe ML. The chicken chorioallantoic membrane model in biology, medicine and bioengineering. Angiogenesis. 2014 Oct;17(4):779–804.

88. Nonn O, Debnath O, Valdes DS, Sallinger K, Secener AK, Fischer C, et al. Senescent Syncytiotrophoblast Secretion During Early Onset Preeclampsia. Hypertension. 2024 Oct 23;HYPERTENSIONAHA.124.23362.

89. Wang L, Wang H, Zhu M, Ni X, Sun L, Wang W, et al. Platelet-derived TGF-β1 induces functional reprogramming of myeloid-derived suppressor cells in immune thrombocytopenia. Blood. 2024 Jul 4;144(1):99–112.

90. Haider S, Lackner AI, Dietrich B, Kunihs V, Haslinger P, Meinhardt G, et al. Transforming growth factor-β signaling governs the differentiation program of extravillous trophoblasts in the developing human placenta. Proc Natl Acad Sci. 2022 Jul 12;119(28):e2120667119.

91. Anitua E, Zalduendo M, Troya M, Alkhraisat MH, Blanco-Antona LA. Platelet-Rich Plasma as an Alternative to Xenogeneic Sera in Cell-Based Therapies: A Need for Standardization. Int J Mol Sci. 2022 Jun 11;23(12):6552.

92. Humar R, Schaer DJ, Vallelian F. Erythrophagocytes in hemolytic anemia, wound healing, and cancer. Trends Mol Med. 2022 Nov;28(11):906–15.

93. Abbas Y, Carnicer-Lombarte A, Gardner L, Thomas J, Brosens JJ, Moffett A, et al. Tissue stiffness at the human maternal–fetal interface. Hum Reprod. 2019 Oct 2;34(10):1999–2008.

94. Hindriks G, Ijsseldijk M, Sonnenberg A, Sixma J, De Groot P. Platelet adhesion to laminin: role of Ca2+ and Mg2+ ions, shear rate, and platelet membrane glycoproteins. Blood. 1992 Feb 15;79(4):928–35.

95. Cho J, Mosher DF. Role of fibronectin assembly in platelet thrombus formation. J Thromb Haemost. 2006 Jul;4(7):1461–9.

96. Moroi M, Jung SM. Platelet receptors for collagen. Thromb Haemost. 1997 Jul;78(1):439–44.

97. Apps R, Sharkey A, Gardner L, Male V, Trotter M, Miller N, et al. Genome-wide expression profile of first trimester villous and extravillous human trophoblast cells. Placenta. 2011 Jan;32(1):33–43.

98. Chen Z, Yu M, Yan J, Guo L, Zhang B, Liu S, et al. PNOC Expressed by B Cells in Cholangiocarcinoma Was Survival Related and LAIR2 Could Be a T Cell Exhaustion Biomarker in Tumor Microenvironment: Characterization of Immune Microenvironment Combining Single-Cell and Bulk Sequencing Technology. Front Immunol. 2021 Mar 24;12:647209.

99. Founds SA, Fallert-Junecko B, Reinhart TA, Parks WT. LAIR2-expressing extravillous trophoblasts associate with maternal spiral arterioles undergoing physiologic conversion. Placenta. 2013 Mar;34(3):248–55.

100. Founds SA, Fallert-Junecko B, Reinhart TA, Conley YP, Parks WT. LAIR2 localizes specifically to sites of extravillous trophoblast invasion. Placenta. 2010 Oct;31(10):880–5.

101. Liu J, Zhao H, Zhou F, Huang Y, Chen X, Wang S, et al. Human-specific LAIR2 contributes to the high invasiveness of human extravillous trophoblast cells. Reprod Biol. 2019 Sep;19(3):287–92.

102. Illsley NP, DaSilva-Arnold SC, Zamudio S, Alvarez M, Al-Khan A. Trophoblast invasion: Lessons from abnormally invasive placenta (placenta accreta). Placenta. 2020 Dec;102:61–6.

103. Founds SA, Conley YP, Lyons-Weiler JF, Jeyabalan A, Allen Hogge W, Conrad KP. Altered Global Gene Expression in First Trimester Placentas of Women Destined to Develop Preeclampsia. Placenta. 2009 Jan;30(1):15–24.

104. Abbas Y, Turco MY, Burton GJ, Moffett A. Investigation of human trophoblast invasion *in vitro*. Hum Reprod Update. 2020 Jun 18;26(4):501–13.

105. Io S, Kondoh E, Chigusa Y, Kawasaki K, Mandai M, Yamada AS. New era of trophoblast research: integrating morphological and molecular approaches. Hum Reprod Update. 2020 Sep 1;26(5):611–33.

106. Orendi K, Gauster M, Moser G, Meiri H, Huppertz B. The choriocarcinoma cell line BeWo: syncytial fusion and expression of syncytium-specific proteins. REPRODUCTION. 2010 Nov;140(5):759–66.

107. Hiden U, Wadsack C, Prutsch N, Gauster M, Weiss U, Frank HG, et al. The first trimester human trophoblast cell line ACH-3P: A novel tool to study autocrine/paracrine regulatory loops of human trophoblast subpopulations – TNF-α stimulates MMP15 expression. BMC Dev Biol. 2007 Dec 19;7(1):137.

108. King A, Thomas L, Bischof P. Cell Culture Models of Trophoblast II: Trophoblast Cell Lines— A Workshop Report. Placenta. 2000 Mar;21:S113–9.

109. Abou-Kheir W, Barrak J, Hadadeh O, Daoud G. HTR-8/SVneo cell line contains a mixed population of cells. Placenta. 2017 Feb;50:1–7.

110. Sun C, James JL, Murthi P. Three-Dimensional In Vitro Human Placental Organoids from Mononuclear Villous Trophoblasts or Trophoblast Stem Cells to Understand Trophoblast Dysfunction in Fetal Growth Restriction. In: Raha S, editor. Trophoblasts [Internet]. New York, NY: Springer US; 2024 [cited 2025 Feb 10]. p. 235–45. (Methods in Molecular Biology; vol. 2728). Available from: https://link.springer.com/10.1007/978-1-0716-3495-0_19

111. Gamage TKJB, Schierding W, Tsai P, Ludgate JL, Chamley LW, Weeks RJ, et al. Human trophoblasts are primarily distinguished from somatic cells by differences in the pattern rather than the degree of global CpG methylation. Biol Open. 2018 Aug 8;7(8):bio034884.

112. Okae H, Toh H, Sato T, Hiura H, Takahashi S, Shirane K, et al. Derivation of Human Trophoblast Stem Cells. Cell Stem Cell. 2018 Jan;22(1):50-63.e6.

113. James JL, Hurley DG, Gamage TKJB, Zhang T, Vather R, Pantham P, et al. Isolation and characterisation of a novel trophoblast side-population from first trimester placentae. REPRODUCTION. 2015 Nov;150(5):449–62.

114. Sun C, Chamley LW, James JL. Organoid generation from trophoblast stem cells highlights distinct roles for cytotrophoblasts and stem cells in organoid formation and expansion. Placenta. 2024 Dec;S0143400424007914.

115. Sheridan MA, Zhao X, Fernando RC, Gardner L, Perez-Garcia V, Li Q, et al. Characterization of primary models of human trophoblast. Development. 2021 Nov 1;148(21):dev199749.

116. Oeller M, Laner-Plamberger S, Krisch L, Rohde E, Strunk D, Schallmoser K. Human Platelet Lysate for Good Manufacturing Practice-Compliant Cell Production. Int J Mol Sci. 2021 May 13;22(10):5178.

117. Zarà M, Vismara M, Dona GD, Trivigno SMG, Amadio P, Sandrini L, et al. The Impact of Platelet Isolation Protocol on the Release of Extracellular Vesicles. Front Biosci-Landmark. 2022 May 18;27(5):161.

The following tools were used to optimize the language of the text:

DeepL Write, DeepL SE, 2024/2025 https://www.deepl.com/en/write
DeepL Translator, DeepL SE, 2024/2025, https://www.deepl.com/en/translator

Figures were partly created with BioRender.com:

2024 BioRender, 2024/2025, https://www.biorender.com

RBMO

ELSEVIER

ARTICLE

Platelet-derived factors dysregulate placental sphingosine-1-phosphate receptor 2 in human trophoblasts

BIOGRAPHY

Freya Lyssy is a PhD candidate of the Division of Cell Biology, Histology and Embryology at the Medical University of Graz, Austria. Her research focus mainly deals with the role of maternal platelet-derived factors in early human placenta development.

Freya Lyssy[1], Jacqueline Guettler[1,*], Beatrice A Brugger[1], Christina Stern[2], Désirée Forstner[1], Olivia Nonn[1,3,4,5], Cornelius Fischer[5,6], Florian Herse[3], Stefan Wernitznig[1], Birgit Hirschmugl[2], Christian Wadsack[2], Martin Gauster[1]

KEY MESSAGE

The placental S1P receptor subtypes are differentially expressed across gestation and located on diverse cell types of the human placenta. Because platelets contain considerable amounts of S1P, the down-regulation of S1PR2 in response to platelet-derived factors may represent a negative feedback regulation to prevent exaggerated S1P signalling in villous trophoblasts.

ABSTRACT

Research question: Sphingosine-1-phosphate (S1P) is an essential and bioactive sphingolipid with various functions, which acts through five different G-protein-coupled receptors (S1PR1–5). What is the localization of S1PR1–S1PR3 in the human placenta and what is the effect of different flow rates, various oxygen concentrations and platelet-derived factors on the expression profile of S1PR in trophoblasts?

Design: Expression dynamics of placental S1PR1–S1PR3 were determined in human first trimester ($n = 10$), pre-term ($n = 9$) and term ($n = 10$) cases. Furthermore, the study investigated the expression of these receptors in different primary cell types isolated from human placenta, verified the findings with publicly available single-cell RNA-Seq data from first trimester and immunostaining of human first trimester and term placentas. The study also tested whether the placental S1PR subtypes are dysregulated in differentiated BeWo cells under different flow rates, different oxygen concentrations or in the presence of platelet-derived factors.

Results: Quantitative polymerase chain reaction revealed that *S1PR2* is the predominant placental S1PR in the first trimester and reduces towards term ($P < 0.0001$). *S1PR1* and *S1PR3* increased from first trimester towards term ($P < 0.0001$). S1PR1 was localized in endothelial cells, whereas S1PR2 and S1PR3 were predominantly found in villous trophoblasts. Furthermore, *S1PR2* was found to be significantly down-regulated in BeWo cells when co-incubated with platelet-derived factors ($P = 0.0055$).

Conclusion: This study suggests that the placental S1PR repertoire is differentially expressed across gestation. *S1PR2* expression in villous trophoblasts is negatively influenced by platelet-derived factors, which could contribute to down-regulation of placental S1PR2 over time of gestation as platelet presence and activation in the intervillous space increases from the middle of the first trimester onwards.

[1] Division of Cell Biology, Histology and Embryology, Gottfried Schatz Research Center, Medical University of Graz, Austria
[2] Department of Obstetrics and Gynaecology, Medical University of Graz, Austria
[3] Charité-Universitätsmedizin Berlin, Corporate Member of Freie Universität Berlin and Humboldt-Universität zu Berlin, Berlin, Germany
[4] Experimental Clinical Research Centre, Max Delbrueck Center for Molecular Medicine in the Helmholtz Association and Charité Berlin, Germany
[5] Max-Delbrück-Center for Molecular Medicine in the Helmholtz Association (MDC), Berlin, Germany
[6] Institute for Medical Systems Biology (BIMSB), Berlin, Germany

KEYWORDS
Placenta
Platelet-derived factors
Pregnancy
Sphingosine-1-phosphate receptor

*Corresponding author. E-mail address: jacqueline.guettler@medunigraz.at (J. Guettler). https://doi.org/10.1016/j.rbmo.2023.04.006 1472-6483/
Declaration: The authors report no financial or commercial conflicts of interest.

INTRODUCTION

Sphingosine-1-phosphate (S1P) is an essential and bioactive sphingolipid associated with the regulation of various cellular functions such as differentiation, proliferation, apoptosis, cell motility and calcium signalling (*Bryan and Del Poeta, 2018*; *Maceyka* et al., *2012*). Moreover, S1P regulates vascular development during embryogenesis and has differential effects on motility, contraction, angiogenesis and vascular permeability, all of which are important to both maintenance and termination of pregnancy (*Spiegel and Milstien, 2003*; *Yamamoto* et al., *2010*). The structure of S1P consists of a polar head group, a phosphate group and a long-chain sphingoid base backbone, the sphingosine group (*Książek* et al., *2015*). It originates from phosphorylation of sphingosine by either sphingosine kinase 1 (SPHK1) or sphingosine kinase 2 (SPHK2). The concentration of S1P is controlled by two specific S1P phosphatases or an S1P lyase, which either remove the phosphate group or irreversibly degrade S1P (*Maceyka* et al., *2012*; *Tukijan* et al., *2018*). The major source of plasma S1P are red blood cells, vascular endothelial cells and activated platelets, making S1P a blood-borne lipid mediator, found in association with albumin and lipoproteins such as high-density lipoprotein (HDL) (*Patanapirunhakit* et al., *2021*). Although studies have shown that erythrocytes are the major source of S1P in blood plasma, platelets are also found to generate and store large quantities of S1P. Recent studies suggest that S1P is essential in thrombus formation due to its increased release during blood clot formation. The augmentation of S1P plasma concentrations by activated platelets is also assumed to play an important role in the repair of injured endothelial vessels (*Tukijan* et al., *2018*). S1P signalling is mediated by five different G-protein-coupled receptors (S1PR1–5), which were originally referred to as Edg for endothelial differentiation gene (S1PR1/Edg-1, S1PR2/Edg-5, S1PR3/Edg-3, S1PR4/Edg-6 and S1PR5/Edg-8) (*Kerage* et al., *2014*). The expression of these receptors is tissue- and cell type-specific. While S1PR1 is ubiquitously expressed, S1PR2 and S1PR3 are more restricted in expression and are mainly found in the gastrointestinal, vascular and central nervous systems. S1PR4 is prevailingly expressed in lymphoid tissues, whereas S1PR5 is primarily found in the nervous system (*Takabe* et al., *2008*).

Various cell types express different combinations of these receptors and the distribution of the receptors on different cell types and the coupling of receptors to different G-subunits allows S1P to influence numerous pathways in different ways. Because the commercial availability of antibodies for S1PR4 and S1PR5 is limited and their expression has been reported to be restricted to lymphoid tissue and the central nervous system, the main focus in this study was on S1PR1–3 (*Obinata and Hla, 2019*).

In fact, S1P signalling is increasingly becoming the focus of pregnancy research (see *Fakhr* et al., *2021*, for a comprehensive review). Its functions have an impact on female reproductive organs before and during pregnancy, including progesterone production in the corpus luteum, differentiation of the endometrium (i.e. decidualization) and placenta development. In human pregnancy, trophoblast invasion into the maternal decidua, as well as fusion of mononucleated cytotrophoblasts into the multinucleated syncytiotrophoblast, are mandatory steps in placentation, both of which are described to be regulated by S1P. Moreover, S1P is suggested to regulate vascular function and immune cell trafficking at the maternal–fetal interface and to play a powerful role in establishing an adequate uteroplacental microvasculature and development of immune tolerance of the mother towards the fetus (*Nagamatsu* et al., *2014*). However, an increasing body of evidence suggests that S1P signalling pathways are dysregulated in pregnancy pathologies such as pre-eclampsia and intrauterine growth restriction (IUGR). Accordingly, circulating S1P plasma concentrations were significantly higher in women diagnosed with pre-eclampsia when compared with controls (*Charkiewicz* et al., *2017*). Besides, placental S1P receptor subtypes are dysregulated in placental tissues from pregnancies complicated by severe pre-eclampsia (*Dobierzewska* et al., *2016*; *Li* et al., *2014*). Both aberrant trophoblast differentiation and turbulent blood flow (high-velocity jets and vortices), combined with elevated blood pressure in the intervillous space and increased wall shear stress at the villous syncytiotrophoblast surface, are suggested to be involved in the pathophysiology of pre-eclampsia (*Drewlo* et al., *2020*; *Roth* et al., *2017*). Notably, shear stress has been shown to induce S1PR1 expression in endothelial cells (*Aoki* et al., *2007*; *Josipovic* et al., *2018*), tempting speculation on the impact of onset of uteroplacental blood perfusion on placental S1P receptor subtype expression.

The aim of the present study was to analyse the expression dynamics of placental S1PR across different stages of gestation and to determine their expression in various placental cell types. Because platelets might be the first amongst maternal blood cells able to enter the early intervillous space through interstices of extravillous trophoblast columns (*Guettler* et al., *2021*; *Sato* et al., *2005*), this study investigated whether or not the S1PR subtype repertoire is dysregulated in human trophoblasts in response to platelet-derived factors. Also tested was whether onset of uteroplacental perfusion with maternal blood could affect the placental S1PR repertoire by analysing the receptor expression in regard to different flow rates and oxygen concentrations.

MATERIALS AND METHODS

Human placental tissue samples

The study was approved by the ethical committee of the Medical University of Graz (31-019 ex 18/19, approved 2 December 2022). First trimester placental tissues (n = 10) were obtained with written informed consent from women undergoing legal elective surgical pregnancy terminations between weeks 6 and 12 of gestation. Pre-term (n = 9) and term (n = 10) placental tissue was collected with written informed consent. Pre-term placental tissues were obtained mostly by Caesarean section because of placenta praevia with or without velamentous insertion of the cord and vaginal bleeding or cervical insufficiency from women who had no clinical evidence of infection. Villous tissue from all placentas was fixed in formalin and embedded in paraffin. Furthermore, additional tissue pieces were thoroughly rinsed in phosphate-buffered saline and dissected into small pieces of approximately 5 × 5 mm, before they were snap-frozen in liquid nitrogen and stored at −80°C until further analyses. Characteristics of the study population are shown in TABLE 1.

Culture of BeWo cell line

Trophoblast cell line BeWo was purchased from the European Collection of Cell Cultures (ECACC) and was cultured in DMEM/F12 (1:1, Gibco™, Life Technologies, Paisley, UK) supplemented

TABLE 1 CHARACTERISTICS OF THE STUDY GROUP

Characteristic	First trimester (*n* = 10)	Pre-term (*n* = 9)	Term (*n* = 10)	*P*-value
Maternal age (years)	31.4 (8.7)	34.8 (2.5)	32.0 (2.9)	NS[a]
Maternal BMI (kg/m^2)	24.1 (6.7)	23.8 (4.4)	22.8 (2.8)	NS[a]
Gestational age (days)	53.9 (6.9)	244.7 (6.1)	276.0 (3.4)	<0.0001[b]
Fetal weight (g)	–	2401 (338.3)	3604 (362.3)	<0.0001[b]
Placental weight (g)	–	510.0 (110.5)	633.9 (129.3)	0.0471[b]
Delivery mode (spontaneous/section)	–	1/8	5/5	–
Fetal sex (male/female)	6/4	8/1	6/4	–

Data are presented as mean (SD) or number.

[a] Differences between all groups were calculated using one-way ANOVA, with post-hoc differences by Tukey's multiple comparison test. (Maternal age: first trimester versus pre-term $P = 0.4027$, first trimester versus term $P = 0.9727$, pre-term versus term $P = 0.5107$; BMI: first trimester versus pre-term $P = 0.9845$, first trimester versus term $P = 0.8143$, pre-term versus term $P = 0.9042$)

[b] Differences pre-term versus term were assessed using the unpaired Student's *t*-test.

ANOVA = analysis of variance; BMI = body mass index; NS = not significant.

with 10% FCS (Gibco), 0.1 U/ml penicillin and 0.1 μg/ml streptomycin (Gibco) and 1% (v/v) L-glutamine (Gibco; 200 mmol/l 100X) in a humidified atmosphere of 5% CO_2 at 37°C (*Forstner et al., 2020*). Cells between passage 10 and 20 were used for in-vitro experiments. For differentiation, 2×10^5 cells per well were plated in 12-well dishes (Nunc^{TM} Lab-Tek^{TM}, Thermo Scientific, NY, USA) 1 day prior to the start of the experiment in the above-described culture medium. Next day, culture medium was exchanged with medium including 20 μmol/l forskolin (Bio-Techne, Tocris, Abingdon, UK) and cells were incubated for another 48 h. Dimethylsulphoxide (DMSO) served as solvent control for forskolin and was applied at a final concentration of 0.1% (v/v). Thereafter, cells were incubated under hypoxic conditions with 5% CO_2 and either 2.5%, 12% or 21% O_2 concentrations at 37°C for 24 h in a hypoxic workstation (BioSpherix; Redfield, NY, USA). After culture, cell lysates and supernatants were collected for further analysis.

Fluidic flow culture of BeWo cells

BeWo cells were seeded on coverslips in a 12-well dish (Nunc Lab-Tek, Thermo Scientific) with a density of 2×10^5 cells per well in DMEM/F-12 (1:1, Gibco) 1 day prior to the start of the experiment. Next day, cells were treated with forskolin (Bio-Techne, Tocris) with a final concentration of 20 μmol/l for 48 h. Thereafter, cells on coverslips were transferred to flow chambers (Kirkstall; QV500), which were connected to a tubing system (Kirkstall; $2 \times 1/16'$ diameter 22 cm length, $1 \times 3/32'$ diameter 22 cm length) and a 30 ml reservoir bottle. The flow system was placed in a TEB500 flow bioreactor (Ebers Medical Technology, Zaragoza, Spain). Each flow cycle included two chambers, which were perfused with 12 ml fresh media from the reservoir. Pumps were set to a perfusion rate of 1 ml/min and 3 ml/min and culture conditions were set to 2.5% O_2 and 5% CO_2 at 37°C for an experiment duration of 24 h. For static controls, forskolin-differentiated BeWo cells, grown on coverslips, were transferred to 6-well dishes (Nunc Lab-Tek, Thermo Scientific) containing 6 ml fresh culture media. Static controls were cultured in parallel to flow cultures in the TEB500 flow bioreactor. The experiments were performed four times with different cell passages.

Co-incubation of platelet-derived factors with BeWo cells

BeWo cells were seeded in a 12-well dish (Nunc Lab-Tek, Thermo Scientific) with a density of 2×10^5 cells per well in DMEM/F-12 (1:1, Gibco) 1 day prior to the start of the experimental. Next day, cells were treated with forskolin (Bio-Techne; Tocris) to undergo differentiation into multinucleated syncytia at a final concentration of 20 μmol/l for 48 h. After differentiation three different treatments were started for 24 h. For treatment with platelet-derived factors, platelets were first isolated from whole blood of pregnant donors (see Platelet isolation below); 2.25×10^5 to 3.13×10^5 platelets per μl in a total of 500 μl were transferred into a polycarbonate cell culture insert (Nunc Lab-Tek, Thermo Scientific) located above the well containing the differentiated BeWo cells. The insert prevented direct cell contact of platelets and trophoblasts, as platelets also express the S1P receptors and therefore the results would have been compromised by direct contact. Platelets in the insert were activated with 1 IU/ml thrombin directly administered into the culture medium. Control cells cultured in transwell dishes were subjected to either control medium DMEM/F-12, or control medium supplemented with 1 IU/ml thrombin (Sigma-Aldrich, St. Louis, MO, USA). After 24 h culture, cell lysates and supernatants were collected for further analysis.

Isolation of placental primary cells

Primary endothelial cells were isolated from term placentas of healthy pregnancies as previously described by *Lang et al. (2008)*. In brief, arterial and venous chorionic blood vessels were resected and washed with HBSS (Gibco). Arterial endothelial cells (ECA) and venous endothelial cells (ECV) were isolated by separate perfusion of chorionic arteries and veins with collagenase/dispase (0.1/0.8 U/ml, Roche, Vienna, Austria) dissolved in HBSS, pre-warmed to 37°C. The obtained cell suspension was centrifuged and the cell pellet was resuspended in EGM-MV medium (Lonza, Verviers, Belgium) and plated on culture plates. ECA were incubated at 37°C with 12% O_2 and 5% CO_2. ECV were incubated at 37°C, 21% O_2 and 5% CO_2.

Primary trophoblasts were isolated from term placentas of healthy pregnancies as previously described by *Loegl et al. (2017)*. In brief, placental villous tissue was minced and digested with trypsin/dispase/DNase (Gibco/Roche/Sigma) solution for 90 min. Cell suspension was centrifuged on a Percoll gradient (Sigma) at 4°C for 30 min at 300*g*. Trophoblast-enriched layers were

purified by immunodepletion of contaminating cells using beads conjugated to MCA-81 antibody (Serotec, Puchheim, Germany) against HLA-A, B and C. Trophoblasts were then seeded in each well of a 6-well plate (Nunc Lab-Tek, Thermo Scientific) in 2 ml DMEM (Gibco) containing 10% FCS (Gibco), 0.1 U/ml penicillin and 0.1 μg/ml streptomycin (Gibco) at 37°C and 21% O_2 and 5% CO_2.

Platelet isolation

Citrated whole blood (5 × 3.5 ml VACUETTE® tubes per patient) was collected from healthy term donors before Caesarean section. Donors signed written informed consents. Blood samples were centrifuged at 100*g* for 15 min at room temperature. Afterwards, platelet-rich plasma (PRP) was gently mixed in equal amount with a wash buffer consisting of distilled water with 128 mmol/l NaCl (Supelco®, Merck, Darmstadt, Germany), 11 mmol/l glucose (Sigma), 7.5 mmol/l Na_2HPO_4 (Merck), 4.8 mmol/l sodium citrate (Sigma-Aldrich), 4.3 mmol/l NaH_2PO_4 (Lactan, Graz, Austria), 2.4 mmol/l citric acid (Merck) and 0.35% bovine serum albumin (Biowest, Nuaillé, France) with addition of 2.5 ng/μl prostaglandin (Cayman Chemical Company, Ann Arbor, MI, USA). After centrifugation at 1962*g* for 15 min at room temperature, the pellet was resuspended in 10 ml wash buffer and centrifuged again at 1962*g* for 15 min at room temperature. After centrifugation, platelets were resuspended in DMEM/F12 (1:1, Gibco) supplemented with 0.1 U/ml penicillin and 0.1 μg/ml streptomycin (Gibco) and 1% (v/v) L-glutamine (Gibco; 20 mmol/l 100X) to physiological platelet concentrations. Platelet number was determined using a Sysmex KX-21NTM (Sysmex, Horgen, Switzerland).

qPCR analysis

Total RNA from cell lysates and placental tissue was isolated with an ExtractMe Total RNA Kit (Blirt, Gdansk, Poland) according to the manufacturer's protocol. Quality check and amount calculation by NanoDrop (ND-1000, Peqlab Biotechnology GmbH, Erlangen, Germany) was followed by reverse transcription of 1 μg total RNA per reaction using a High-Capacity cDNA Reverse Transcription Kit (Applied Biosystems, Foster City, CA, USA) according to the manufacturer's manual. qPCR was performed with SYBR Green (Biozym, Vienna, Austria) using the Bio-Rad CFX384 Touch Real-Time PCR Detection System (Bio-Rad, Hercules, CA, USA) with the specific primers shown in Supplementary Table 1. Cq values were automatically determined using single thresholds and normalized expression (ΔΔCq analysis, all primers confirmed to have equivalent amplification efficiencies), automatically generated by Bio-Rad CFX Manager 3.1 software. The expression of *GAPDH* or *TBP* was used as reference.

Immunoblotting

Placental primary cells were washed with HBSS and homogenized in RIPA Buffer (Sigma-Aldrich) supplemented with cOmplete™ Mini protease inhibitor (Roche, Mannheim, Germany). Total protein concentration was determined using the Lowry method; 20 μg of total protein were loaded on precast 10% Bis-Tris gel (NuPAGE™, Novex, Life Technologies). Proteins were blotted on a 0.45 μm nitrocellulose membrane (Hybond, Amersham Biosciences, GE Healthcare Life Sciences, Little Chalfont, UK) and blotting efficiency was determined with Ponceau staining (Ponceau S solution, Sigma-Aldrich). Primary antibodies were diluted as described in Supplementary Table 2 and incubated on membranes overnight at 4°C. HRP-conjugated goat anti-mouse and goat anti-rabbit IgG (1:5000, Bio-Rad) were used as secondary antibodies and incubated on membranes for 2 h at room temperature. Immunodetection was performed with a chemiluminescent immunodetection kit (WesternBright Chemilumineszenz Substrat für Film, Biozym) according to the manufacturer's instructions. Images were acquired with an iBright CL 1000 Imaging System (Thermo Fisher Scientific) and band densities were analysed with Image Studio Lite 5.2. Results are presented as a ratio of band densities of target protein and reference protein beta-actin.

Immunohistochemistry

Human formalin-fixed paraffin-embedded (FFPE) first trimester and term placenta tissues were cut into 5 μm slices and mounted on Superfrost Plus slides (Thermo Fisher Scientific). After undergoing standard deparaffinization, sections were subjected to an antigen retrieval in Epitope Retrieval Solution pH 9.0 (Novocostra, Leica) or citrate buffer pH 6.0 for two times 20 min at 150 W in a laboratory microwave (Miele, Guetersloh, Germany). Immunohistochemistry was performed with primary antibodies and IgG-negative controls as indicated in Supplementary Table 2 using the UltraVision Large Volume Detection System HRP Polymer Kit (Thermo Fisher Scientific) as previously described (*Blaschitz* et al., *2015*; *Siwetz* et al., *2015*). The slides were covered with Kaiser's Glycerin Gelatine (Merck) and a cover slip. The negative control for CD42b has previously been verified in *Guettler* et al. *(2021)* Supplementary Figure 1b (CD42b) and 1 h (neg ctrl rabbit)) in FFPE human platelets. Images were obtained with an Olympus microscope (BX3-CBH).

Immunofluorescence staining

For immunofluorescence double staining, sections were deparaffinized and subjected to the appropriate antigen retrieval (Supplementary Table 2). Afterwards, slides were blocked with Ultra V (Thermo Fisher Scientific) for 10 min at room temperature. Primary antibodies and IgG-negative controls were diluted in antibody diluent (Dako) (Supplementary Table 2) and added to the slides for 45 min at room temperature. Slides were washed three times in PBS. Secondary fluorescence-labelled antibodies (Supplementary Table 2) were diluted 1:200 in PBS and slides were incubated for 30 min at room temperature. After washing three times with PBS, DAPI was diluted 1:2000 in PBS and incubated on the slides for 5 min. Slides were washed again three times with PBS, left to dry and mounted with ProLong Gold Antifade reagent (Invitrogen). Images were obtained with an Olympus VS200 Slide Scanner.

Analysis of single-cell RNA sequencing data

Single-cell data from first trimester placenta were obtained from *Vento-Tormo* et al. *(2018)* and procedures for analysing the data were previously described therein. In brief, cells extracted from tissue were counted with a Neubauer haemocytometer and loaded in a 10x-Genomic Chromium to profile gene expression before libraries were sequenced on an Illumina HiSeq 4000. Only cells with more than 300 detected genes and less than 20% total mitochondrial gene expression were used for further analysis (*Vento-Tormo* et al., *2018*). Further bioinformatical analysis was done using R package Seurat (*Butler* et al., *2018*) and RStudio to visualize gene expression data in a dot plot.

Transmission electron microscopy

The membrane was cut from the insert after termination of the cell culture

experiment and transferred into 2% paraformaldehyde (Diapath S.P.A., Martinengo BG, Italy) and 2.5% glutaraldehyde (Electron Microscopy Sciences, Hartfield, USA) in 0.1 mol/l dimethyl arsenic acid sodium buffer (cacodylate buffer) pH 7.4 for 30 min at room temperature. The sample was washed in 0.1 mol/l cacodylate buffer pH 7.4 twice for 15 min at room temperature and afterwards it was post fixed with 2% osmium tetroxide (Electron Microscopy Sciences) in 0.1 mol/l cacodylate buffer pH 7.4 for 30 min. After rinsing in 0.1 mol/l cacodylate buffer pH 7.4 the sample was stored in the buffer overnight at 4°C. The next day the membrane was dehydrated in a graded ethanol series (50–96%) for 15 min each and two times 100% ethanol for 7 min. The resin infiltration started with 2:1 100% EtOH/Polybed embedding resin (Polysciences, Inc., Warrington, PA, USA) for 45 min, followed by 1:1 100% EtOH/Polybed embedding resin for 45 min and afterwards 1:2 100% EtOH/Polybed embedding resin overnight at 4°C. The next day pure Polybed resin at room temperature for 90 min was followed by another step of pure Polybed resin but with 1.5% DMP30 for 120 min at 45°C. The sections were embedded in pure Polybed resin with 1.5% DMP30 in silicone forms and polymerized at 60°C for 3 days. For sectioning of semi-thin (500 nm) and ultra-thin (70 nm) sections, an ultra-microtome (Leica, Vienna, Austria) was used. Semi-thin sections were stained with 1% toluidine blue solution (Sigma-Aldrich) for an overview and to identify the region of interest (ROI). The block was trimmed to the ROI and ultra-thin sections were collected on 200-mesh copper grids. Grids were subjected to a staining protocol with lead citrate and platinum blue prior to electron microscope imaging (Ultra-stainer, Leica). Stained grids were examined by a Zeiss 900 TEM (Carl Zeiss Microscopy GmbH, Jena, Germany) operated at 80 kV.

Statistical analysis

All data were analysed using GraphPad Prism Version 9.0.0 and are presented as mean with SD or SEM as stated in figure legends. Standard normality was tested by performing the Shapiro–Wilk test and significance was tested with one-way analysis of variance followed by Tukey's multiple comparison test in order to compare groups with one another. Student's *t*-test was used when only two groups were compared.

RESULTS

S1PR2 is the predominant placental S1PR in the first trimester and declines significantly towards term

In order to determine temporal expression of placental S1PR across different stages of human pregnancy, placental tissues from healthy women undergoing either elective termination of pregnancy during first trimester or delivery at pre-term and term were subjected to quantitative gene expression analysis for S1PR subtypes. There were no differences between subjects in terms of maternal age and body mass index; significant differences were seen between pre-term and term cases in gestational age ($P < 0.0001$), fetal weight ($P < 0.0001$) and placental weight ($P = 0.0471$) (TABLE 1). Analysis of *S1PR* in human first trimester placental tissue revealed *S1PR2* as the predominant *S1PR*, which was expressed approximately two-fold higher than *S1PR1* and *S1PR3* ($P = 0.0039$) (FIGURE 1A). Comparison of the placental *S1PR* expression between first trimester samples and pre-term (FIGURE 1B) and term cases (FIGURE 1C) showed a substantial change in the expression pattern over time of gestation. While the expression levels of *S1PR1* (FIGURE 1D) and *S1PR3* (FIGURE 1F) strongly increased by about 20- to 30-fold towards term ($P < 0.0001$ first trimester versus term, both *S1PR1* and *S1PR3*), placental *S1PR2* expression significantly declined in pre-term and almost vanished at term, when compared with first trimester ($P < 0.0001$) (FIGURE 1E).

S1PR are differentially expressed across different placental cell types

Immunohistochemical staining of first trimester as well as term placental tissue showed that S1PR1 expression was restricted to endothelial cells (FIGURE 2A and 2D), while S1PR2 and S1PR3 were predominantly found in the syncytiotrophoblast and cytotrophoblasts (FIGURE 2B, 2C, 2E, 2F). Negative controls using rabbit IgG revealed no staining on term placenta for both antigen retrieval protocols (FIGURE 2G and 2H).

Analysis of publicly available scRNA-Seq data from human first trimester placenta (*Vento-Tormo* et al., *2018*) provided an insight into placental S1PR expression on a single-cell level. A dot plot of single-cell transcriptomes from first trimester placenta samples showed considerable *S1PR2* expression in the syncytiotrophoblast and the villous cytotrophoblast populations, in concordance with the immunohistochemical findings. Moreover, *S1PR2* was expressed in fibroblasts and a small proportion of extravillous trophoblasts. scRNA-Seq data for *S1PR1* confirmed localization of the receptor in fetal–placental endothelial cells, while *S1PR3* was detected mainly in placental fibroblasts, decidual stroma cells and to some extent in villous cytotrophoblasts and decidual natural killer cells (FIGURE 2I).

Double immunofluorescence staining confirmed the expression of S1PR2 in villous syncytiotrophoblast, but did not show its expression on extravillous trophoblasts (FIGURE 2J). Moreover, S1PR2 was expressed on the outer layer of the decidual epithelium (FIGURE 2K). S1PR3 gave immunofluorescence signals in the cytotrophoblast layer and in the proximal parts of the trophoblast cell columns right before these cells developed their extravillous character and started invading into the maternal decidua (FIGURE 2V). A strong staining of S1PR3 was also observed in decidual stroma cells (FIGURE 2M). Immunofluorescence negative controls using rabbit and mouse IgG revealed no staining on first trimester placenta (FIGURE 2N and 2O).

Next, mRNA as well as protein expression levels of the three receptors in primary placental endothelial cells and trophoblasts were analysed (FIGURE 3). *S1PR1* was significantly higher expressed in arterial as well as venous endothelial cells compared with primary trophoblasts ($P < 0.0001$) (FIGURE 3A–C). In contrast, *S1PR2* expression was significantly increased in primary trophoblast cells compared with endothelial cells ($P = 0.0262$) (FIGURE 3D–F). S1PR3 showed somewhat adverse expression levels between qPCR, where it was expressed in all three cell types, and immunoblotting, where it was present in trophoblast cells and to some extent in endothelial cells, especially venous endothelial cells ($P = 0.0182$, $P = 0.0064$, respectively) (FIGURE 3G–I).

S1PR2 and S1PR3 are dysregulated by platelet-derived factors

The next aim was to determine potential effects of fluidic flow on S1PR expression in differentiated BeWo cells, mimicking placental syncytiotrophoblasts exposed to maternal blood flow. For this purpose, BeWo cells were first stimulated with forskolin to undergo differentiation and syncytialization, and were afterwards

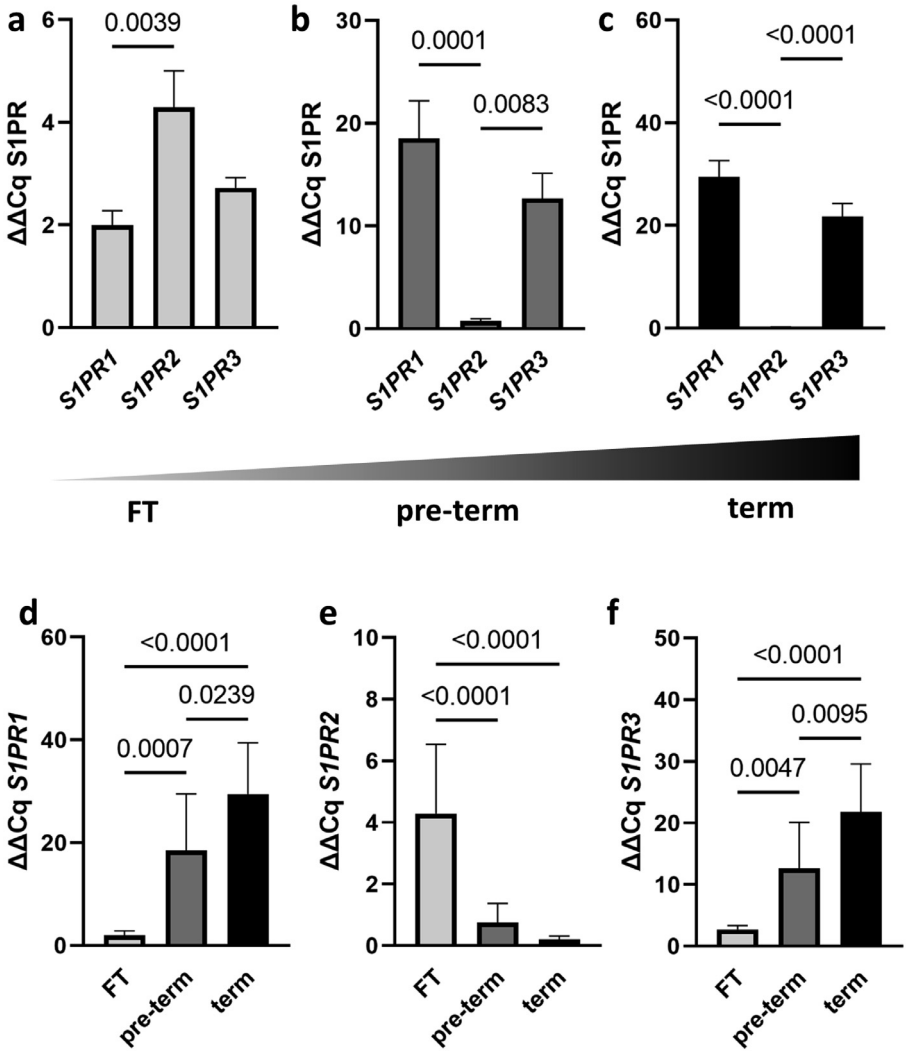

FIGURE 1 Differential placental S1PR expression across human gestation. Human placental tissue was subjected to qPCR analysis of three different S1PR subtypes (*S1PR1*–*S1PR3*) in first trimester (a, $n = 10$), pre-term (b, $n = 9$) and term (c, $n = 10$) samples. Expression levels of *S1PR1* (d), *S1PR2* (e) and *S1PR3* (f) were compared between first trimester, pre-term and term cases using one-way ANOVA. Data are presented as mean ΔΔCq ± SEM, with *GAPDH/TBP* used as reference. ANOVA = analysis of variance; FT = first trimester; qPCR = quantitative polymerase chain reaction.

cultured under fluidic flow. qPCR analysis showed no influence on the expression level of *S1PR2* and *S1PR3* in response to flow rates of 1 ml/min and 3 ml/min, respectively (FIGURE 4A and 4B).

To determine whether the physiological rise in intervillous oxygen tension during the course of pregnancy may cause the observed longitudinal expression changes of placental S1P receptors, the next test was whether different in-vitro oxygen concentrations can affect *S1PR* in differentiated BeWo cells. During the first trimester oxygen concentrations range between 2 and 3% in the intervillous space and increase during the ongoing development to about 8–10% during the second trimester. In order to determine oxygen effects, a rather broad range was tested, including 2.5% O_2 during the first trimester, 12% O_2 to mirror the rise in oxygen concentration and lastly 21% O_2 as a control to depict an atmospheric state. *S1PR2* did not show significant differences in expression at 2.5%, 12% and 21% oxygen (FIGURE 4**c**); *S1PR3* on the other hand showed no significant change from 2.5% to 12% O_2 but from there a significant decrease when cultured under 21% O_2 ($P = 0.0240$) (FIGURE 4D).

As platelets are the first maternal blood cells that establish contact to fetal-derived trophoblast cells, the effect of co-incubation of platelets and trophoblast cells was examined. As platelets express various S1P receptors (Supplementary Figure 1), experiments with direct co-incubation of platelets and trophoblast cells would be difficult to analyse because expression of the cellular origin of a certain receptor cannot be verified. To exclude this possibility, co-incubation experiments were conducted with an insert to keep the trophoblast samples free of platelet RNA (FIGURE 4E–G). However, the platelet-derived factors may well diffuse through the 0.4 μm membrane of the insert and act on underlying BeWo cells. qPCR analysis after co-cultures revealed that *S1PR2* was significantly down-regulated in BeWo cells upon treatment with platelet-derived factors when compared with controls ($P = 0.0055$) (FIGURE 4H). It is worth noting that thrombin itself, used as an agonist to activate platelets, had an impact on the *S1PR2* expression level ($P = 0.0461$). Contrary effects, although not significant, could be seen in the expression of *S1PR3*,

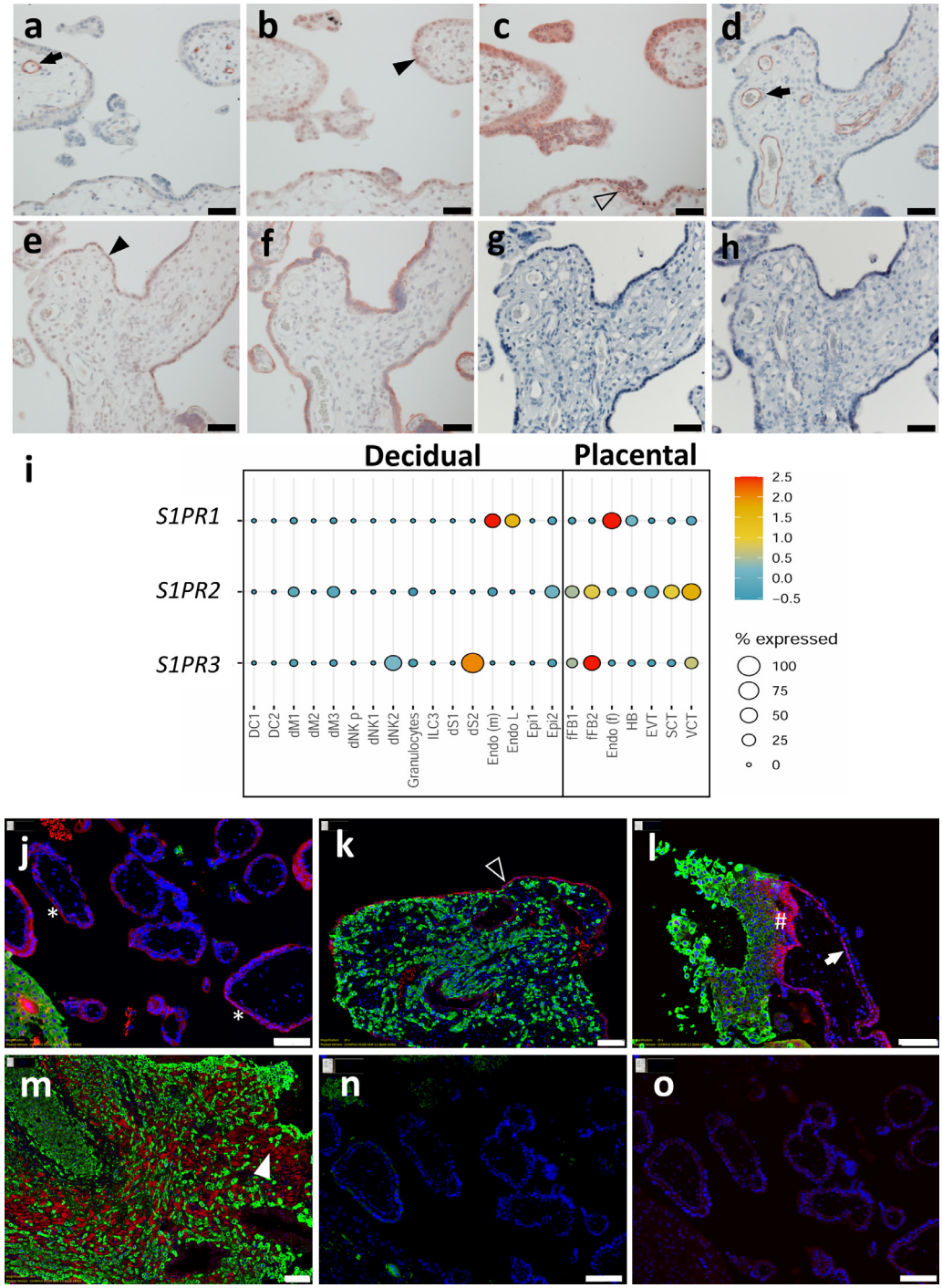

FIGURE 2 Differential expression of S1PR1, S1PR2 and S1PR3 across different cell types of the human placenta. First trimester placenta (a–c) and term placenta (d–f) were stained for antibodies S1PR1 (a and d), S1PR2 (b and e) and S1PR3 (c and f). Fetal–placental endothelial cells: black arrow, cytotrophoblast: open arrowhead, syncytiotrophoblast: black arrowhead. Negative controls rabbit IgG in term placenta for both antigen retrieval protocols (pH6 in g and pH9 in h). Scale bars represent 50 μm. Single-cell RNA-Seq expression levels of S1P receptor subtypes (i). Published data for first trimester placenta from *Vento-Tormo* et al. *(2018)* were analysed. Intensity and colour scale (raw counts) show the gene expression level and dot circumference shows % of cells within a cell type group expressing a gene. DC = dendritic cells; dM = decidual macrophages; dNK = decidual natural killer cells; dS = decidual stromal cells; Endo = endothelial cells; Epi = epithelial glandular cells; EVT = extravillous trophoblast; f = fetal; FB = fibroblasts; HB = Hofbauer cells; ILC = innate lymphocyte cells; L = lymphatic; m = maternal; p = proliferative; SCT = syncytiotrophoblast; VCT = villous cytotrophoblast. First trimester placentas were stained with immunofluorescence double staining for HLA-G (j–m) (FITC – green) and S1PR2 (j and k) or S1PR3 (l and m) (Cy3 – red). Villous syncytiotrophoblast (*), lining at the decidual border (white open arrowhead), cytotrophoblasts (white arrow), the first proximal parts of the trophoblast cell column (#), decidual stroma cells (white arrowhead). Negative control rabbit and mouse IgG on first trimester placenta (mouse IgG – FITC in n and rabbit IgG – Cy3 in o). Scale bars represent 100 μm.

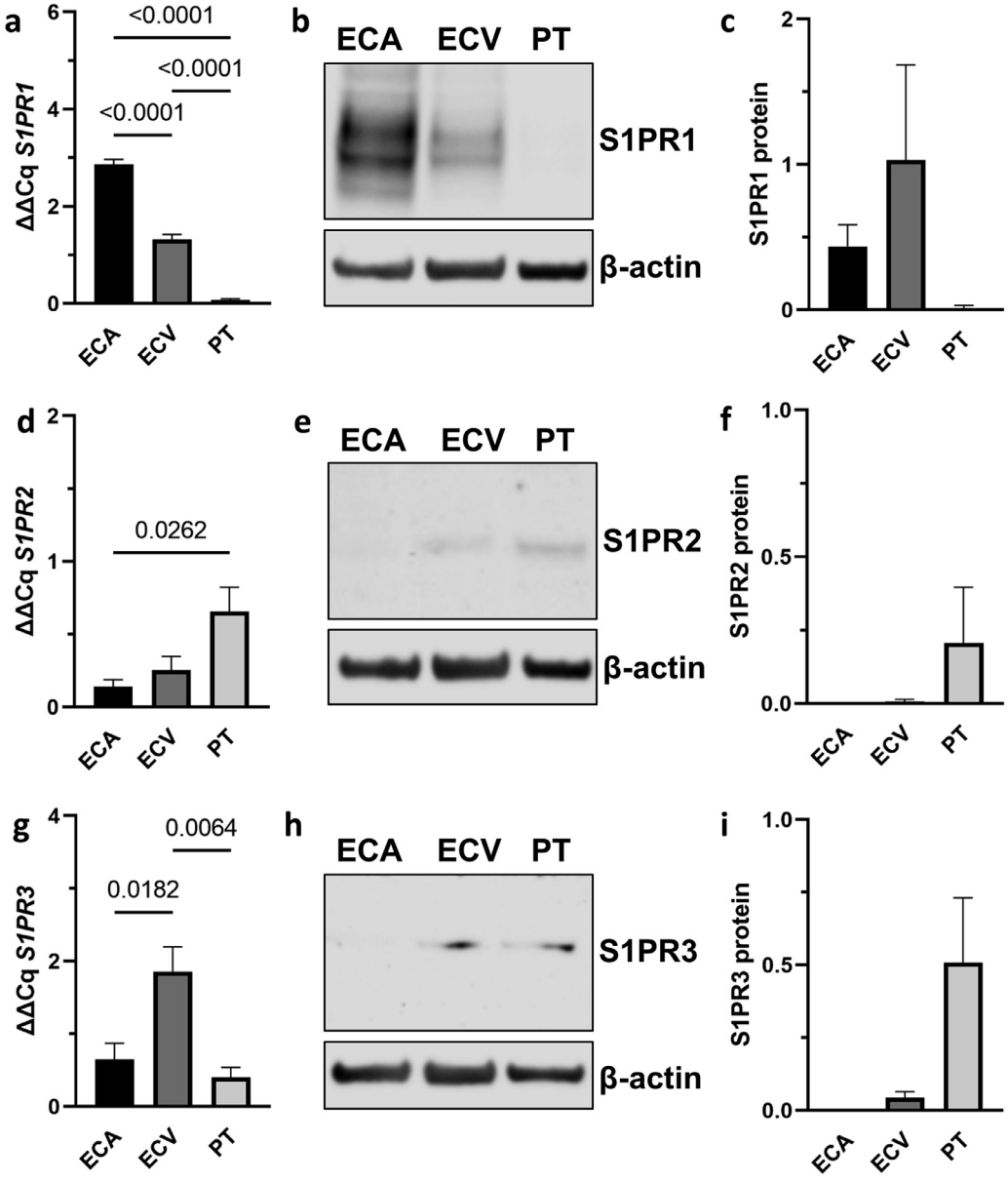

FIGURE 3 Differential expression of S1PR1, S1PR2 and S1PR3 across isolated primary cells of the human placenta. mRNA was investigated in arterial endothelial cells (ECA), venous endothelial cells (ECV) and primary trophoblasts (PT) ($n = 4$ each group) for *S1PR1* (a), *S1PR2* (d), *S1PR3* (g) and protein expression ($n = 3$ each group) for S1PR1 (43 kDa) (b and c), S1PR2 (50–60 kDa) (e and f) and S1PR3 (42 kDa) (h and i). Data are presented as mean ± SEM. *GAPDH/TBP* was used as reference gene for quantitative polymerase chain reaction, and β-actin (42 kDa) as reference protein in densitometry analysis. Differences were assessed by one-way analysis of variance, with post-hoc differences by Tukey's multiple comparison test.

which increased in the presence of both thrombin alone and platelet-derived factors (FIGURE 4I).

DISCUSSION

This study demonstrates the spatiotemporal expression of different S1PR in the human placenta across gestation. While placental *S1PR* subtypes 1 and 3 increase with gestational age, *S1PR2* is predominantly expressed in the first trimester villous trophoblast compartment and sharply declines towards term. In human trophoblasts, S1P action is suggested to inhibit differentiation through G(i)-coupled S1P receptor interaction, leading to the inhibition of adenylate cyclase and reduced production of intracellular cAMP (*Johnstone* et al., *2005*; *Singh* et al., *2012*). However, whether or not this inhibitory effect is mediated through a particular S1PR, e.g. through the prevailing S1PR2 in first trimester placenta, still remains to be determined. Of note, S1P acts as a potent inhibitor of extravillous trophoblast migration, predominantly through S1PR2/Gα12/13 and Rho activation (*Westwood* et al., *2017*). Moreover, S1PR2 is involved in S1P-induced expression and secretion of IL6 in BeWo cells (*Goyal* et al., *2013*). Based on these previous and our own studies, it is tempting to speculate that the predominant S1PR2 expression in human first trimester placenta is involved in regulating trophoblast differentiation and migration/invasion processes, both essential for early placentation. Later on in

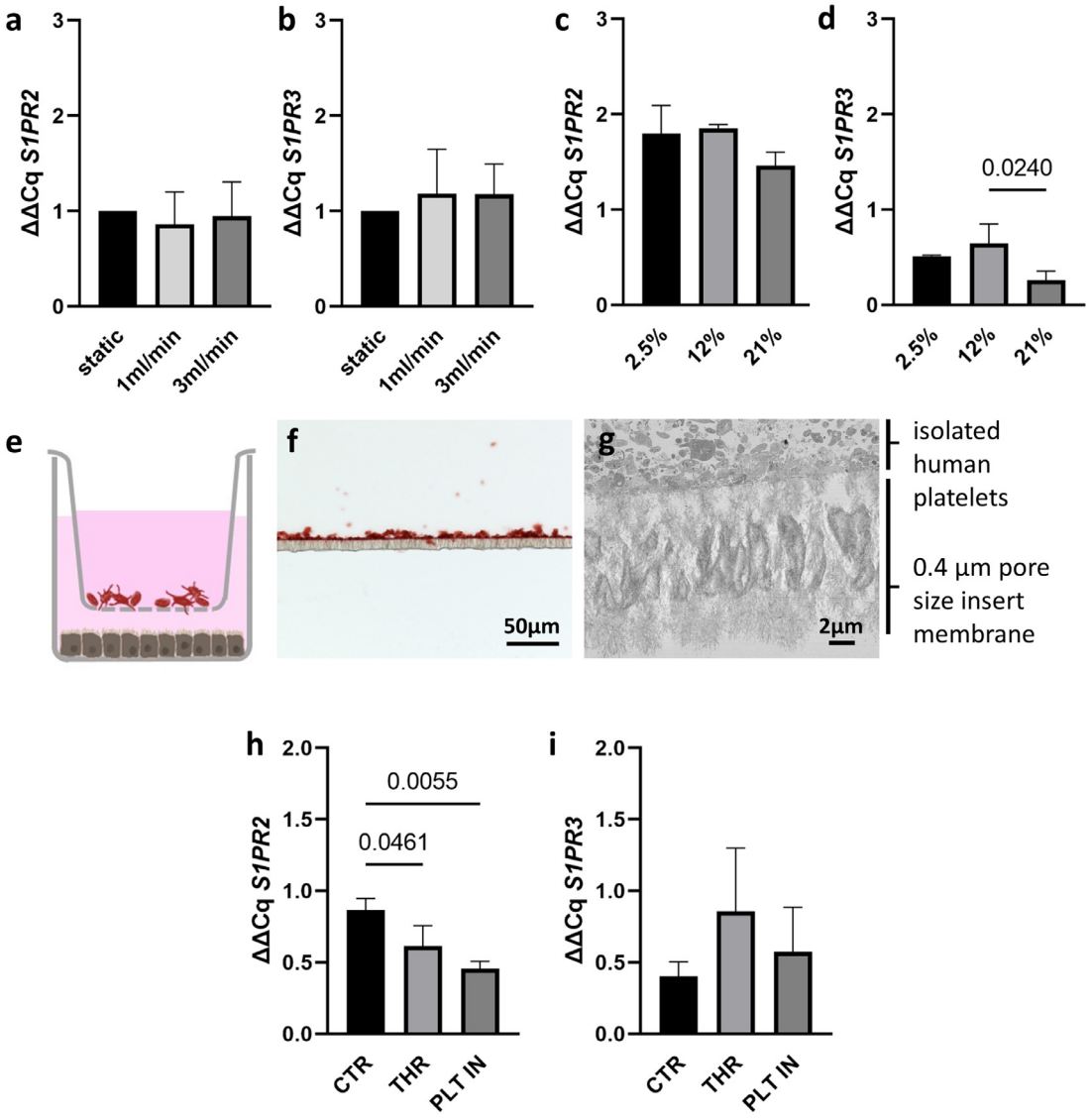

FIGURE 4 Effect of fluidic flow, different oxygen concentrations and platelet-derived factors on S1PR2 and S1PR3 expression in trophoblast cell line BeWo. BeWo cells were stimulated with forskolin (20 μmol/l) for 48 h to undergo differentiation under static conditions. Thereafter, cells were cultured under fluidic flow culture with indicated flow rates of 1 ml/min and 3 ml/min, respectively, for 24 h. Expression levels of *S1PR2* (a) and *S1PR3* (b) were compared with quantitative polymerase chain reaction (qPCR) between cells cultured under static control conditions and different flow rates (n = 4 independent experiments). After 48 h of differentiation, BeWo cells were cultured under three different oxygen concentrations (2.5%, 12% and 21% O_2) for 24 h. Expression levels of *S1PR2* (c) and *S1PR3* (d) were compared with qPCR between the different oxygen concentrations (n = 3 independent experiments). After 48 h of differentiation BeWo cells were co-incubated with freshly isolated human platelets from pregnant donors. 2.25 $\times$ 10^5 to 3.13 $\times$ 10^5 platelets per μl in a total of 500 μl were loaded into an insert and activated with thrombin (1 IU/ml). Released platelet cargo could penetrate through the 0.4 μm insert membrane to get in contact with the underlying layer of trophoblast cells (e). The insert membrane was embedded for immunohistochemistry after the experiment and stained for platelet marker CD42b (f) scale bar represents 50 μm. The membrane was also embedded for transmission electron microscopy to further visualize the membrane and the incubated platelets on one side of the membrane (g). Scale bar represents 2 μm. Expression of *S1PR2* (h) and *S1PR3* (i) were compared with qPCR between the control (CTR), thrombin control (THR) and platelet-derived factors (PLT IN) (n = 3 independent experiments). All data are presented as mean $\Delta\Delta$Cq $\pm$ SD, *GAPDH/TBP* was used as reference gene for qPCR and differences assessed by one-way analysis of variance with post-hoc differences by Tukey's multiple comparison test.

pregnancy, when the initial phase of rapid cell mass expansion and invasion is replaced by metabolic processes, expression of the placental S1PR repertoire may shift to meet these demands. Significantly reduced levels of *S1PR1* and *S1PR3* in non-severe as well as severe pre-eclampsia cases are suggested to be responsible for impaired vasculogenesis/angiogenesis observed during this syndrome (*Dobierzewska* et al., *2016*), and may be a sign for an insufficient shift in the placental S1PR repertoire.

This study confirms the expression of S1PR1 in endothelial cells, which is in agreement with previous studies showing the expression of this receptor subtype in the endothelium of various other organs (*Panetti, 2002*; *Wang* et al., *1999*) and to be strongly induced by shear stress in the vascular network of flow-positive regions (*Josipovic* et al., *2018*; *Jung* et al., *2012*). S1PR2 and S1PR3 were mainly found in

trophoblasts, which is in accordance with the speculations that these two receptor subtypes play a significant role in trophoblast development and remodelling of spiral arteries. This assumption is substantiated by recent studies highlighting the involvement of S1PR2 in trophoblast mobility (*Liao* et al., *2022*).

S1PR are increasingly acknowledged for their role as cellular mechanosensors that convert various physical signals, such as laminar and turbulent flow, into biochemical signals, coupling them with downstream signalling pathways (*Hu* et al., *2022*). In vascular endothelial cells, S1PR1 is described as one of the predominant mechanosensors, which is up-regulated by laminar shear stress itself, as shown in HUVEC cultured under laminar shear stress of 20 dyne/cm^2 (*Aoki* et al., *2007*; *Josipovic* et al., *2018*). During human gestation, uteroplacental blood flow is fully established with transition to the second trimester, causing fluid shear stress that is produced by haemodynamic forces across different trophoblast subtypes (*Brugger* et al., *2020*). Whether onset of maternal blood flow is triggering the observed (up) regulation of placental S1PR towards term remains speculative. Our data from flow culture experiments rather argue against this speculation, because neither *S1PR2* nor *S1PR3* were up-regulated in differentiated BeWo cells in response to fluid flow.

Low oxygen concentrations of about 2–3% in the early developing placenta are a special attribute described for the first couple of weeks during pregnancy, while with ongoing placentation and remodelling of the spiral arteries the oxygen concentration increases to about 8–10% (*Zhao* et al., *2021*). Previous studies have shown a significant up-regulation of SPHK1 under low oxygen tension, but a decrease in expression levels of receptors *S1PR2* and *S1PR3* in pre-eclamptic placentas (*Dobierzewska* et al., *2016*). Because this study found no significant difference in the expression level of *S1PR2* or *S1PR3* when cells were cultured under 2.5% or 12% oxygen, the tremendous difference in the expression pattern of the receptors from first trimester to term is most likely not due to the rise in oxygen concentrations over gestation. The controls incubated at atmospheric conditions (21% oxygen) showed a slight decrease in the expression level of *S1PR2* and even a significant difference in the expression of *S1PR3*, but it can be assumed that this condition is considered rather hyperoxic and therefore not physiologically present in the human placenta (*Burton* et al., *2021*).

During uncomplicated pregnancy, the count of maternal platelets decreases gradually over time of gestation, reaching an overall decrease of about 10% by the end of pregnancy (*Michelson* et al., *2019*). This decrease in platelet count can be explained mainly by haemodilution, and to some extent by accelerated sequestration and consumption of platelets in the utero-placental circulation. Increased mean platelet volume (MPV), as a measure of platelet activation, has been associated with inflammatory pregnancy pathologies, including pre-eclampsia and IUGR (*Guettler* et al., *2022*; *Moser* et al., *2019*). Before haemochorial placentation is fully established, extravillous trophoblasts form plugs within the lumen of spiral arteries to prevent maternal blood cells from entering the intervillous space. However, by the middle of the first trimester these trophoblast plugs become loosely cohesive, forming narrow capillary-shaped channels (*Roberts* et al., *2017*). We and others have found platelets within trophoblast columns and assume that they can enter the channels due to their small diameter of 2–3 μm (*Forstner* et al., *2020*; *Sato* et al., *2005*). Electron microscopy confirmed that these platelets are in an activated state, tempting speculation as to whether released factors can impact the expression of the S1P receptors (*Guettler* et al., *2021*). The extensive reports of the involvement of S1P in inflammatory processes and the fact that a link between a dysfunction in the sphingolipid signature and pre-eclampsia has been discussed before, makes it an obligation to investigate the dysregulation of the receptors upon contact with platelet-derived factors (*Del Gaudio* et al., *2020*; *Dobierzewska* et al., *2016*; *Spiegel and Milstien, 2011*). The approach of incubating platelets from pregnant women in cell culture inserts above trophoblasts without any direct contact provides a perfect model to study the effect of platelet-derived factors without having to deal with the bias that platelets themselves express S1PR.

The effect observed on *S1PR2* and *S1PR3* subtypes upon treatment with thrombin alone can be drawn back to the fact that thrombin is a versatile enzyme, thereby able to bind to numerous substrates and thus affecting the molecular basis of cells in many ways (*Davie and Kulman, 2006*). However, because the difference in expression of *S1PR2* upon treatment with platelet-derived factors is even higher compared with the difference seen with cells treated with thrombin alone, it can be argued that a considerable part of the effect is solely due to factors released from platelets. Interestingly, platelet-derived factors seem to have contrary effects on the expression levels of *S1PR2* and *S1PR3*. The significant down-regulation of *S1PR2* and the tendency of up-regulation of *S1PR3* demonstrated here could be speculated to be in concordance with the opening of the spiral arteries and the influx of maternal blood into the intervillous space at the end of the first trimester of pregnancy. Here, one could speculate that an earlier influx of maternal blood, and thus potential activation of maternal platelets and release of their cargo, would dysregulate the expression pattern of the S1PR too soon and therefore could take part in pregnancy complications with insufficient infiltration and migration of extravillous trophoblasts into the maternal decidua. Further research is necessary to evaluate the timeline of S1PR pattern change and the influence this could have on the developing human placenta. Although the underlying mechanisms of S1PR2 and S1PR3 dysregulation are not widely discussed in the literature, it has been shown that S1PR1 expression on the cell surface is in fact down-regulated by its activation of agonists, like small-molecule FTY720-P, HDL-S1P or albumin-S1P (*Cartier and Hla, 2019*). We suggest a very similar response of S1PR2 due to the fact that it is down-regulated upon excessive release of platelet cargo, which includes S1P.

The lack of data for placental S1PR subtypes 4 and 5 at various stages of pregnancy is a clear limitation of the current study, but may be justified by the fact that accurate detection of endogenous S1PR proteins is *per se* a challenge and specific antibodies have either been discontinued or simply were not available (*Talmont* et al., *2019*). However, comparative S1PR expression data from first trimester, pre-term and term placenta samples, and furthermore the use of platelets from pregnant women, can be considered a strength of this study. This is the first report on S1PR expression analysis in a trophoblast cell line cultured under fluidic flow in combination with low oxygen conditions. Moreover, to our knowledge this is the first paper to discuss the impact of platelet-derived factors on the expression pattern of the S1P receptors in the human trophoblast.

In summary, this study suggests that the placental S1PR repertoire is differently expressed across gestation. The trophoblastic S1PR expression pattern depends on differentiation status of the cells and may be dysregulated in response to platelet-derived factors, including S1P.

DATA AVAILABILITY

Data will be made available on request.

ACKNOWLEDGEMENTS

The authors gratefully acknowledge the excellent technical assistance of Lena Neuper, Christine Daxboeck, Bettina Amtmann and Manuela Stückler. The authors thank Dr Andreas Glasner for recruiting first trimester placental tissue samples for this study.

AUTHOR CONTRIBUTIONS

FL, JG and MG conceived and designed the study, analysed data and drafted the manuscript; FL, JG, BAB, DF, SW, CF and ON performed experiments and analysed data; CS and BH provided material and all authors revised the manuscript.

MG was supported by the Austrian Science Fund (FWF): P 35118, P 33554 and I 3304 and by the Medical University Graz through the PhD programme MolMed. Moreover, MG was supported by funds of the Oesterreichische Nationalbank (Austrian Central Bank, Anniversary Fund, project number: 18175).

SUPPLEMENTARY MATERIALS

Supplementary material associated with this article can be found in the online version at doi:10.1016/j.rbmo.2023.04.006.

REFERENCES

Aoki, S., Osada, M., Kaneko, M., Ozaki, Y., Yatomi, Y., 2007. Fluid shear stress enhances the sphingosine 1-phosphate responses in cell-cell interactions between platelets and endothelial cells. Biochem. Biophys. Res. Commun. 358, 1054–1057. https://doi.org/10.1016/j.bbrc.2007.05.028.

Blaschitz, A., Siwetz, M., Schlenke, P., Gauster, M., 2015. Adhering maternal platelets can contribute to the cytokine and chemokine cocktail released by human first trimester villous placenta. Placenta 36, 1333–1336. https://doi.org/10.1016/j.placenta.2015.09.002.

Brugger, B.A., Guettler, J., Gauster, M., 2020. Go with the flow – trophoblasts in flow culture. Int. J. Mol. Sci. 21, E4666. https://doi.org/10.3390/ijms21134666.

Bryan, A.M., Del Poeta, M., 2018. Sphingosine-1-phosphate receptors and innate immunity. Cell. Microbiol. 20, e12836. https://doi.org/10.1111/cmi.12836.

Burton, G.J., Cindrova-Davies, T., Yung, H.W., Jauniaux, E., 2021. HYPOXIA AND REPRODUCTIVE HEALTH: Oxygen and development of the human placenta. Reprod. Camb. Engl. 161, F53–F65. https://doi.org/10.1530/REP-20-0153.

Butler, A., Hoffman, P., Smibert, P., Papalexi, E., Satija, R., 2018. Integrating single-cell transcriptomic data across different conditions, technologies, and species. Nat. Biotechnol. 36, 411–420. https://doi.org/10.1038/nbt.4096.

Cartier, A., Hla, T., 2019. Sphingosine 1-phosphate: lipid signaling in pathology and therapy. Science 366, eaar5551. https://doi.org/10.1126/science.aar5551.

Charkiewicz, K., Goscik, J., Blachnio-Zabielska, A., Raba, G., Sakowicz, A., Kalinka, J., Chabowski, A., Laudanski, P., 2017. Sphingolipids as a new factor in the pathomechanism of preeclampsia – mass spectrometry analysis. PloS One 12, e0177601. https://doi.org/10.1371/journal.pone.0177601.

Davie, E.W., Kulman, J.D., 2006. An overview of the structure and function of thrombin. Semin. Thromb. Hemost. 32 (Suppl 1), 3–15. https://doi.org/10.1055/s-2006-939550.

Del Gaudio, I., Sasset, L., Di Lorenzo, A., Wadsack, C., 2020. Sphingolipid signature of human feto-placental vasculature in preeclampsia. Int. J. Mol. Sci. 21, 1019. https://doi.org/10.3390/ijms21031019.

Dobierzewska, A., Palominos, M., Sanchez, M., Dyhr, M., Helgert, K., Venegas-Araneda, P., Tong, S., Illanes, S.E., 2016. Impairment of angiogenic sphingosine kinase-1/sphingosine-1-phosphate receptors pathway in preeclampsia. PloS One 11, e0157221. https://doi.org/10.1371/journal.pone.0157221.

Drewlo, S., Johnson, E., Kilburn, B.A., Kadam, L., Armistead, B., Kohan-Ghadr, H.-R., 2020. Irisin induces trophoblast differentiation via AMPK activation in the human placenta. J. Cell. Physiol. 235, 7146–7158. https://doi.org/10.1002/jcp.29613.

Fakhr, Y., Brindley, D.N., Hemmings, D.G., 2021. Physiological and pathological functions of sphingolipids in pregnancy. Cell. Signal. 85, 110041. https://doi.org/10.1016/j.cellsig.2021.110041.

Forstner, D., Maninger, S., Nonn, O., Guettler, J., Moser, G., Leitinger, G., Pritz, E., Strunk, D., Schallmoser, K., Marsche, G., Heinemann, A., Huppertz, B., Gauster, M., 2020. Platelet-derived factors impair placental chorionic gonadotropin beta-subunit synthesis. J. Mol. Med. Berl. Ger. 98, 193–207. https://doi.org/10.1007/s00109-019-01866-x.

Goyal, P., Brünnert, D., Ehrhardt, J., Bredow, M., Piccenini, S., Zygmunt, M., 2013. Cytokine IL-6 secretion by trophoblasts regulated via sphingosine-1-phosphate receptor 2 involving Rho/Rho-kinase and Rac1 signaling pathways. Mol. Hum. Reprod. 19, 528–538. https://doi.org/10.1093/molehr/gat023.

Guettler, J., Forstner, D., Cvirn, G., Maninger, S., Brugger, B.A., Nonn, O., Kupper, N., Pritz, E., Wernitznig, S., Dohr, G., Hutter, H., Juch, H., Isermann, B., Kohli, S., Gauster, M., 2021. Maternal platelets pass interstices of trophoblast columns and are not activated by HLA-G in early human pregnancy. J. Reprod. Immunol. 144, 103280. https://doi.org/10.1016/j.jri.2021.103280.

Guettler, J., Forstner, D., Gauster, M., 2022. Maternal platelets at the first trimester maternal-placental interface – small players with great impact on placenta development. Placenta 125, 61–67. https://doi.org/10.1016/j.placenta.2021.12.009.

Hu, Y., Chen, M., Wang, M., Li, X., 2022. Flow-mediated vasodilation through mechanosensitive G protein-coupled receptors in endothelial cells. Trends Cardiovasc. Med. 32, 61–70. https://doi.org/10.1016/j.tcm.2020.12.010.

Johnstone, E.D., Chan, G., Sibley, C.P., Davidge, S.T., Lowen, B., Guilbert, L.J., 2005. Sphingosine-1-phosphate inhibition of placental trophoblast differentiation through a G(i)-coupled receptor response. J. Lipid Res. 46, 1833–1839. https://doi.org/10.1194/jlr.M500095-JLR200.

Josipovic, I., Pflüger, B., Fork, C., Vasconez, A.E., Oo, J.A., Hitzel, J., Seredinski, S., Gamen, E., Heringdorf, D.M.Z., Chen, W., Looso, M., Pullamsetti, S.S., Brandes, R.P., Leisegang, M.S., 2018. Long noncoding RNA LISPR1 is required for S1P signaling and endothelial cell function. J. Mol. Cell. Cardiol. 116, 57–68. https://doi.org/10.1016/j.yjmcc.2018.01.015.

Jung, B., Obinata, H., Galvani, S., Mendelson, K., Ding, B., Skoura, A., Kinzel, B., Brinkmann, V., Rafii, S., Evans, T., Hla, T., 2012. Flow-regulated endothelial S1P receptor-1 signaling sustains vascular development. Dev. Cell 23, 600–610. https://doi.org/10.1016/j.devcel.2012.07.015.

Kerage, D., Brindley, D.N., Hemmings, D.G., 2014. Review: novel insights into the regulation of vascular tone by sphingosine 1-phosphate. Placenta 35 (Suppl), S86–S92. https://doi.org/10.1016/j.placenta.2013.12.006.

Książek, M., Chacińska, M., Chabowski, A., Baranowski, M., 2015. Sources, metabolism, and regulation of circulating sphingosine-1-phosphate. J. Lipid Res. 56, 1271–1281. https://doi.org/10.1194/jlr.R059543.

Lang, I., Schweizer, A., Hiden, U., Ghaffari-Tabrizi, N., Hagendorfer, G., Bilban, M., Pabst, M.A., Korgun, E.T., Dohr, G., Desoye, G., 2008. Human fetal placental endothelial cells have a mature arterial and a juvenile venous phenotype with adipogenic and osteogenic differentiation potential. Differ. Res. Biol. Divers. 76, 1031–1043. https://doi.org/10.1111/j.1432-0436.2008.00302.x.

Li, Q., Pan, Z., Wang, X., Gao, Z., Ren, C., Yang, W., 2014. miR-125b-1-3p inhibits trophoblast cell invasion by targeting sphingosine-1-phosphate

receptor 1 in preeclampsia. Biochem. Biophys. Res. Commun. 453, 57–63. https://doi.org/10.1016/j.bbrc.2014.09.059.

Liao, J., Zheng, Y., Hu, M., Xu, P., Lin, L., Liu, X., Wu, Y., Huang, B., Ye, X., Li, S., Duan, R., Fu, H., Huang, J., Wen, L., Fu, Y., Kilby, M.D., Kenny, L.C., Baker, P.N., Qi, H., Tong, C., 2022. Impaired sphingosine-1-phosphate synthesis induces preeclampsia by deactivating trophoblastic YAP (yes-associated protein) through S1PR2 (sphingosine-1-phosphate receptor-2)-induced actin polymerizations. Hypertension 79, 399–412. https://doi.org/10.1161/HYPERTENSIONAHA.121.18363.

Loegl, J., Nussbaumer, E., Cvitic, S., Huppertz, B., Desoye, G., Hiden, U., 2017. GDM alters paracrine regulation of feto-placental angiogenesis via the trophoblast. Lab. Investig. J. Tech. Methods Pathol. 97, 409–418. https://doi.org/10.1038/labinvest.2016.149.

Maceyka, M., Harikumar, K.B., Milstien, S., Spiegel, S., 2012. Sphingosine-1-phosphate signaling and its role in disease. Trends Cell Biol 22, 50–60. https://doi.org/10.1016/j.tcb.2011.09.003.

Michelson, A.D., Cattaneo, M., Frelinger, A.L., Newman, P.J, 2019. Platelets, fourth ed. Elsevier/Academic Press, London.

Moser, G., Guettler, J., Forstner, D., Gauster, M., 2019. Maternal platelets — friend or foe of the human placenta? Int. J. Mol. Sci. 20, E5639. https://doi.org/10.3390/ijms20225639.

Nagamatsu, T., Iwasawa-Kawai, Y., Ichikawa, M., Kawana, K., Yamashita, T., Osuga, Y., Fujii, T., Schust, D.J., 2014. Emerging roles for lysophospholipid mediators in pregnancy. Am. J. Reprod. Immunol. 72, 182–191. https://doi.org/10.1111/aji.12239.

Obinata, H., Hla, T., 2019. Sphingosine 1-phosphate and inflammation. Int. Immunol. 31, 617–625. https://doi.org/10.1093/intimm/dxz037.

Panetti, T., 2002. Differential effects of sphingosine 1-phosphate and lysophosphatidic acid on endothelial cells. Biochim. Biophys. Acta 1582, 190–196. https://doi.org/10.1016/S1388-1981(02)00155-5.

Patanapirunhakit, P., Karlsson, H., Mulder, M., Ljunggren, S., Graham, D., Freeman, D., 2021. Sphingolipids in HDL — potential markers for adaptation to pregnancy? Biochim. Biophys. Acta Mol. Cell Biol. Lipids 1866, 158955. https://doi.org/10.1016/j.bbalip.2021.158955.

Roberts, V.H.J., Morgan, T.K., Bednarek, P., Morita, M., Burton, G.J., Lo, J.O., Frias, A.E., 2017. Early first trimester uteroplacental flow and the progressive disintegration of spiral artery plugs: new insights from contrast-enhanced ultrasound and tissue histopathology. Hum. Reprod. 32, 2382–2393. https://doi.org/10.1093/humrep/dex301.

Roth, C.J., Haeussner, E., Ruebelmann, T., Koch, F.V., Schmitz, C., Frank, H.-G., Wall, W.A., 2017. Dynamic modeling of uteroplacental blood flow in IUGR indicates vortices and elevated pressure in the intervillous space—a pilot study. Sci. Rep. 7, 40771. https://doi.org/10.1038/srep40771.

Sato, Y., Fujiwara, H., Zeng, B.-X., Higuchi, T., Yoshioka, S., Fujii, S., 2005. Platelet-derived soluble factors induce human extravillous trophoblast migration and differentiation: platelets are a possible regulator of trophoblast infiltration into maternal spiral arteries. Blood 106, 428–435. https://doi.org/10.1182/blood-2005-02-0491.

Singh, A.T., Dharmarajan, A., Aye, I.L.M.H., Keelan, J.A., 2012. Sphingosine—sphingosine-1-phosphate pathway regulates trophoblast differentiation and syncytialization. Reprod. Biomed. Online 24, 224–234. https://doi.org/10.1016/j.rbmo.2011.10.012.

Siwetz, M., Sundl, M., Kolb, D., Hiden, U., Herse, F., Huppertz, B., Gauster, M., 2015. Placental fractalkine mediates adhesion of THP-1 monocytes to villous trophoblast. Histochem. Cell Biol. 143, 565–574. https://doi.org/10.1007/s00418-014-1304-0.

Spiegel, S., Milstien, S., 2003. Sphingosine-1-phosphate: an enigmatic signalling lipid. Nat. Rev. Mol. Cell Biol. 4, 397–407. https://doi.org/10.1038/nrm1103.

Spiegel, S., Milstien, S., 2011. The outs and the ins of sphingosine-1-phosphate in immunity. Nat. Rev. Immunol. 11, 403–415. https://doi.org/10.1038/nri2974.

Takabe, K., Paugh, S.W., Milstien, S., Spiegel, S., 2008. Inside-out' signaling of sphingosine-1-phosphate: therapeutic targets. Pharmacol. Rev. 60, 181–195. https://doi.org/10.1124/pr.107.07113.

Talmont, F., Moulédous, L., Baranger, M., Gomez-Brouchet, A., Zajac, J.-M., Deffaud, C., Cuvillier, O., Hatzoglou, A., 2019. Development and characterization of sphingosine 1-phosphate receptor 1 monoclonal antibody suitable for cell imaging and biochemical studies of endogenous receptors. PloS One 14, e0213203. https://doi.org/10.1371/journal.pone.0213203.

Tukijan, F., Chandrakanthan, M., Nguyen, L.N., 2018. The signalling roles of sphingosine-1-phosphate derived from red blood cells and platelets. Br. J. Pharmacol. 175, 3741–3746. https://doi.org/10.1111/bph.14451.

Vento-Tormo, R., Efremova, M., Botting, R.A., Turco, M.Y., Vento-Tormo, M., Meyer, K.B., Park, J.-E., Stephenson, E., Polański, K., Goncalves, A., Gardner, L., Holmqvist, S., Henriksson, J., Zou, A., Sharkey, A.M., Millar, B., Innes, B., Wood, L., Wilbrey-Clark, A., Payne, R.P., Ivarsson, M.A., Lisgo, S., Filby, A., Rowitch, D.H., Bulmer, J.N., Wright, G.J., Stubbington, M.J.T., Haniffa, M., Moffett, A., Teichmann, S.A., 2018. Single-cell reconstruction of the early maternal-fetal interface in humans. Nature 563, 347–353. https://doi.org/10.1038/s41586-018-0698-6.

Wang, F., Van Brocklyn, J.R., Hobson, J.P., Movafagh, S., Zukowska-Grojec, Z., Milstien, S., Spiegel, S., 1999. Sphingosine 1-phosphate stimulates cell migration through a Gi-coupled cell surface receptor. J. Biol. Chem. 274, 35343–35350. https://doi.org/10.1074/jbc.274.50.35343.

Westwood, M., Al-Saghir, K., Finn-Sell, S., Tan, C., Cowley, E., Berneau, S., Adlam, D., Johnstone, E.D., 2017. Vitamin D attenuates sphingosine-1-phosphate (S1P)-mediated inhibition of extravillous trophoblast migration. Placenta 60, 1–8. https://doi.org/10.1016/j.placenta.2017.09.009.

Yamamoto, Y., Olson, D.M., van Bennekom, M., Brindley, D.N., Hemmings, D.G., 2010. Increased expression of enzymes for sphingosine 1-phosphate turnover and signaling in human decidua during late pregnancy. Biol. Reprod. 82, 628–635. https://doi.org/10.1095/biolreprod.109.081497.

Zhao, H., Wong, R.J., Stevenson, D.K., 2021. The impact of hypoxia in early pregnancy on placental cells. Int. J. Mol. Sci. 22, 9675. https://doi.org/10.3390/ijms22189675.

Received 16 January 2023; received in revised form 22 March 2023; accepted 11 April 2023.

Supplementary Materials

Platelet-derived factors deregulate placental sphingosine-1-phosphate receptor 2 in human trophoblast cells

Freya Lyssy[1], Jacqueline Guettler[1]*, Beatrice A. Brugger[1], Christina Stern[2], Désirée Forstner[1], Olivia Nonn[1,3,4,5], Cornelius Fischer[5,6], Florian Herse[3], Stefan Wernitznig[1], Birgit Hirschmugl[2], Christian Wadsack[2], Martin Gauster[1]

[1]Division of Cell Biology, Histology and Embryology; Gottfried Schatz Research Center, Medical University of Graz; Austria
[2]Department of Obstetrics and Gynaecology, Medical University of Graz; Austria
[3]Charité-Universitätsmedizin Berlin, Corporate Member of Freie Universität Berlin and Humboldt-Universität zu Berlin, Berlin; Germany
[4]Experimental Clinical Research Centre, Max Delbrueck Center for Molecular Medicine in the Helmholtz Association and Charité Berlin; Germany
[5]Max-Delbrück-Center for Molecular Medicine in the Helmholtz Association (MDC), Berlin; Germany
[6]Institute for Medical Systems Biology (BIMSB), Berlin; Germany

*Correspondence:
Jacqueline Guettler, https://orcid.org/0000-0002-8141-5712
Division of Cell Biology, Histology and Embryology,
Gottfried Schatz Research Center,
Medical University of Graz,
Neue Stiftingtalstraße 6, Graz 8010, Austria
Tel: +43 316 385 71878, Fax: +43 316 385 79612
E-mail: jacqueline.guettler@medunigraz.at

Supplemental Table 1

qPCR Primer Sequences

Gene	forward	reverse
GAPDH	ACCCACTCCTCCACCTTTGA	CTGTTGCTGTAGCCAAATTCG
TBP	TGACCCAGCATCACTGTTTC	CCAGCACACTCTTCTCAGCA
S1PR1	CCTCCGTGTTCAGTCTCCTC	AGTTATTGCTCCCGTTGTGG
S1PR2	CGGCCTAGCCAGTTCTGA AA	AATGGCGCAACAGAGGATGA
S1PR3	CAGCCCCGCTTCCCTTTG	CATCACTTGGCATTCACAGACG

Supplemental Table 2

Antibodies used for Immunohistochemistry (IHC), Immunofluorescence staining (IF) and Immunoblotting (IB)

Protein	Host Species	Company	AG retrieval	Dilution IHC	Dilution IF	Dilution IB
S1PR1	Rabbit	abcam	pH 6	1:1000	1:500	1:1000
S1PR2	Rabbit	Invitrogen	pH 9	1:200	1:100	1:400
S1PR3	Rabbit	abcam	pH 9	1:200	1:100	1:1000
HLA-G	Mouse	BD Pharmingen	pH 9	-	1:1000	-
CD68	Mouse	Thermo Scientific	pH 9	-	1:100	-
CD42b	Rabbit	Proteintech Europa	pH 9	1:1000	1:500	-
IgG	Rabbit	Cell Signaling	pH6/pH9	1:200	1:200	-
IgG1	Mouse	Dako	pH9		1:1000	
β-actin	Mouse	abcam	-	-	-	1:500.000
DAPI	-	Invitrogen	-	-	1:2000	-
Alexa Fluor 488	Goat anti mouse	Invitrogen	-	-	1:200	-
Alexa Fluor 555	Goat anti rabbit	Invitrogen	-	-	1:200	-

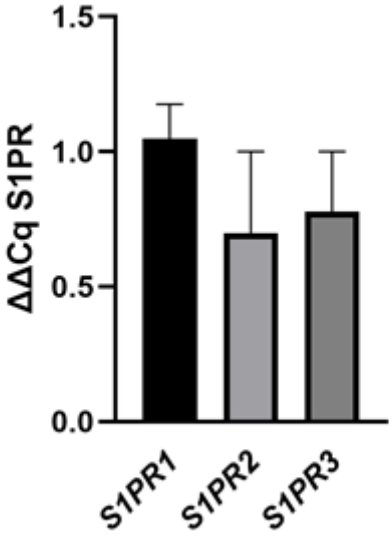

Supplemental Figure 1

S1P receptor expression in isolated human platelets

qPCR for *S1PR1*, *S1PR2* and *S1PR3* in human platelets (n=3). Data shown as mean ΔΔCq ± SD, *GAPDH/TBP* was used as reference gene.

Placenta xxx (xxxx) xxx

Contents lists available at ScienceDirect

Placenta

journal homepage: www.elsevier.com/locate/placenta

The chicken chorioallantoic membrane assay revisited – A face-lifted approach for new perspectives in placenta research

Freya Lyssy [a], Désirée Forstner [a], Beatrice A. Brugger [a], Kaja Ujčič [a], Jacqueline Guettler [a], Nadja Kupper [a], Stefan Wernitznig [a], Christine Daxboeck [a], Lena Neuper [a], Amin El-Heliebi [a], Teresa Kloimboeck [b], Julia Kargl [b], Berthold Huppertz [a], Nassim Ghaffari-Tabrizi-Wizsy [c,1], Martin Gauster [a,*,1]

[a] Division of Cell Biology, Histology and Embryology, Gottfried Schatz Research Center, Medical University of Graz, Austria
[b] Division of Pharmacology, Otto Loewi Research Center, Medical University of Graz, Austria
[c] Division of Immunology, Research Unit CAM Lab, Otto Loewi Research Center, Medical University of Graz, Austria

ARTICLE INFO

Keywords:
Placenta
Trophoblast invasion
Chorioallantoic membrane assay
Spheroid

ABSTRACT

The study of very early human placentation is largely limited due to ethical restrictions on the use of embryonic tissue and the fact that the placental anatomy of common laboratory animal models varies considerably from that of humans. In recent years several promising models, including trophoblast stem cell-derived organoids, have been developed that have also proven useful for the study of important trophoblast differentiation processes. However, the consideration of maternal blood flow in trophoblast invasion models currently appears to be limited to animal models. An almost forgotten model to study the invasive behavior of trophoblasts is to culture them in vitro on the chicken chorioallantoic membrane (CAM), showing an extraembryonic vascular network in its mesenchymal stroma that is continuously perfused by the chicken embryonic blood circulation.

Here, we present an extension of the previously described *ex ovo* CAM assay and describe the use of cavity-bearing trophoblast spheroids obtained from the first trimester cell line ACH-3P. We demonstrate how spheroids penetrated the CAM and that erosion of CAM vessels by trophoblasts led to filling of the spheroid cavities with chicken blood, mimicking initial steps of intervillous space blood perfusion. Moreover, we prove that this model is useful for state-of-the-art techniques including immunofluorescence and *in situ* padlock probe hybridization, making it a versatile tool to study aspects of trophoblast invasion in presence of blood flow.

1. Introduction

The possibilities to study early human placental development in more detail are to this day still very limited. Ethical and regulatory restrictions to use human embryonic tissue and the lack of suitable animal models complicate the establishment of appropriate experimental setups for the investigation of human trophoblast differentiation and invasion processes [1,2]. In particular, the search for adequate approaches for trophoblast studies that take blood flow into account is still ongoing [3]. One model that has mostly been overlooked to study the invasive behavior of trophoblasts in the last years is the avian chorioallantoic membrane (CAM) assay. The CAM of a chicken embryo shows a three-layered structure, including an external chorionic epithelium, an intermediate, highly vascularized mesenchymal layer (formed by fusion of the chorionic and the allantoic mesoderm), and an inner allantoic epithelium [4,5]. The chicken embryo is naturally immunodeficient at early stages and therefore capable of accepting any kind of allo- or xenografts, such as human cancer cells. Therefore, this model has proven to be quite helpful for investigating tumor formation and growth, metastasis or even angiogenesis in cancer research [4,5]. However, the numerous possible applications of this method in other research areas beyond cancer research should not be neglected. In fact, to some extend this method has already been described in regard to human placenta and embryonic development. Since the early 2000's, some publications have

* Corresponding author. Division of Cell Biology, Histology and Embryology, Gottfried Schatz Research Center, Medical University of Graz, Neue Stiftingtalstraße 6, Graz, 8010, Austria.
E-mail address: martin.gauster@medunigraz.at (M. Gauster).
[1] these authors equally contributed to this manuscript.

https://doi.org/10.1016/j.placenta.2024.04.013
Received 28 February 2024; Received in revised form 9 April 2024; Accepted 29 April 2024
Available online 30 April 2024

shown the application of various placenta-derived cell lines in CAM assays and proven its potential to study complex morphoregulatory processes, such as invasion [6,7]. Others went even one step further and incubated placental tissue of decidual origin as well as placental villi on the CAM to investigate angiogenesis within the "maternal-fetal" interface [8,9]. However, the great potential of this assay to become a more frequently used method in placenta research has not been widely considered yet.

As mentioned before, the use of embryonic tissue is very limited due to ethical and legal concerns. More and more alternative models are established to not only overcome this particular challenge but also to reduce the need for animal models in general. One state-of-the-art technique that has been developed and continues to evolve are 3D cell culture models [10]. For example, the use of stem cell-derived organoids has become a standardized method to mimic certain interactions or mechanisms in a spatial cellular network. However, the generation of trophoblast organoids may be hampered not only by the need for primary first trimester tissue, but also the rather high costs associated with these procedures. These obstacles can be overcome with differentiation of human induced pluripotent stem cells (hiPSCs) that can efficiently self-organize into 3D stem-cell-derived trophoblast organoids [11,12]. Besides the requirement of complex culture media supplemented with signaling inhibitors and recombinant growth factors, another drawback of these protocols seems to be the very long cultivation time, ranging between 10 and 30 days, until the first 3D structures are formed. Therefore, formation of spheroids out of immortalized trophoblast cell lines has recently been suggested as a rather basic but highly efficient and reliable method [13,14].

Here, we first describe the generation of spheroids using the human first trimester trophoblast cell line ACH-3P [15] and how their specific three-dimensional structure can be of use in several research questions. In a further step we present the application of this 3D cell culture model on the chicken CAM assay. With the combination of these two approaches, we would like to introduce an alternative and unique method for studying trophoblast differentiation and invasion characteristics in the presence of blood flow.

2. Materials and methods

2.1. Culture of the trophoblast cell line ACH-3P and generation of spheroids

The human first trimester trophoblast cell line ACH-3P [15] was kindly provided by Gernot Desoye (Department of Obstetrics and Gynecology, Medical University of Graz, Austria). Cells were cultured in DMEM/F12 (1:1, Gibco, life technologies; Paisley, UK) supplemented with 10 % FCS (Gibco), 0.1 U/ml penicillin and 0.1 μg/ml streptomycin (Gibco) and 1 % (v/v) L-glutamine (Gibco; 20 mM 100X) in a humidified atmosphere of 5 % CO_2 at 37 °C. Cells were incubated with selection medium every 10th passage containing 5.7 μM azaserin and 100 μM hypoxanthine. For spheroid formation 2.5 x 10^4 cells were seeded in 100 μl culture medium in each well of a Nunclon™ Sphera™ treated 96-Well, U-Shaped-Bottom Microplate (Thermo Fisher Scientific, Waltham, MA, USA). These plates feature a special surface coating that prevents cell attachment and enables spheroid formation, generating one spheroid per well (Fig. 1a). After 24 h of cultivation, spheroids were either used for further assays or directly fixed in formalin and embedded in paraffin.

2.2. Chicken chorioallantoic membrane (CAM) assay

For the *ex ovo* chorioallantoic membrane assay fertilized white Lohmann chicken eggs (Schropper GmbH, Gloggnitz, Austria) were washed and incubated for 3 days at 37.6 °C and 40–60 % humidity [16]. On day three of incubation, eggs were carefully cracked and content transferred into sterile weighing boats (100 ml, 85x85 × 24 mm, VWR®, Avantor, Vienna, Austria) (Fig. 1g), covered with plastic lids (square Petri dish with grid, 10 × 15 mm, Bartelt, Graz, Austria) and further incubated under the same conditions as mentioned above for eggs. On day 10 after fertilization, silicone rings of 5 mm diameter were placed on the CAM of each embryo, avoiding placement directly on bigger blood vessels (Fig. 1h). Up to five ACH-3P spheroids were placed in each silicone ring and chicken embryos were further incubated. In the initial

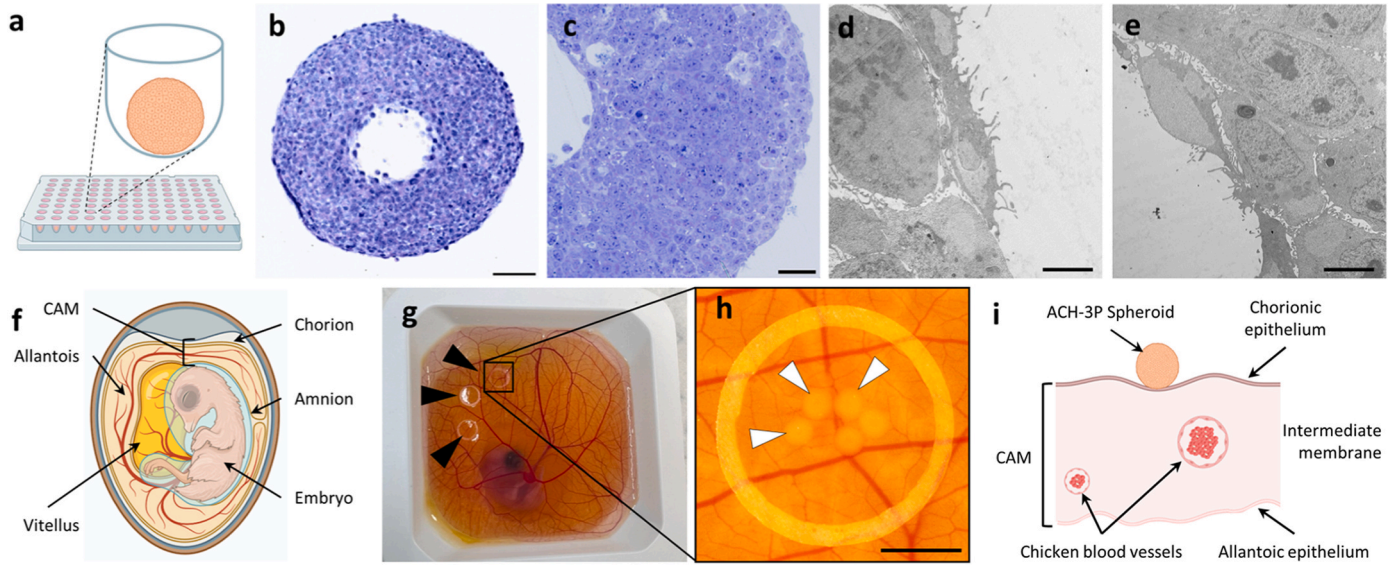

Fig. 1. *ACH-3P spheroid formation and experimental setup of the CAM assay*
ACH-3P cells were seeded in anti-adhesive multi-well plates to form one spheroid per well after 24 h (**a**). H&E staining of FFPE spheroid sections showed an overall cross diameter of approx. 750 μm and revealed a cavity in the center (**b**). Semi-thin sections were stained with toluidine blue (**c**) and subsequent TEM analyses showed microvilli-like protrusions on outermost cell layers of the spheroid (**d**) as well as on cells lining the spheroid cavity (**e**). The chorioallantoic membrane (CAM) is a multi-layered and highly vascularized extraembryonic structure of a chicken egg (**f**). For CAM invasion assays, silicone rings were placed between larger blood vessels (**g**, black arrowheads) and spheroids were seeded within the rings (**h**, white arrowheads). Spheroids were then in direct contact with the uppermost layer of the CAM (**i**). Scale bar in (**b**) represents 100 μm. Scale bar in (**c**) represents 50 μm. Scale bars in (**d** and **e**) represent 5 μm. Scale bar in (**h**) represents 2 mm. Parts of the figure were created with BioRender.com.

phase of the assay, the CAMs were checked every 2 h for the penetration behavior of the spheroids. As soon as petechiae were visible under the microscope (Olympus SZX16), which occurred on average between 20 and 40 h after starting the xenografting (i.e. transfer of spheroids to CAMs), the experiments were terminated. Pieces with attached and invaded ACH-3P spheroids were cut from the egg and were formalin-fixed and paraffin-embedded (FFPE) according to standard protocols. The assays were performed using 38 individual chicken eggs and 4 different passages of ACH-3P cells.

2.3. Hematoxylin and eosin staining

After FFPE-processing, we sectioned the tissue block (5 μm) and stained every 10th slide for hematoxylin and eosin (H&E) to determine the degree of invasion. For H&E staining, spheroid and CAM sections were incubated in acid hemalaun for 10 min according to Mayer (Hematoxylin monohydrate, Merck) directly after standard deparaffinization steps. Subsequently, sections were incubated briefly in 1 % ammonia water (Ammonia solution 25 %, Merck) to change the pH-value. After incubation in 1 % aqueous eosin (Eosin Y (yellowish), Sigma-Aldrich) for 1 min, slides were permanently mounted with Cytoseal (Glas™ Tissue Mount™, Tissue-Tek®, Sakura Finetek Germany GmbH, Umkirch, Germany) and a cover slip. Images were obtained with an Evident Olympus VS200 Slide Scanner (Evident Corporation, Tokyo, Japan).

2.4. Immunohistochemistry

FFPE tissue of the CAM assay was cut into 5 μm sections and mounted on Superfrost Plus slides (Thermo Fisher Scientific). After standard deparaffinization procedures, sections underwent antigen retrieval in an Epitope Retrieval Solution pH 9.0 (Novocostra, Leica) or citrate buffer pH 6.0 for two times 20 min at 150 W in a laboratory microwave (Miele; Guetersloh, Germany). Immunohistochemistry was performed with primary antibodies as indicated in Table 1 using the UltraVision Large Volume Detection System HRP Polymer Kit (Thermo Fisher Scientific) as previously described [17]. Nuclei were stained with hemalaun and slides were mounted with Kaiser's Glycerin Gelatine (Merck). Images were obtained with an Evident Olympus VS200 Slide Scanner (Evident).

2.5. Immunofluorescence staining

For immunofluorescence double staining, 5 μm FFPE CAM sections were deparaffinized and subjected to antigen retrieval with Epitope Retrieval Solution pH 9.0 (Novocostra, Leica). Slides were blocked with Ultra V block (Thermo Fisher Scientific) for 10 min at room temperature (RT) and primary antibodies (Table 1) were diluted in antibody diluent (Dako) and added to the slides for 45 min at RT. After three washing steps with PBS, slides were incubated with secondary fluorescence-labeled antibodies (Table 1) diluted 1:200 in PBS for 30 min at RT. Slides were washed three times with PBS before incubating with DAPI (1:2000 in PBS) for 5 min. Thereafter, slides were washed three times with aqua dest., left to dry and mounted with ProLong Gold Antifade reagent (Invitrogen). Images were obtained with an Evident Olympus VS200 Slide Scanner (Evident).

2.6. Transmission electron microscopy (TEM)

Spheroids were transferred into 2 % paraformaldehyde (Sigma-Aldrich, USA) and 2.5 % glutaraldehyde (Electron Microscopy Sciences; Hartfield, USA) in 0.1 M dimethyl arsenic acid sodium buffer (cacodylate buffer) pH 7.4 for 2 h at RT. Samples were washed with 0.1 M cacodylate buffer pH 7.4 twice for 30 min at RT and afterwards post fixed with 2 % osmium tetroxide (Electron Microscopy Sciences, Hartfield, USA) in 0.1 M cacodylate buffer pH 7.4 for 1 h. After rinsing in 0.1 M cacodylate buffer pH 7.4, the samples were stored in buffer over night at 4 °C. The following day spheroids were dehydrated in a graded ethanol series (50–96 %) for 30 min each and two times in 100 % ethanol for 15 min. The resin infiltration started with 2:1100 % EtOH/TAAB embedding resin (TAAB Laboratory Equipment Ltd; Aldermasten, UK) for 1 h, followed by 1:1100 % EtOH/TAAB embedding resin for 3 h and afterwards with 1:2100 % EtOH/TAAB embedding resin over night at 4 °C. The next day, sections were incubated in pure TAAB resin at RT twice for 90 min. The samples were embedded in TAAB resin in silicone forms and polymerized at 60 °C for 3 days. For sectioning of semi-thin (500 nm) and ultra-thin (70 nm) sections, an ultra-microtome (Leica, Vienna, Austria) was used. Semi-thin sections were stained with 1 % toluidine blue solution (Sigma-Aldrich, USA) for an overview and to identify the region of interest (ROI). The block was trimmed to the ROI and ultra-thin sections were collected on 200 mesh copper grids. Grids were subjected to a staining protocol with lead citrate (Leica, Vienna, Austria) and platinum blue (Science Services, Munich, Germany) prior to EM imaging (Ultra-stainer, Leica). Stained grids were examined by a Zeiss 900 TEM (Carl Zeiss Microscopy GmbH, Jena, Germany) operated at 80 kV.

2.7. In situ padlock probe hybridization

The mRNA transcripts encoding human Actin Beta (*ACTB*) were visualized with *in situ* padlock probe hybridization as described previously [18–20]. Sequences for padlock probe design were retrieved from the National Center for Biotechnology Information (NCBI) with the GenBank accession number NM_001101.5 (ACTB). In short, cDNA was produced using a reverse transcription primer specific to the target. Subsequently, padlock probes were hybridized to the cDNA. Following ligation, circularized padlock probes underwent amplification through rolling circle amplification, and were visualized with fluorescently labeled detection probes in the channel Atto488 (ACTB). Positive signals of ACTB were confirmed with Cy7 fluorescent detection probes. All oligonucleotide sequences are available in Table 2.

3. Results and discussion

3.1. Generation of ACH-3P trophoblast spheroids

To generate spheroids from the first trimester trophoblast cell line

Table 1
Antibodies used for staining.

antibody	clone/order #	company	species	AG retrieval	Dilution IHC	Dilution IF
CK7	DB 051	DB Biotech	rabbit	pH9	1:200	1:100
CK7	OV-TL 12/30	Thermo Fisher	mouse	pH9	1:200	1:100
HLA-G	4H84	BD Pharmingen	mouse	pH9	1:2000	1:1000
vWF	A0082	Dako	rabbit	pH9	1:400	1:200
Cleaved CASP3	5A1E	Cell Signaling	rabbit	pH6	1:100	–
Ki67	C16–I	Dako	mouse	pH6	1:100	–
Alexa Fluor 555		Invitrogen	mouse	–	–	1:200
Alexa Fluor 633		Invitrogen	rabbit	–	–	1:200
DAPI		Invitrogen	–	–	–	1:2000

Table 2
Materials used for in-situ padlock probe hybridization.
The + symbol indicates that the following base is LNA (locked nucleic acid) modified. The padlock probe was 5′-phosphorylated and underlined sequences indicate the targeted complement sequence. Atto488 and CY7 are fluorescent labels.

		Sequence 5'→3'
Primer	ACTB_LNA	C + GG + GC + GG + CG + GATCGGCAAAG
Padlock Probe	plp_ACTB	/5Phos/AGCCTCGCCTTTGCCTCTACGAGTTTGCAGTCACGTGCGTCTATTTAGTGGAGCCGGTTGCTACGATGACTCACGCCCCGCGAGCACAG
Detection Oligos	D1	Atto488-TCTACGAGTTTGCAGTCACG
	D2	CY7-UGCGUCUAUUUAGUGGAGCC

ACH-3P, cells were seeded and incubated in non-adhesive U-bottom 96-well plates, leading to spheroid formation within 24 h. Of note, a single spheroid formed in each well, which mostly appeared in a perfect round shape with an average diameter of about 750 μm (Fig. 1a and b), and interestingly had a cavity in the center (Fig. 1b). The advantage of this simple, high-throughput approach is the consistent, repeatable spheroid generation of uniform size that we observed across different cell passages. So far, several methods have been developed for growing spheroids, which can be categorized into two groups: scaffold-based and scaffold-free approaches [21]. Scaffold-based methods include the use of biomaterials such as hydrogel, biofilms or even particles which favor self-assembly of the cells leading to organization into 3D structures [22]. So-called technical methods include for example the pellet formation, hanging drop, liquid overlay, spinner culture or rotating wall vessel technique, to name a few. Scaffold-free methods are often the preferred approach since they are usually inexpensive, simple and provide a high yield [23]. However, some of these approaches are time-consuming, inefficient, may lead to inconsistent spheroid size and carry the risk of cell damage due to fluidic shear stress [24]. TEM analysis of the ACH-3P spheroid ultrastructure showed in general a high compactness of the spheroid wall, composed of dense layers of round to polygonal cells, whereas in some regions small intercellular channels have formed, leading to a more loosely cohesive environment (Fig. 1c). In contrast, the outermost cell layer of the spheroids (Fig. 1d) as well as cells lining the cavity in the center (Fig. 1e) showed a more elongated, squamous shape and cells formed microvilli-like protrusions on their surfaces.

Although this method is not suited for every type of cell, ACH-3P cells have proven suitable for this method without any difficulty. So far, we have no conclusive explanation as to why the spheroids form a cavity and whether they could close during prolonged cultivation. However, it is worth noting that we found a way to co-incubate ACH-3P cells together with isolated maternal platelets in non-adhesive U-bottom 96-well plates to study the interaction between these two different cells types during spheroid formation. Interestingly, platelets were predominantly located in the cavity of the spheroids, suggesting that gravity and cell size/density could play a substantial role in the formation of these spheroid types (unpublished data). Furthermore, small gaps and capillary-sized intercellular channels in between the spheroids' walls may enable nutrient and oxygen supply, to even the innermost part of the spheroids. This might explain that when checking for apoptosis, we hardly found any cleaved caspase 3 positive cells in the spheroids (data not shown). This seems surprising, considering the rather large diameter of the ACH-3P spheroids and the fact that other protocols mentioned problems with hypoxic cores and insufficient nutrient supply when spheroids grow bigger in size [21].

Taken together, we found this spheroid approach helpful for the subsequent CAM assay, as spheroids are easy to handle due to their rather big size (even with the naked eye) and can be easily coordinated in time to match the spheroid growth with access to chicken eggs.

3.2. Transfer of ACH-3P spheroids on the CAM

Originally the CAM assay was performed *in ovo*, where only a small window was introduced in the shell of the chicken egg for the application of test material. However, the setup was not ideal, since it did not seem practical for accessing and visualizing the CAM [25]. Therefore, the so-called *ex ovo* technique was established, where the egg is carefully cracked and displayed in a sterile dish, ensuring that the CAM part is located on top (Fig. 1f and g). The disadvantage of this method is the lower survival rate of the embryos due to potential small ruptures of the yolk membrane. Nevertheless, this problem can be reduced when gently cracking the egg and reducing the total impact [16,26]. Moreover, it seems like a crucial step to further incubate the embryos in confined curved spaces (e.g. weighing boat, Fig. 1g) rather than flat dishes to avoid excessive distention of the yolk sac [25].

During the performance of the CAM assay, another critical step is the arrangement of silicone rings on the chicken membrane, which will later on be the site of spheroid incubation. When placing spheroids on the CAM, it is of utmost importance to keep the rings, i.e. the intended area of invasion, from touching large blood vessels in order to prevent excessive bleedings too early during the experiment. Therefore, silicone rings were placed between bigger blood vessels and care was taken to avoid areas directly above the embryo or too close to the rim of the dish. We introduced up to three silicone rings per embryo and incubated five ACH-3P spheroids per ring (Fig. 1g and h). The key for a successful CAM assay is to find a good balance between cell number, an adequate CAM area and yield by the end of the experiment. In our experience, the risk of losing or destroying the sample during transfer, incubation or subsequent embedding was too high when applying only one spheroid per ring. We have also refrained from incubating more than 5 spheroids in order to prevent an overflow of spheroids in the limited space of the silicone rings as wells as exhausting the chicken embryo right away with a too big xenograft mass. After transferring spheroids into the rings, they were in direct contact with the uppermost CAM layer – the chorionic epithelium –from the moment of seeding onwards (Fig. 1i). A major advantage of this setup is that no additional culture medium or other supporting materials were required, such as the frequently reported use of Matrigel®, or similar materials to improve the environment for the cells and to promote their attachment and invasion.

3.3. Penetration of the CAM by ACH-3P spheroids

Soon after the transfer of ACH-3P spheroids to the CAM, macroscopic changes, i.e. appearance of small petechiae in areas within the silicone rings, could be observed, usually after 20 h–24 h (Fig. 2k). While CAM assays with various tumor cells were continued for several days in our lab, we were forced to end experiments after a maximum of 48 h [25,27]. As soon as bleedings were observed, experiments were terminated and CAMs subjected to histological surveys. Routine H&E staining of CAM sections revealed that ACH-3P spheroids completely penetrated the CAM as a solid, dense cell mass and reached the allantoic epithelium within less than 24 h (Fig. 2a). Surprisingly, the invaded ACH-3P cell mass still showed cavities reminiscent of the original spheroid cavities (Fig. 2a). All of the cavities were lined again by cells that showed an elongated, squamous shape. What was even more astonishing, was the fact that some of these cavities were filled with embryonic chicken blood cells (Fig. 2b), explaining the macroscopically visible appearance of petechiae. It is worth mentioning at this point that erythrocytes and thrombocytes of the chicken – in contrast to those of human – contain nuclei, not only in the embryonic but also in the adult state. At the

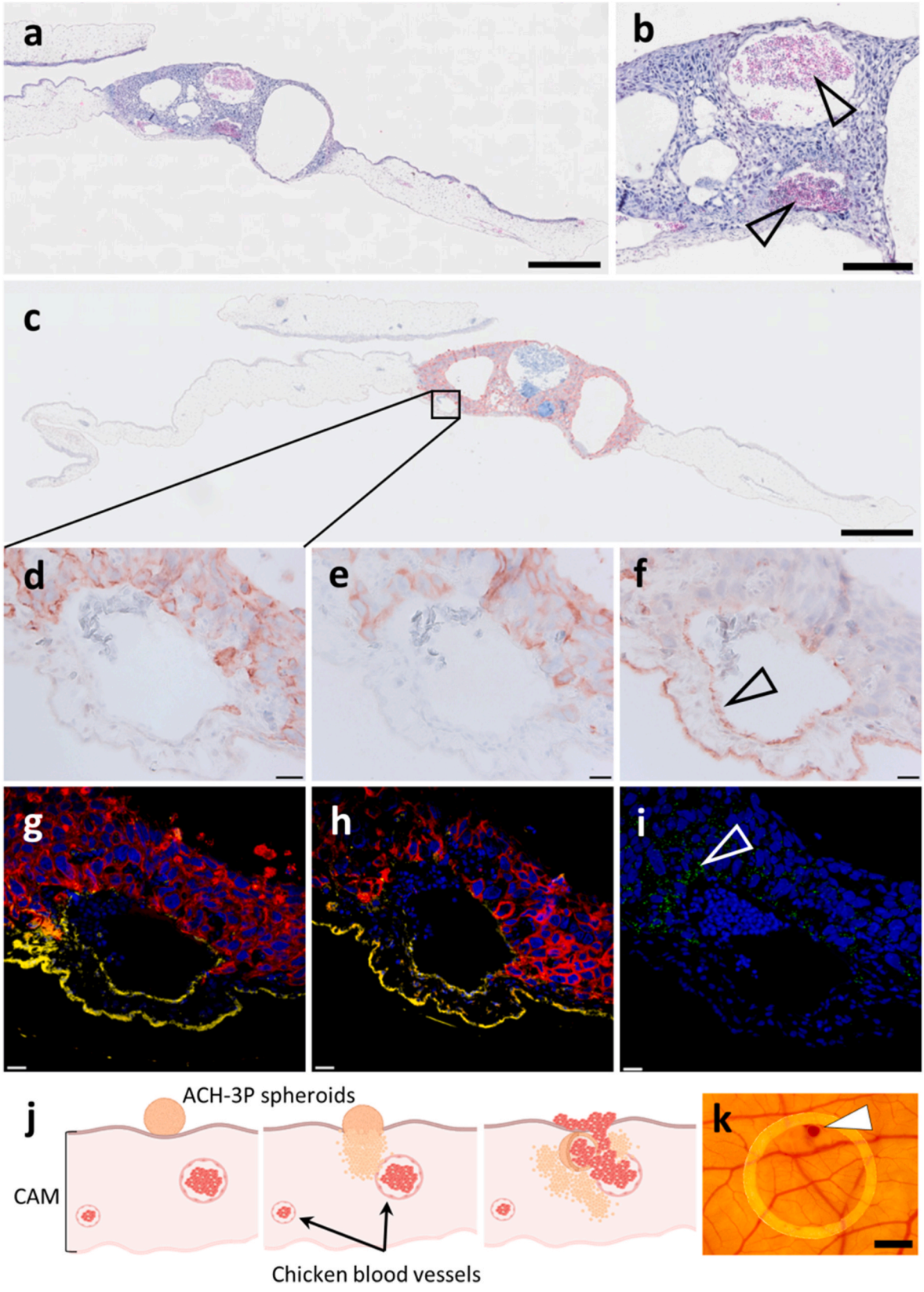

(caption on next page)

Fig. 2. *Invasion of ACH-3P spheroids into the CAM*
H&E staining of FFPE CAM sections showed that spheroid cavities were present after implantation. All of them were lined by flat ACH-3P cells (**a**) and some were filled with chicken blood cells approx. 24 h after transfer of spheroids to the CAM (**b**, arrowheads). Immunohistochemical staining for keratin 7 (CK7) confirmed the human origin of the ACH-3P cells and showed the massive but clearly defined area of invasion, extending to the allantoic epithelium (**c**). Staining of serial sections for CK7 (**d**) and HLA-G (**e**) confirmed the extravillous phenotype of the invading ACH-3P cells, which eroded chicken blood vessels, as determined by vWF staining (**f**). Note that the anti-human vWF antibody showed cross reactivity with the allantoic membrane (**f**). Immunofluorescence double staining for vWF (yellow) and CK7 (red) (**g**) or vWF (yellow) and HLA-G (red) (**h**) verified observations from immunohistochemistry. FFPE sections of the invaded CAM were suitable for the padlock probe *in-situ* hybridization approach, which allowed detection of human *ACTB* mRNA (encoding actin beta) exclusively in ACH-3P cells (**i**, arrowhead). Spheroids were invading the CAM, eventually reaching and eroding CAM blood vessels (**j**), enabling entry of chicken blood cells into the cavities of the ACH-3P spheroids, which then appeared as petechiae on the CAM (**k**, arrowhead). Scale bars in (**a**) and (**c**) represent 500 μm. Scale bar in (**b**) represents 200 μm and those in (**d**) to (**i**) represent 20 μm. Scale bar in (**k**) represents 2 mm. Parts of the figure were created with BioRender.com.

moment we cannot provide an explanation why there was no clotting observed in the trophoblast-lined cavities. However, the lack of adequate blood coagulation stimuli was obviously the reason for chicken embryo exsanguination, observed during preliminary experiments, when suspensions of the trophoblast cell line Jeg-3 were applied to the CAM (data not shown). Nevertheless, it is tempting to compare the blood filling of the spheroid cavities with initial steps of early blood leakage through the trophoblast shell into the developing intervillous space. The trophoblast shell represents the outermost site of the placenta encircling the embryo and is formed by proliferating cytotrophoblasts at distal sites, expanding laterally around day 15 post-conception [28,29].

Although primarily the source for extravillous trophoblast formation involved in spiral artery remodeling, the trophoblastic shell is suggested to protect the early developing placental villi from maternal red blood cells and oxidative stress. Much of our understanding of the very early stages of human placentation is based on observations of placenta-*in situ* specimen by Hamilton and Boyd from the 1960s [30], as well as on even older surveys such as by Dr. Peters at the end of 19th century (Hubert Peters, "*Einbettung des menschlichen Eies*", 1899). Of note, one photomicrograph of a 26 day post-fertilisation placenta-*in-situ* specimen (H710) from the Boyd Collection that was recently reviewed and published by Burton and Jauniaux [29], showed intercellular clefts within the trophoblast shell together with red blood cells between adjacent developing placental villi, suggesting that maternal blood can leak through these gaps of the trophoblastic shell. However, it is important to stress that the cavities of the used ACH-3P spheroids definitely do not resemble the intervillous space, as they are lined by mononucleated cells rather than a syncytiotrophoblast.

Immunohistochemical staining for keratin 7 (CK7) (Fig. 2c and d) and HLA-G (Fig. 2e) confirmed the extravillous phenotype of the invaded ACH-3P cell mass, which had eroded CAM blood vessels, as determined by vWF staining (Fig. 2f). However, it should be stressed at this point that an anti-human von Willebrand factor (vWF) antibody was used to detect the chicken endothelium, which unfortunately showed cross reactivity with the allantoic epithelium. Subsequent immunofluorescence double staining for either keratin 7 or HLA-G in combination with vWF was consistent with observations from immunohistochemistry (Fig. 2g and h). Due to the issue of (interspecies) cross-reactivity of antibodies and as a proof of principle, we finally tested the possibility to run a padlock probe-based *in situ* hybridization protocol on CAMs invaded by ACH-3P spheroids. Targeting human ACTB mRNA (encoding human actin beta) showed specific punctate signals exclusively in areas of invaded ACH-3P cells (Fig. 2i), suggesting that this method can be used as an alternative approach for the analysis of CAM invasion assays when antibodies are not available. Based on our observations, we propose the concept that ACH-3P spheroids penetrate the CAM and thereby form a massive but clearly defined area of invasion that extends to the allantoic epithelium. Erosion of CAM blood vessels by invading ACH-3P cells, enables entry of embryonic chicken blood cells into the ACH-3P spheroid cavities, which seem to persist during invasion (Fig. 2j).

3.4. Limitations of the approach

During the beginning of human pregnancy, extravillous trophoblasts invade the maternal decidua and interact with uterine immune cells [31]. One major limitation of the CAM approach is the fact that during this early stage of development the chicken embryo is immunocompromised and therefore there is no active interaction between immune cells from the host with the invading trophoblasts. Moreover, the immortalized trophoblast cell line ACH-3P was used, which maintained its proliferative phenotype during invasion into the CAM (data not shown). This is in contrast to the *in vivo* situation where extravillous trophoblasts lose their proliferative capacity during differentiation towards the invasive phenotype. In addition, the spheroids used herein are not composed of different trophoblast linages, as shown for primary trophoblast-derived organoids [32], and thus do not completely resemble normal first trimester placenta.

We have recently proposed that maternal platelets – due to their small size of approx. 2–3 μm – could be the first to enter the early intervillous space through narrow intercellular trophoblast gaps [33]. Unfortunately, this study question cannot be addressed in this invasion model, since chicken blood cells with thrombocytes spanning from 4 to 5 μm and erythrocytes from 10 to 12 μm seem quite big compared to human [34]. Finally, it is important to recognize that the absence of the decidual microenvironment is another constraint of the model. Decidual stromal cells and their released factors, as well as immune cells, including uterine natural killer cells, macrophages, T cells, and dendritic cells, play key roles in immune tolerance and regulate invasion of extravillous trophoblasts [35]. Beside immunological aspects, mechanical forces may have profound effects on trophoblast differentiation and migration, as suggested by a recent study, showing higher tissue stiffness of the decidua basalis than decidua parietalis or 3D Matrigel [36]. Tissue stiffness of the CAM may differ from the physiological situation in the decidua basalis and thus affect invasion behavior.

3.5. Outlook

Despite its limitations, the CAM approach offers some potential strengths and opportunities that should be mentioned. First of all, the CAM assay is not legally classified as animal experiments in EU countries and therefore does not require ethical approval [5]. Besides ethical considerations, the blood circulation in CAM vessels could provide a simple way to study aspects of trophoblast – vessel interactions, including penetration and replacement of the endothelium by invading trophoblasts. In addition, this model could be an attractive approach to study how shear stress of circulating "*natural*" blood affects trophoblasts. In this regard, the role of mechanosensitive channels, such as the recently identified TRPV6 [37] in trophoblast microvilli formation could be characterized in more depth. Moreover, the roles of pro- and anticoagulant factors, such as tissue factor (TF) and tissue factor pathway inhibitor (TFPI), as well as components of the fibrinolytic system, including tissue-type plasminogen activator (T-PA) and its primary inhibitor, plasminogen activator inhibitor type-1 (PAI-1) during the invasion of a functioning viable blood vessel by trophoblasts could be studied through loss or gain of function experiments. In addition, effects of anticoagulant agents such as low dose aspirin (LDA) and low molecular weight heparin (LMWH), which are controversially discussed for their role in preventing or treating placenta-mediated pregnancy

complications, may be elucidated at the molecular level in invading trophoblasts. In contrast to conventional fluidic shear stress studies, using cell culture medium, additional aspects such as shear stress by circulating blood cells and the colloid osmotic pressure of the blood plasma may be considered in the CAM model. With the emergence of new trophoblast stem-cell derived organoids and the establishment of novel gene editing approaches, we strongly believe that the CAM assay will have its renaissance and can represent a face-lifted approach for new perspectives in placenta research.

Grant support

M. Gauster was supported by the Austrian Science Fund (FWF): 10.55776/P33554 and 10.55776/P35118, and by the Medical University Graz through the PhD program MolMed.

CRediT authorship contribution statement

Freya Lyssy: Writing – review & editing, Writing – original draft, Visualization, Methodology, Investigation, Formal analysis, Data curation, Conceptualization. **Désirée Forstner:** Writing – review & editing, Methodology, Investigation. **Beatrice A. Brugger:** Writing – review & editing, Methodology, Investigation. **Kaja Ujčič:** Writing – review & editing, Methodology, Investigation. **Jacqueline Guettler:** Writing – review & editing, Methodology, Investigation. **Nadja Kupper:** Writing – review & editing, Methodology, Investigation. **Stefan Wernitznig:** Writing – review & editing, Methodology, Investigation. **Christine Daxboeck:** Writing – review & editing, Methodology. **Lena Neuper:** Writing – review & editing, Methodology. **Amin El-Heliebi:** Writing – review & editing, Methodology. **Teresa Kloimboeck:** Methodology, Investigation. **Julia Kargl:** Writing – review & editing, Supervision, Investigation. **Berthold Huppertz:** Writing – review & editing. **Nassim Ghaffari-Tabrizi-Wizsy:** Writing – review & editing, Supervision, Methodology. **Martin Gauster:** Writing – review & editing, Writing – original draft, Visualization, Supervision, Project administration, Funding acquisition, Conceptualization.

Declaration of competing interest

All authors declare that they have no conflicts of interest (both financial and personal), and affirm that the material is original. All involved people have read and approved the manuscript.

Acknowledgements

The authors gratefully appreciate the excellent technical assistance of Waltraud Huber. Figures were in part created with BioRender (https://www.biorender.com; license granted to Julia Kargl)

References

[1] S. Io, E. Kondoh, Y. Chigusa, K. Kawasaki, M. Mandai, A.S. Yamada, New era of trophoblast research: integrating morphological and molecular approaches, Hum. Reprod. Update 26 (2020) 611–633, https://doi.org/10.1093/humupd/dmaa020.

[2] Y. Abbas, M.Y. Turco, G.J. Burton, A. Moffett, Investigation of human trophoblast invasion *in vitro*, Hum. Reprod. Update 26 (2020) 501–513, https://doi.org/10.1093/humupd/dmaa017.

[3] B.A. Brugger, J. Guettler, M. Gauster, Go with the flow—trophoblasts in flow culture, Int. J. Mol. Sci. 21 (2020) 4666, https://doi.org/10.3390/ijms21134666.

[4] D. Fischer, G. Fluegen, P. Garcia, N. Ghaffari-Tabrizi-Wizsy, L. Gribaldo, R.Y.-J. Huang, V. Rasche, D. Ribatti, X. Rousset, M.T. Pinto, J. Viallet, Y. Wang, R. Schneider-Stock, The CAM model—Q&A with experts, Cancers 15 (2022) 191, https://doi.org/10.3390/cancers15010191.

[5] R. Schneider-Stock, D. Ribatti, The CAM assay as an alternative in vivo model for drug testing, in: M. Schäfer-Korting, S. Stuchi Maria-Engler, R. Landsiedel (Eds.), Organotypic Models Drug Dev, Springer International Publishing, Cham, 2020, pp. 303–323, https://doi.org/10.1007/164_2020_375.

[6] R. Schneider, M. Borges, M. Kadyrov, Forskolin-induced differentiation of BeWo cells stimulates increased tumor growth in the chorioallantoic membrane (CAM) of the Turkey (Meleagris gallopavo) egg, Ann. Anat. - Anat. Anz. 193 (2011) 220–223, https://doi.org/10.1016/j.aanat.2011.02.007.

[7] T. Laurin, U. Schmitz, D. Riediger, H.G. Frank, C. Stoll, Die Chorioallantoismembran befruchteter Vogeleier als Substrat zur Testung der Invasivität von Karzinomen, Mund-, Kiefer- Gesichtschirurgie 8 (2004), https://doi.org/10.1007/s10006-004-0543-y.

[8] T. Stallmach, C. Duc, E. Van Praag, C. Mumenthaler, C. Ott, S.A. Kolb, G. Hebisch, R. Steiner, Feto-maternal interface of human placenta inhibits angiogenesis in the chick chorioallantoic membrane (CAM) assay, Angiogenesis 4 (2001) 79–84, https://doi.org/10.1023/A:1016769416713.

[9] C. Liang, Y. Li, H. Qin, M.N. Ramzan, H. Wang, S. Liu, Q. Yan, Role of poFUT1 and O-fucosylation in placental angiogenesis, Biol. Reprod. 108 (2023) 553–563, https://doi.org/10.1093/biolre/ioad011.

[10] S.A. Yi, Y. Zhang, C. Rathnam, T. Pongkulapa, K. Lee, Bioengineering approaches for the advanced organoid research, Adv. Mater. 33 (2021) 2007949, https://doi.org/10.1002/adma.202007949.

[11] R.M. Karvas, S.A. Khan, S. Verma, Y. Yin, D. Kulkarni, C. Dong, K. Park, B. Chew, E. Sane, L.A. Fischer, D. Kumar, L. Ma, A.C.M. Boon, S. Dietmann, I.U. Mysorekar, T.W. Theunissen, Stem-cell-derived trophoblast organoids model human placental development and susceptibility to emerging pathogens, Cell Stem Cell 29 (2022) 810–825.e8, https://doi.org/10.1016/j.stem.2022.04.004.

[12] Z. Li, O. Kurosawa, H. Iwata, Development of trophoblast cystic structures from human induced pluripotent stem cells in limited-area cell culture, Biochem. Biophys. Res. Commun. 505 (2018) 671–676, https://doi.org/10.1016/j.bbrc.2018.09.181.

[13] B. Dietrich, V. Kunihs, J. Pollheimer, M. Knöfler, S. Haider, 3D organoid formation and EVT differentiation of various trophoblastic cell lines, Placenta 133 (2023) 19–22, https://doi.org/10.1016/j.placenta.2023.01.005.

[14] L. Wen, F. Tang, Organoid research on human early development and beyond, Mediev. Rev. 2 (2022) 512–523, https://doi.org/10.1515/mr-2022-0028.

[15] U. Hiden, C. Wadsack, N. Prutsch, M. Gauster, U. Weiss, H.-G. Frank, U. Schmitz, C. Fast-Hirsch, M. Hengstschläger, A. Pötgens, A. Rüben, M. Knöfler, P. Haslinger, B. Huppertz, M. Bilban, P. Kaufmann, G. Desoye, The first trimester human trophoblast cell line ACH-3P: a novel tool to study autocrine/paracrine regulatory loops of human trophoblast subpopulations – TNF-α stimulates MMP15 expression, BMC Dev. Biol. 7 (2007) 137, https://doi.org/10.1186/1471-213X-7-137.

[16] E.I. Deryugina, J.P. Quigley, Chick embryo chorioallantoic membrane model systems to study and visualize human tumor cell metastasis, Histochem. Cell Biol. 130 (2008) 1119–1130, https://doi.org/10.1007/s00418-008-0536-2.

[17] F. Lyssy, J. Guettler, B.A. Brugger, C. Stern, D. Forstner, O. Nonn, C. Fischer, F. Herse, S. Wernitznig, B. Hirschmugl, C. Wadsack, M. Gauster, Platelet-derived factors dysregulate placental sphingosine-1-phosphate receptor 2 in human trophoblasts, Reprod. Biomed. Online 47 (2023) 103215, https://doi.org/10.1016/j.rbmo.2023.04.006.

[18] A. El-Heliebi, K. Kashofer, J. Fuchs, S.W. Jahn, C. Viertler, A. Matak, P. Sedlmayr, G. Hoefler, Visualization of tumor heterogeneity by in situ padlock probe technology in colorectal cancer, Histochem, Cell Biol. 148 (2017) 105–115, https://doi.org/10.1007/s00418-017-1557-5.

[19] B.A. Brugger, L. Neuper, J. Guettler, D. Forstner, S. Wernitznig, D. Kummer, F. Lyssy, J. Feichtinger, J. Krappinger, A. El-Heliebi, L. Bonstingl, G. Moser, G. Rodriguez-Blanco, O.A. Bachkönig, B. Gottschalk, M. Gruber, O. Nonn, F. Herse, S. Verlohren, H.-G. Frank, N. Barapatre, C. Kampfer, H. Fluhr, G. Desoye, M. Gauster, Fluid shear stress induces a shift from glycolytic to amino acid pathway in human trophoblasts, Cell Biosci. 13 (2023) 163, https://doi.org/10.1186/s13578-023-01114-3.

[20] O. Nonn, C. Fischer, S. Geisberger, A. El-Heliebi, T. Kroneis, D. Forstner, G. Desoye, A.C. Staff, M. Sugulle, R. Dechend, U. Pecks, M. Kollmann, C. Stern, J. E. Cartwright, G.S. Whitley, B. Thilaganathan, C. Wadsack, B. Huppertz, F. Herse, M. Gauster, Maternal angiotensin increases placental leptin in early gestation via an alternative renin-angiotensin system pathway: suggesting a link to preeclampsia, Hypertension 77 (2021) 1723–1736, https://doi.org/10.1161/HYPERTENSIONAHA.120.16425.

[21] O. Habanjar, M. Diab-Assaf, F. Caldefie-Chezet, L. Delort, 3D cell culture systems: tumor application, advantages, and disadvantages, Int. J. Mol. Sci. 22 (2021) 12200, https://doi.org/10.3390/ijms222212200.

[22] N.-E. Ryu, S.-H. Lee, H. Park, Spheroid culture system methods and applications for mesenchymal stem cells, Cells 8 (2019) 1620, https://doi.org/10.3390/cells8121620.

[23] S. Gunti, A.T.K. Hoke, K.P. Vu, N.R. London, Organoid and spheroid tumor models: techniques and applications, Cancers 13 (2021) 874, https://doi.org/10.3390/cancers13040874.

[24] T.-C. Tseng, C.-W. Wong, F.-Y. Hsieh, S.-H. Hsu, Biomaterial substrate-mediated multicellular spheroid formation and their applications in tissue engineering, Biotechnol. J. 12 (2017), https://doi.org/10.1002/biot.201700064.

[25] M. Naik, P. Brahma, M. Dixit, A cost-effective and efficient chick ex-ovo CAM assay protocol to assess angiogenesis, Methods Protoc 1 (2018) 19, https://doi.org/10.3390/mps1020019.

[26] P. Nowak-Sliwinska, T. Segura, M.L. Iruela-Arispe, The chicken chorioallantoic membrane model in biology, medicine and bioengineering, Angiogenesis 17 (2014) 779–804, https://doi.org/10.1007/s10456-014-9440-7.

[27] N. Ghaffari-Tabrizi-Wizsy, C.A. Passegger, L. Nebel, F. Krismer, G. Herzer-Schneidhofer, G. Schwach, R. Pfragner, The avian chorioallantoic membrane as an alternative tool to study medullary thyroid cancer, Endocr. Connect. 8 (2019) 462–467, https://doi.org/10.1530/EC-18-0431.

[28] M. Knofler, S. Haider, L. Saleh, J. Pollheimer, T.K.J.B. Gamage, J. James, Human placenta and trophoblast development: key molecular mechanisms and model

systems, Cell. Mol. Life Sci. CMLS (2019), https://doi.org/10.1007/s00018-019-03104-6.

[29] G.J. Burton, E. Jauniaux, The cytotrophoblastic shell and complications of pregnancy, Placenta 60 (2017) 134–139. S0143-4004(17)30303-X [pii].

[30] W.J. Hamilton, J.D. Boyd, Development of the human placenta in the first three months of gestation, J. Anat. 94 (1960) 297–328.

[31] S. Vondra, A.-L. Höbler, A.I. Lackner, J. Raffetseder, Z.N. Mihalic, A. Vogel, L. Saleh, V. Kunihs, P. Haslinger, M. Wahrmann, H. Husslein, R. Oberle, J. Kargl, S. Haider, P. Latos, G. Schabbauer, M. Knöfler, J. Ernerudh, J. Pollheimer, The human placenta shapes the phenotype of decidual macrophages, Cell Rep. 42 (2023) 111977, https://doi.org/10.1016/j.celrep.2022.111977.

[32] M.J. Shannon, G.L. McNeill, B. Koksal, J. Baltayeva, J. Wächter, B. Castellana, M. S. Peñaherrera, W.P. Robinson, P.C.K. Leung, A.G. Beristain, Single-cell assessment of primary and stem cell-derived human trophoblast organoids as placenta-modeling platforms, Dev. Cell 59 (2024) 776–792.e11, https://doi.org/10.1016/j.devcel.2024.01.023.

[33] J. Guettler, D. Forstner, M. Gauster, Maternal platelets at the first trimester maternal-placental interface - small players with great impact on placenta development, Placenta 125 (2022) 61–67, https://doi.org/10.1016/j.placenta.2021.12.009.

[34] Casimir Jamroz, A.M. Lucas, Atlas of Avian Hematology/Alfred M. Lucas, Casimir Jamroz, U.S. Dept. of Agriculture, Washington, D.C., 1961, https://doi.org/10.5962/bhl.title.6392.

[35] J. Krstic, A. Deutsch, J. Fuchs, M. Gauster, T. Gorsek Sparovec, U. Hiden, J. C. Krappinger, G. Moser, K. Pansy, M. Szmyra, D. Gold, J. Feichtinger, B. Huppertz, (Dis)similarities between the decidual and tumor microenvironment, Biomedicines 10 (2022) 1065, https://doi.org/10.3390/biomedicines10051065.

[36] Y. Abbas, A. Carnicer-Lombarte, L. Gardner, J. Thomas, J.J. Brosens, A. Moffett, A. M. Sharkey, K. Franze, G.J. Burton, M.L. Oyen, Tissue stiffness at the human maternal–fetal interface, Hum. Reprod. 34 (2019) 1999–2008, https://doi.org/10.1093/humrep/dez139.

[37] S. Miura, K. Sato, M. Kato-Negishi, T. Teshima, S. Takeuchi, Fluid shear triggers microvilli formation via mechanosensitive activation of TRPV6, Nat. Commun. 6 (2015) 8871, https://doi.org/10.1038/ncomms9871.

Received: 19 December 2024 | Revised: 14 March 2025 | Accepted: 17 March 2025

https://doi.org/10.1016/j.jtha.2025.03.020

ORIGINAL ARTICLE

Maternal platelet-derived factors induce trophoblastic *LAIR2* expression to promote trophoblast invasion and inhibit platelet activation at the fetal-maternal interface

Freya Lyssy[1] | Désirée Forstner[1] | Jacqueline Guettler[1] | Nadja Kupper[1] | Kaja Ujčič[1] | Lena Neuper[1] | Christine Daxboeck[1] | Amin El-Heliebi[1] | Daniel Kummer[1] | Julian C. Krappinger[1] | Djenana Vejzovic[2] | Beate Rinner[2] | Gerhard Cvirn[3] | Stefan Wernitznig[1] | Gerit Moser[1] | Daniela S. Valdes[4,5] | Florian Herse[4,5] | Anna-Lena Höbler[6] | Jürgen Pollheimer[6] | Joanna L. James[7] | Julia Feichtinger[1] | Martin Gauster[1]

[1]Division of Cell Biology, Histology and Embryology, Gottfried Schatz Research Center, Medical University of Graz, Graz, Austria

[2]Division of Biomedical Research, Core Facility Alternative Biomodels and Preclinical Imaging, Medical University of Graz, Graz, Austria

[3]Division of Physiological Chemistry, Otto Loewi Research Center, Medical University of Graz, Graz, Austria

[4]Max-Delbrück-Center for Molecular Medicine in the Helmholtz Association (MDC), Berlin, Germany

[5]Experimental and Clinical Research Center, a cooperation between the Max-Delbrück-Center for Molecular Medicine in the Helmholtz Association and the Charité–Universitätsmedizin Berlin, Berlin, Germany

[6]Department of Obstetrics and Gynecology, Reproductive Biology Unit, Maternal-Fetal Immunology Group, Medical University of Vienna, Vienna, Austria

[7]Department of Obstetrics, Gynaecology and Reproductive Sciences, Faculty of Medical and Health Sciences, University of Auckland, Auckland, New Zealand

Correspondence
Martin Gauster and Julia Feichtinger, Division of Cell Biology, Histology and Embryology, Gottfried Schatz Research Center, Medical University of Graz, Neue Stiftingtalstraße 6, Graz 8010, Austria.
Email: martin.gauster@medunigraz.at and julia.feichtinger@medunigraz.at

Funding information
M. Gauster was supported by the Austrian Science Fund (FWF): 10.55776/P35118 and 10.55776/I6907 and by the Medical University Graz through the PhD program MolMed. F. Lyssy was supported through the PhD program MolMed at the Medical University of Graz, and through the Marietta Blau Grant by the Austrian Federal Ministry for Education, Science and

Abstract

Background: During human placentation, extravillous trophoblasts (EVTs) arising from cell column trophoblasts (CCTs) invade the highly differentiated uterine mucosa, called decidua, where they erode blood vessels and replace vascular endothelial cells. Maternal platelets have been detected in intercellular gaps of CCTs, but their physiological role remains unclear.

Objectives: This study aimed to elucidate the impact of platelet-derived factors on trophoblasts that are exposed to maternal platelets through erosion of decidual blood vessels.

Methods: Trophoblast cell line ACH-3P spheroids were incubated either with platelet-derived factors or isolated platelets obtained from pregnant women and then subjected to RNA sequencing followed by validation using quantitative polymerase chain reaction, ELISA, and *in situ* padlock hybridization. Among the deregulated genes, leukocyte

Manuscript handled by: Shrey Kohli

Final decision: Shrey Kohli, 17 March 2025

Research (OeAD; BMBWF). F. Herse was supported by Deutsche Forschungsgemeinschaft (DFG) (HE6249/5-1; HE6249/7-1; HE6249/7-2; HE6249/5-3).

associated immunoglobulin-like receptor 2 (*LAIR2*) expression was confirmed in first trimester placenta and primary trophoblast organoids. The functional role of LAIR2 in trophoblast invasion and platelet activation was studied.

Results: Platelet-derived factors altered the transcriptional profile of ACH-3P spheroids, including deregulation of genes linked to embryonic development. Among them, LAIR2 was exclusively detected in CCTs and invaded EVTs of first trimester decidua. Histology showed extravasated maternal erythrocytes within interstitial gaps of highly invaded decidua samples, coinciding with LAIR2-positive EVTs. LAIR2 inhibited type 1 collagen-induced platelet activation and enhanced invasiveness of trophoblasts.

Conclusion: This study suggests that maternal platelet-derived factors affect the transcriptional profile of trophoblasts, including upregulation of *LAIR2*, which may be involved in fine-tuning the coagulation of maternal blood leaking from eroded decidual blood vessels and could increase the invasiveness of EVTs into the decidua through an autocrine mechanism.

KEYWORDS
first trimester, placenta, platelets, pregnancy

1 | INTRODUCTION

Human gestation is initiated by embryo implantation, which includes the anchoring of the blastocyst to the endometrial epithelium. While the inner cell mass of the blastocyst, the embryoblast, proceeds to develop into the embryo, amnion, and umbilical cord, the outer trophectoderm layer of the blastocyst provides the basis for the formation of the placenta by providing the source of specialized epithelial cells termed trophoblasts. Following implantation, the trophectoderm starts to proliferate and differentiate, fusing to a multinucleated syncytium, the so-called primitive syncytiotrophoblast (SCT). In this early stage, the primitive SCT possesses all necessary enzymes to penetrate the maternal endometrium, now referred to as the decidua [1,2]. Eventually, vacuoles start to grow in the primitive SCT, leading to the formation of lacunae, which are separated by SCT trabeculae and are precursors of the intervillous space [1]. These trabeculae then develop into primary villi, consisting of cytotrophoblasts (CTBs) as well as a layer of true SCT (that will form the surface of the placenta), before colonization of the extraembryonic mesoderm and development of placental blood vessels give rise to secondary villi and then tertiary villi, respectively. At the distal parts of the evolving villi, trophoblasts penetrate through the SCT and form trophoblast cell columns (CCTs), which eventually anchor the developing placenta to the decidua. Trophoblasts from distal areas of cell columns differentiate into an invading phenotype, the so-called extravillous trophoblast (EVT) [3]. This area has also been referred to as a transition zone, showing more intercellular space between the trophoblasts than in the proximal compact zone of cell columns, enabling a possible route for maternal blood plasma components to enter the early intervillous space [4]. There, EVTs are embedded in a self-secreted matrix of laminins, collagen type IV, vitronectin, heparan sulfate, and cellular fibronectins termed matrix-type fibrinoid [4,5]. Moreover, differentiation into the invasive phenotype is associated with an integrin switch and the expression of the bona fide EVT marker, major histocompatibility complex, class I, G (HLA-G). Failure in EVT lineage formation and differentiation can result in pregnancy complications such as preeclampsia, fetal growth restriction, and pregnancy loss [6]. EVTs invade the decidual stroma and its vessels, including uterine lymphatics, veins, and spiral arteries, forming trophoblast plugs within the latter to inhibit maternal blood cells from entering the early intervillous space. However, by the middle of the first trimester, cells in these trophoblast plugs become loosely cohesive, forming capillary sized channels [7]. Due to their small diameter of only 2 to 3 μm, platelets might be the first among the circulating maternal blood cells that can traverse these intercellular gaps. In fact, we and others have found platelets in between these trophoblast cell gaps, leading to the conclusion that maternal platelets might reach the intervillous space even before uteroplacental perfusion is fully established [8,9].

Several studies have reported a decrease in maternal platelet count during progression of pregnancy [10]. The decrease in mean platelet count gradually occurs from first trimester to second and third, with an overall decline of approximately 10% across gestation considered normal. This decline is a result of both dilution of platelet numbers by maternal blood plasma volume expansion and accelerated platelet sequestration and consumption in the utero-placental circulation [11–13]. It has been reported that in normal human pregnancy, maternal platelets can contribute to perivillous fibrin deposition, which can indirectly contribute to shaping of placental villi and intervillous space. However, excessive platelet activation at the fetal-maternal interface can lead to activation of inflammasomes in the

placental SCT, triggering a sterile inflammation of the placenta and potentially causing systemic inflammatory response in the mother. The question of whether maternal platelets are friend or foe of the human placenta remains unanswered [14].

Based on our recent observations showing maternal platelets in the intercellular space of CCTs, this study aimed to test the hypothesis that maternal platelets and their derived factors play a role in trophoblasts during the initial phase of placental development. For this purpose, platelets from pregnant women were cocultured with trophoblast spheroids and the latter subjected to molecular downstream analyses. Among the numerous genes involved in invasion and placentation processes, we identified leukocyte associated immunoglobulin-like receptor 2 (*LAIR2*) was deregulated in response to maternal platelet activation. This gene encodes a soluble receptor apparently highly expressed in distal parts of CCTs of anchoring villi during the first trimester and is associated with invasion capacities of EVTs.

2 | MATERIALS AND METHODS

2.1 | Platelet isolation and preparation of platelet releasate

This study was approved by the ethical committee of the Medical University of Graz (31-019 ex 18/19). Platelets were isolated as previously described [15,16]. The isolation protocol is provided in the Supplementary Material. Platelets were either directly used for coincubation with ACH-3P spheroids, aggregometry measurements, or further processed. For the generation of platelet releasate (PR), platelets were then incubated with one of the following agonists: 1 U/mL thrombin (Merck, Darmstadt KGaA), 10 μM ADP (2-methylthioadenosine diphosphate; Tocris), 1 μg/mL collagen type 1 (COL1A1; Chrono-Log Corporation), 50 μM thrombin receptor activator peptide 6 (TRAP6; HY-P0078, MedChemExpress) for 30 minutes at 37 °C. If not stated otherwise, PR used for experiments was activated with thrombin. For thrombin-induced PR preparation, thrombin was inactivated with 1.1 U/mL hirudin (Merck, Darmstadt KGaA) and platelets were centrifuged at 1962 × *g* for 15 minutes. The supernatant containing the released factors from activated platelets (PR), not platelets themselves, was collected, aliquoted, and stored at −80 °C for subsequent experiments. Characteristics of the study group are shown in Supplementary Table S1.

2.2 | Culture of trophoblast cell line ACH-3P and spheroid formation

The human first trimester trophoblast cell line ACH-3P [17] was kindly provided by Gernot Desoye (Department of Obstetrics and Gynecology, Medical University Graz, Austria). Cells were cultured as previously described [18]. Details are provided in the Supplementary Material. For spheroid formation, 2.5 × 10^4 cells were cultured per well of a Nunclon Sphera-treated 96-well, U-shaped-bottom microplate (Thermo Fisher Scientific). After 12 hours, cell spheroids were incubated with PR pooled from 10 independent pregnant donors (mean platelets/μL: 163 ± 44 × 10^3, mean gestational age: 270 ± 8 days) in a 1:2 dilution with culture medium. After culture, ≥8 spheroids were pooled and lysed with respective lysis buffer and vigorous up and down pipetting. Cell lysates were stored at −80 °C until further analysis. Four or more spheroids that underwent the same treatment were pooled and formalin-fixed and paraffin embedded (FFPE) according to standard procedure.

2.3 | LAIR2 silencing

ACH-3P cells were seeded in 24-well plates at a density of 1 × 10^5 cells per well and cultured for 24 hours. Cells were then transfected with a predesigned small interfering RNA (siRNA) targeting human *LAIR2* (5 pM, Silencer siRNA, Thermo Fisher Scientific) or nontargeting negative control siRNA (5 pM, Silencer siRNA, Thermo Fisher Scientific) using Lipofectamine as a transfection reagent in 1 ml Dulbecco's Modified Eagle Medium/F12 (1:1; Gibco, Life Technologies) supplemented only with 1% (v/v) L-glutamine (20 mM 100X; Gibco) for 24 hours.

2.4 | Viability and apoptosis determination for 3-dimensional (3D) cell culture

For viability and apoptosis determination, the commercially available CellTiter-Glo 3D Cell Viability Assay (Promega) and Caspase-Glo 3/7 (Promega) assays were performed according to the manufacturer's protocol. In brief, ACH-3P cells were seeded 24 hours prior to treatment as described previously to allow spheroid formation. PR in a 1:2 dilution was added directly to each well and incubated for 24 hours. The respective amount of culture medium was used as a vehicle control, whereas 10 μM staurosporine (Alexis Corporation) served as a control for apoptosis induction. After 24 hours of treatment, bioluminescence signals were measured using a CLARIOstar microplate reader (BMG Labtech). All values were blank adjusted (medium only). Cell viabilities were normalized to controls using GraphPad Prism.

2.5 | Coculture of ACH-3P spheroids with human platelets

ACH-3P cells were coincubated with isolated human platelets in a Nunclon Sphera-treated 96-well, U-shaped bottom microplate (Thermo Fisher Scientific). In each well, 2.5 × 10^4 cells were cultured and mixed with isolated human platelets (267 ± 44 × 10^3 platelets/μL) in an approximate 1:500 cell-to-platelet ratio, in the abovementioned ACH-3P media with or without 1 U/mL thrombin (Merck) for platelet activation. Controls were treated with the respective amount of the

ACH-3P culture medium without platelets or thrombin. After 24 hours, spheroids from each condition were pooled and either subjected to FFPE procedures or cell lysates were collected and stored at −80 °C until further analysis.

2.6 | RNA sequencing (RNA-seq) and bioinformatics analysis

Total RNA from matched PR-treated and control ACH-3P spheroids (5 per condition) was isolated with SV Total RNA Isolation System (Promega) according to the manufacturer's protocol. RNA samples were then sent to GENEWIZ from Azenta Life Sciences and subjected to RNA quantification using Qubit 4.0 Fluorometer (Life Technologies), and RNA integrity was checked with RNA Kit on Agilent 5300 Fragment Analyzer, RNA integrity number >9 (Agilent Technologies). Ribosomal RNA depletion was achieved using the NEBNext rRNA Depletion Kit (Human/Mouse/Rat Cat. No. E6310). RNA-seq library preparation was performed using the NEBNext Ultra RNA Library Prep Kit for Illumina following the manufacturer's recommendations (New England Biolabs). Samples were sequenced on the Illumina NovaSeq 6000 instrument in a paired-end configuration, resulting in 2 × 250 bp read pairs.

RNA-seq analysis of the 10 samples was performed within Galaxy [19]. A description of the analysis is provided in the Supplementary Material. All raw RNA-seq files are provided through the National Center for Biotechnology Information (NCBI) Short Read Archive, accession number PRJNA1194512.

2.7 | Quantitative polymerase chain reaction (qPCR) analysis

Total RNA was isolated from pooled spheroid or organoid samples using the SV Total RNA Isolation System (Promega) according to the manufacturer's protocol. In addition, to spheroids and organoids, 100 µL of fresh culture medium supplemented with PR and 100 µL conditioned culture medium collected after cell culture were subjected to RNA isolation and subsequent qPCR analysis. A detailed description of the qPCR analysis is provided in the Supplementary Material. Primer sequences are shown in Supplementary Table S2.

2.8 | Analysis of single–nucleus RNA-sequencing data

Single–nucleus RNA-sequencing (snRNA-seq) human first trimester placental villi datasets from Nonn et al. [20] (n = 10 healthy tissues, n = 145,637 nuclei) were accessed from Zenodo (10.5281/zenodo.8159511) and used without additional preprocessing. Matrices were loaded into R (v4.1.2) and *LAIR2* expression visualized using Seurat (v4.1.0). Details about the analysis are provided in the Supplementary Material.

2.9 | *In situ* padlock probe analysis

The mRNA transcripts of *LAIR2* were visualized with *in situ* padlock probe hybridization as described previously [21,22]. Sequences for padlock probe design with the GenBank accession number NM_002288.6 (*LAIR2*) were obtained from NCBI. A detailed description of this method is provided in the Supplementary Material. Sequences of primers and padlock probes are shown in Supplementary Table S3.

2.10 | Primary trophoblast isolation and organoid formation

First trimester placental tissue was obtained from Auckland Medical Aid Centre, Auckland, New Zealand, after obtaining ethical approval from the Northern X Ethics Committee (NTX/12/06/057/AM012) and written informed consent. Primary mononuclear villous trophoblasts were isolated and cultured as organoids as previously described, with minor changes [23]. The detailed protocol is provided in the Supplementary Material. When most of the organoids reached a size of 200 to 500 µm, they were either stimulated to undergo differentiation toward the EVT lineage or maintained in trophoblast organoid media (TOM) as previously described [24]. To stimulate EVT differentiation, TOM was exchanged for extravillous trophoblast medium 1 (see Supplementary Material). Medium was changed every 2 to 3 days. After 7 days of culture in extravillous trophoblast medium 1 or respective TOM, half of the control organoids and half of the EVT-induced organoids were treated with PR pooled from 11 pregnant donors in a 1:2 dilution with the respective culture medium. The remaining organoids underwent medium change in their respective culture media. After 24 hours of incubation, all organoids from 2 wells of the same condition were pooled and cell lysates were collected and stored at −80 °C until further analysis. For FPPE processing, all organoids from 4 wells of the same condition were pooled.

2.11 | ELISA

LAIR2 levels were measured from pooled protein lysates of ACH-3P spheroids treated in presence or absence of PR using a LAIR2 ELISA kit (ELH-LAIR2, RayBiotech Life Inc), according to manufacturer's manual. Further description of this method is stated in the Supplementary Material.

2.12 | Immunohistochemistry

FFPE spheroids, organoids, or placenta tissue were cut into 5 µm sections and mounted on Superfrost Plus slides (Thermo Fisher Scientific). After standard deparaffinization steps, sections were subjected to antigen retrieval in Epitope Retrieval Solution pH 9.0 (Novocostra, Leica) or citrate buffer pH 6.0 2 times for 20 minutes

each at 150 W in a laboratory microwave (Miele). Immunohistochemistry was performed using primary antibodies specified in Supplementary Table S4 by applying the UltraVision Large Volume Detection System HRP Polymer Kit (Thermo Fisher Scientific) as previously described [25,26]. Hematoxylin was used as nuclei counterstain, and slides were mounted with Kaiser's Glycerin Gelatine (Merck) and a cover slip. Images were obtained with an Evident Olympus VS200 Slide Scanner (Evident Corporation).

2.13 | Immunofluorescence staining

For immunofluorescence double staining, 5 µm sections were mounted on Superfrost Plus slides (Thermo Fisher Scientific) and subjected to antigen retrieval as described above. The staining protocol is described in the Supplementary Material. Images were obtained with an Evident Olympus VS200 Slide Scanner or an Evident FV3000 Confocal Laser Scanning Microscope (Evident).

2.14 | Hematoxylin and eosin staining

After FFPE processing, tissue blocks were cut into 5 µm sections and stained with hematoxylin and eosin as previously described [18]. A brief description can be found in the Supplementary Material. Images were obtained with an Evident Olympus VS200 Slide Scanner (Evident Corporation).

2.15 | Platelet aggregometry

Aggregometry of isolated platelets from pregnant women was assessed using impedance measurements with Chrono-log Model 700 Aggregometer (Chrono-Log Corporation). For activation, either TRAP6 (HY-P0078, MedChemExpress) at a final concentration of 50 µM or Col1 (Chrono-Log Corporation) at a final concentration of 1 µg/mL was added to the platelet suspension. To measure the influence of LAIR2 on platelet activation, agonists were preincubated with or without 1 µg/mL recombinant human (rh)LAIR2 protein (ab182705, abcam) for 30 minutes at ambient temperature before measurements. Further details on the methodology can be found in the Supplementary Material.

2.16 | Invasion assay

To measure the invasion ability of the ACH-3P cells through an extracellular matrix (ECM), a QCM 96-Well Cell Invasion Assay (ECM555, Merck) was performed according to manufacturer's protocol. Cells were seeded with or without 1 µg/mL rhLAIR2 protein (ab182705, abcam). Additionally, we used cells that underwent siRNA-mediated knockdown of *LAIR2* expression prior to this assay. Samples were measured with a CLARIOStar fluorescence plate reader (BMG LABTECH GmbH). Further description of the assay is provided in the Supplementary Material.

2.17 | Statistical analysis

Data were analyzed using GraphPad Prism 10.1.2 and are presented as mean with SD. Standard normality was tested by performing the Shapiro–Wilk test, and significance was tested with one-way analysis of variance (ANOVA) followed by Tukey's multiple comparison test to compare groups with one another. Student's *t*-test was used when only 2 groups were compared.

3 | RESULTS

3.1 | Platelet-derived factors modify the trophoblast gene expression profile

To determine the effect of maternal platelet-derived factors on the gene expression profile of trophoblasts, blood was collected from pregnant women just prior to cesarean section, and platelets were isolated and activated with thrombin. The resulting supernatant was collected and used as PR fraction for subsequent experiments. Trophoblast spheroids, generated from the first trimester trophoblast cell line ACH-3P, were cultured with and without PR and subjected to RNA-seq (Figure 1A). Moreover, the impact of platelet-derived factors on the viability and late apoptosis of ACH-3P spheroids was investigated. While the cell viability was significantly enhanced with PR compared to untreated spheroids (Figure 1B), caspase 3-dependent apoptosis was not induced by this treatment (Figure 1C). RNA-seq and subsequent bioinformatics analysis showed that the presence of PR altered the gene expression profile of the trophoblast spheroids, including 65 significantly up and 13 significantly downregulated genes (Figure 1D, Supplementary Table S5). From this set of deregulated genes, we proceeded to identify those that have been previously discussed in the context of placental development and/or platelet function, such as integrins (*ITGA2*, $\log_2$ fold change (FC) = 1.31; *ITGA3*, $\log_2$FC = 0.86), metalloproteinase (*MMP15*, $\log_2$FC = 0.97), and NOD-like receptor proteins (*NLRP2*, $\log_2$FC = 0.61; *NLRP7*, $\log_2$FC = 0.59) (Figure 1E), and confirmed their deregulation in response to PR via qPCR (Figure 1F). Since platelets have been reported to carry very small amounts of mRNA and exhibit high levels of integrins, culture medium supplemented with PR was subjected to qPCR analysis for *ITGA2*, which, however, showed no signal, ruling out possible data falsification by traces of platelet RNA. Further gene set enrichment analysis revealed several significant gene ontology terms, including but not limited to terms associated with cell migration and adhesion as well as tissue, cellular, and vascular development (Supplementary Figure S1, Supplementary Table S6).

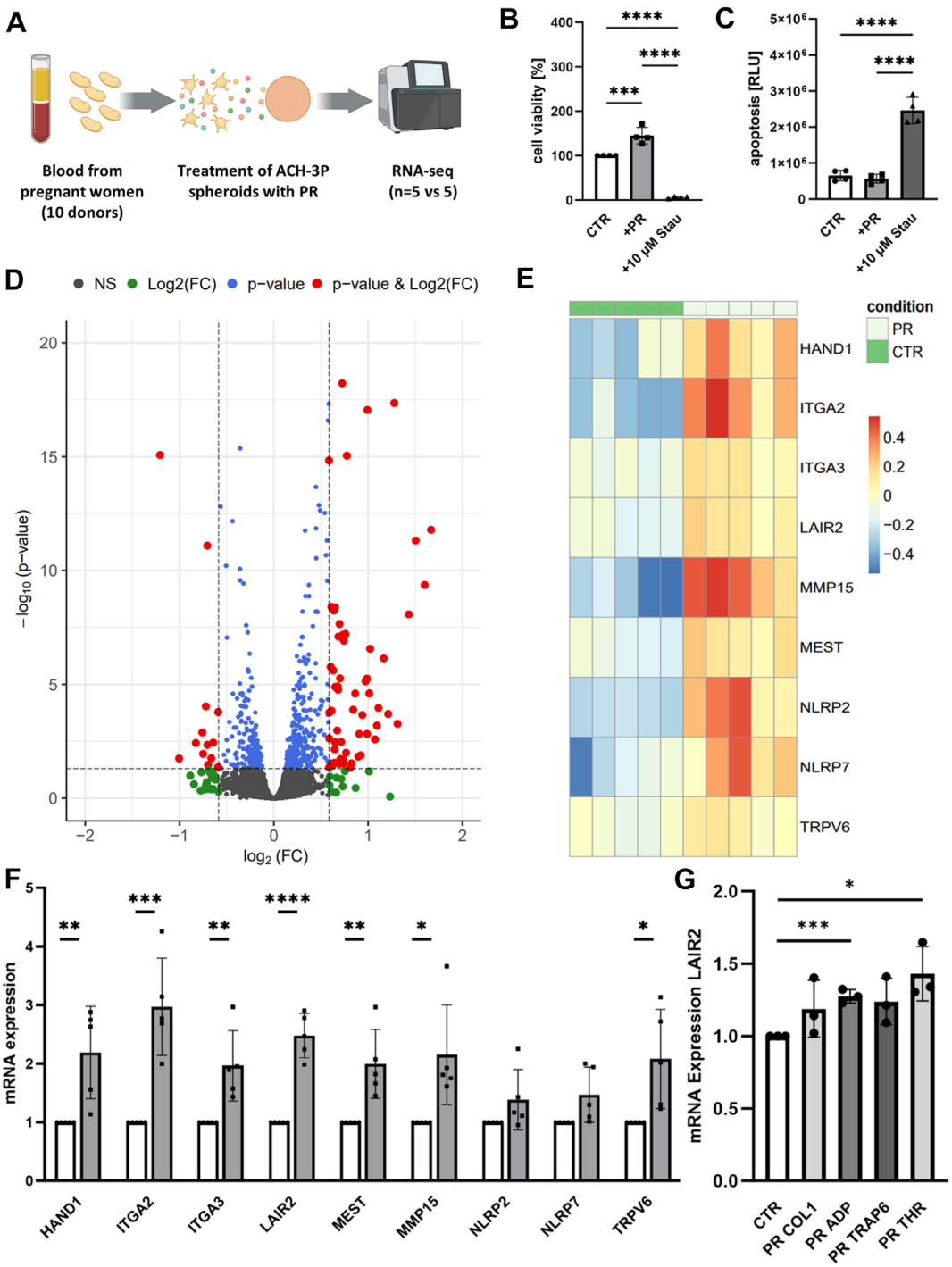

FIGURE 1 Platelet-derived factors modulate transcriptome of trophoblasts. Platelets were isolated from whole blood from pregnant women (n = 10) and activated with thrombin. ACH-3P spheroids were treated with supernatant from activated platelets (platelet releasate fraction, PR) and analyzed by RNA-seq (A). PR enhanced the cell viability of the spheroids (B) but did not affect apoptosis (C) in comparison to control spheroids (CTR). Staurosporine (Stau, 10 µM, 24 hours) was applied to induce apoptosis. RNA-seq data revealed a significant upregulation of 65 genes and a significant downregulation of 13 genes in spheroids upon treatment with PR (D). Gene expression patterns (based on relative rlog values) of genes involved in embryonic or placental development (E). Deregulation of gene expression was confirmed by qPCR (F). *LAIR2* expression was analyzed in ACH-3P monolayer cultures that were incubated with either collagen I-, ADP-, TRAP6- or thrombin-induced PR, which was prepared from 4 different donors (G). Data are presented as mean ± SD. FC, fold change; HAND1, heart and neural crest derivatives expressed 1; ITGA, integrin subunit alpha; LAIR2, leukocyte associated immunoglobulin-like receptor 2; MEST, mesoderm specific transcript; MMP15, matrix metalloproteinase 15; NLRP, NOD-like receptor protein; NS, not significant; qPCR, quantitative polymerase chain reaction; RNA-seq, RNA-sequencing; TRPV6, transient receptor potential cation channel subfamily V member 6. $^{*}P \leq .05$, $^{**}P \leq .01$, $^{***}P \leq .0002$, $^{****}P \leq 0.0001$. Parts of the figure were created with BioRender.com.

3.2 | LAIR2 is highly expressed in invading trophoblasts of the first trimester placenta

From the obtained RNA-seq data set, we identified *LAIR2* (log_2FC = 1.60) as a gene of interest (Figure 1E) potentially linking platelet function and placental development. It is worth mentioning that, besides thrombin-induced PR, COL1A1-, ADP-, and TRAP6-induced PR, although less pronounced, also elicited the same trend of increased *LAIR2* expression in ACH-3P cells grown in monolayers, with only ADP-induced PR reaching statistical significance (Figure 1G). Previous studies have implicated the involvement of LAIR2 in the invasion capacity of EVTs and in uterine spiral artery remodeling, as well as collagen-binding and platelet activation [27–29]. Analysis of our recent snRNA-seq data from human first trimester placenta samples [20] revealed strong expression of *LAIR2* in the CCTs (Figure 2A, B). Immunohistochemical staining was consistent with these findings, showing LAIR2-positive cells throughout cell columns of anchoring villi (Figure 2C). Of note, the platelets themselves were negative for LAIR2 staining (Supplementary Figure S2). To validate snRNA-seq and immunostaining, we performed mRNA-based padlock probe *in situ* hybridization in combination with immunofluorescence staining, which confirmed *LAIR2* expression in trophoblasts positively stained for EVT marker HLA-G in first trimester villous tissue (Figure 2D, E). To further validate *LAIR2* expression in early placental development, we isolated primary trophoblasts from first trimester placental tissue and cultured them as organoids. Interestingly, immunofluorescence double staining confirmed that neither HLA-G (Figure 2F) nor LAIR2 (Figure 2G) was expressed in trophoblast organoids, while organoids in which EVT differentiation was induced showed strong HLA-G expression (Figure 2H) and a trend toward increased *LAIR2* expression (Figure 2I, J). This trend was even more pronounced when organoids in which EVT differentiation was induced were incubated with PR (Figure 2J). However, no statistical significance was reached, likely due to substantial interdonor variations in the primary cells used.

3.3 | Platelets and their released factors induce trophoblastic *LAIR2* expression

To more accurately investigate the influence of maternal platelet activation on trophoblastic *LAIR2* mRNA expression, an *in situ* padlock probe approach was performed on ACH-3P spheroids in the absence and presence of PR from pregnant women. It is worth mentioning that in both settings, cells of the superficial layers of spheroids generally showed more overall, as well as more intensive, signals than the middle layers and the inner core (Figure 3A, D). Although control spheroids showed more evenly distributed signals altogether, *LAIR2* signals clearly accumulated more in PR-treated spheroids (Figure 3E) compared with controls (Figure 3B). *LAIR2* expression was calculated relative to that of actin β (*ACTB*, Figure 3C, F). In line with RNA-seq data, PR-treated spheroids showed an increase in normalized *LAIR2* signals compared to control spheroids (Figure 3G). ELISA analysis of cell protein lysates from ACH-3P spheroids were consistent with the mRNA expression and showed significantly upregulated LAIR2 in spheroids exposed to PR compared to controls (Figure 3H). In addition, ACH-3P cells were cultured to form spheroids either in absence of platelets or presence of nonactivated (ie, resting) and activated platelets. While resting platelets appeared to have no impact on *LAIR2* mRNA expression, thrombin-activated platelets significantly induced *LAIR2* expression in coculture (Figure 3I). Immunohistochemical staining of all 3 groups of spheroids revealed the distinct cavity (Figure 3J), as previously described [18], while platelets, visualized with platelet marker CD42b, accumulated not only in the cavity but also in between trophoblast layers in both resting (Figure 3K) and activated states (Figure 3L).

3.4 | LAIR2 promotes trophoblast invasion and inhibits COL1A1-induced platelet activation

Next, we stained human first trimester decidua samples for HLA-G, confirming substantial invasion of EVTs in decidua basalis samples (Figure 4A), while the decidua parietalis—the noninvaded region of the pregnant uterine mucosa—was, as expected, negative for HLA-G staining (Figure 4B). HLA-G staining revealed erosion of decidual blood vessels (arrowhead in Figure 4A), accompanied by extravasation of maternal blood cells into the decidual stroma. The extravasation was visualized by hematoxylin and eosin staining of consecutive sections, showing erythrocytes in adjacent perivascular areas (Figure 4C), and confirmed by immunostaining for endothelial marker CD31, which also revealed erythrocytes in perivascular areas (Figure 4E). Since leakage of blood into the decidual stroma can be expected to coagulate in presence of ECM components, we stained for COL1A1, a highly thrombogenic ECM protein. In the decidua parietalis, COL1A1 was most prominent in subepithelial areas of the zona compacta (the uppermost densely packed layer, rich in decidual stroma cells and ECM) (Figure 4H), gradually decreasing toward the zona spongiosa (layer showing dilated and differentiated uterine glands), in which it was prevailing in the tunica adventitia of the spiral arteries. COL1A1 was also present in the decidua basalis (Figure 4G), where we observed EVT-eroded blood vessels and extravasated blood. Congruent regions of the decidua basalis positive for HLA-G were also positive for LAIR2 (Figure 4I), whereas the noninvaded decidua parietalis was negative (Figure 4J), cumulatively suggesting that within decidual tissue, only invading EVTs express *LAIR2* at the fetal-maternal interface.

Immunofluorescence staining showed colocalization of HLA-G (green) and LAIR2 (red), confirming the presence of LAIR2 in invaded EVTs in the decidua basalis (Figure 5A–D). Since LAIR2 is a secreted decoy receptor for collagen and collagen is present in the decidua, we next tested whether LAIR2 plays a role in the EVT invasion process. For this purpose, we performed siRNA-mediated silencing of *LAIR2*, which resulted in a 73% knockdown of *LAIR2* expression compared to control (Figure 5E). The subsequent invasion behavior of ACH-3P cells was studied using an ECM invasion assay. The results showed that cell invasion was significantly increased

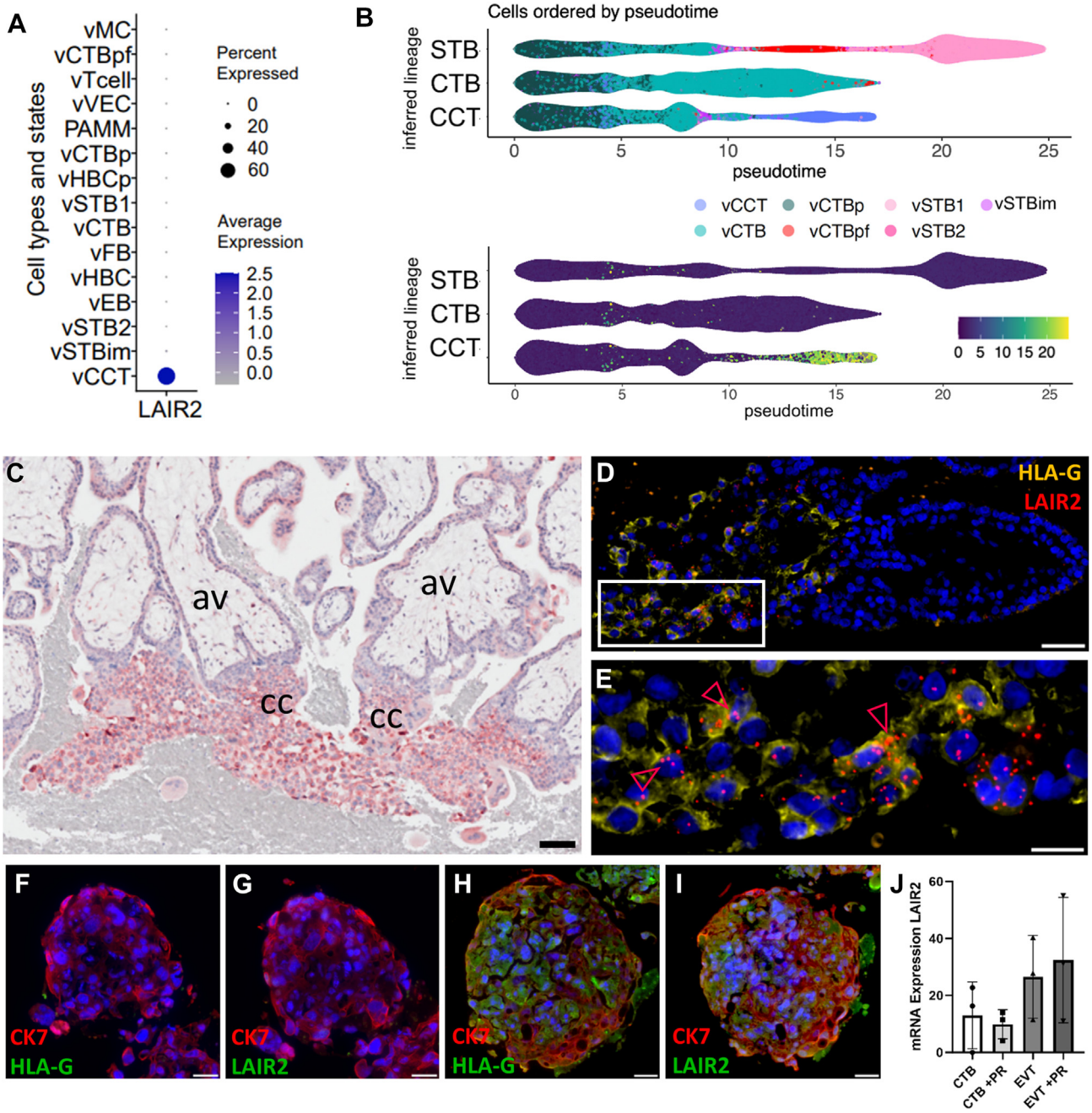

FIGURE 2 Expression of *LAIR2* in human placenta samples. Analysis of snRNA-seq data showed that *LAIR2* is predominantly expressed in the cell column trophoblast (vCCT) population of human villous first trimester placenta; abbreviations for other villus-associated cell populations: myocyte (vMC); prefusion cytotrophoblast (vCTPpf); vascular endothelial cell (vVEC); placenta-associated maternal monocyte/macrophage (PAMM); proliferating cytotrophoblast (vCTBp); proliferating Hofbauer cell (vHBCp); syncytiotrophoblast 1 (vSTB1) and 2 (vSTB2); cytotrophoblast (vCTB); fibroblast (vFB); Hofbauer cell (vHBC); erythroblast (vEB); immature syncytiotrophoblast (vSTBim); (A). Scatter plot of modeled pseudotime values separated by inferred lineage. Each dot represents a nucleus, colored by its annotated cell type or state membership (B). Immunohistochemistry confirmed LAIR2 expression in distal parts of cell columns (cc) of anchoring villi (av) (C). *In situ* padlock probe hybridization approach showing strong LAIR2 mRNA signals (arrowheads) in HLA-G positive (yellow) cells of villous tissue (D and E, enlargement of the boxed region in D). Double immunofluorescence of adjacent section of trophoblast organoids for CK7 (F–I, red) with either HLA-G or LAIR2 (both green) showed that undifferentiated primary trophoblast organoids were negative for HLA-G (F) and LAIR2 (G), while organoids induced to undergo differentiation toward the EVT phenotype showed strong expression of HLA-G (H) and LAIR2 (I). First trimester trophoblast organoids that underwent EVT differentiation showed increased LAIR2 mRNA expression, which is slightly increased in presence of PR (J). Data in J are presented as mean ± SD from 3 different experiments. Scale bar in C represents 100 μm. Scale bars in D and F–I represent 50 μm. Scale bar in E represents 20 μm. CCT, cell column trophoblast; CTB, cytotrophoblast; EVT, extravillous trophoblast; HLA-G, major histocompatibility complex, class I, G; LAIR2, leukocyte associated immunoglobulin-like receptor 2; PR, platelet releasate fraction; snRNA-seq, single–nucleus RNA-sequencing; STB, syncytiotrophoblast.

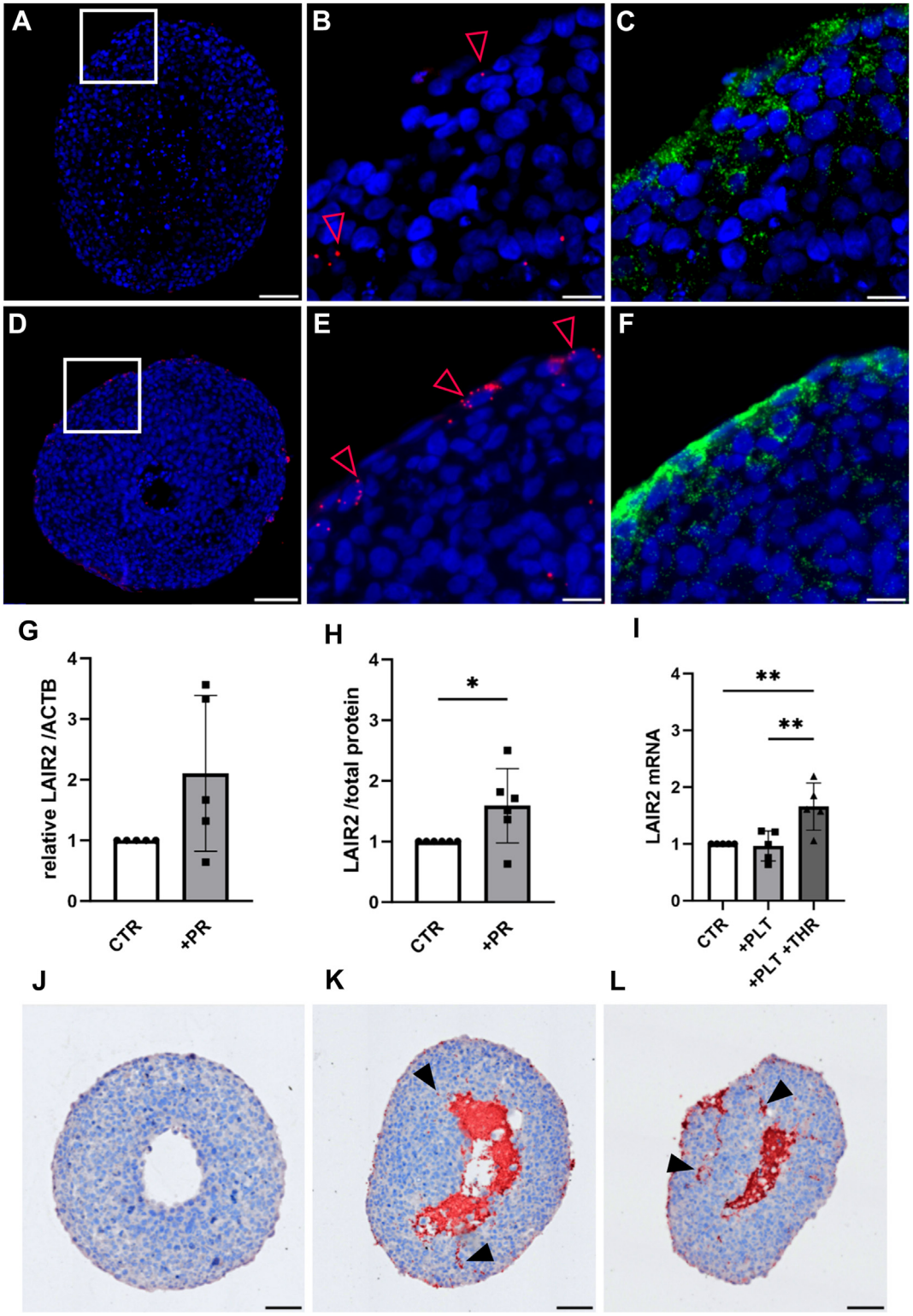

FIGURE 3 Platelets and their derived factors induce *LAIR2* expression of trophoblast spheroids. Padlock probe-based *in situ* hybridization was performed on ACH-3P spheroids incubated in absence (A–C) or presence (D–F) of platelet releasate fraction (PR). Results showed only moderate expression of *LAIR2* in control ACH-3P spheroids (B, arrowheads), while spheroids incubated with PR showed strong signals mostly in the superficial cell layers (E, arrowheads). Expression of actin β (*ACTB*) was used as an internal reference, shown in green (C and F). Software-based analysis of signals in the superficial layers of the spheroids confirmed higher expression of *LAIR2* in PR-treated spheroids (G). ELISA measurements of protein lysates of the spheroids showed significantly increased LAIR2 (H). Coincubation of spheroids with resting platelets (+PLT) showed no effect, whereas activation of the platelets with thrombin (+PLT +THR) significantly increased *LAIR2* expression (I). Spheroids formed cavities in their core (J). Upon coincubation of spheroids with resting (K) or activated platelets (L), platelets can be found—irrespective of their activation status—in the cavities as well as in the intercellular space of trophoblasts (arrowheads). Scale bars in A, D, and J–L represent 100 μm. Scale bars in all other images represent 20 μm. Data are presented as mean ± SD from 5 (A–G and I) or 6 (H) different experiments. CTR, control spheroids; LAIR2, leukocyte associated immunoglobulin-like receptor 2. $^{*}P \leq .05$, $^{**}P \leq .01$.

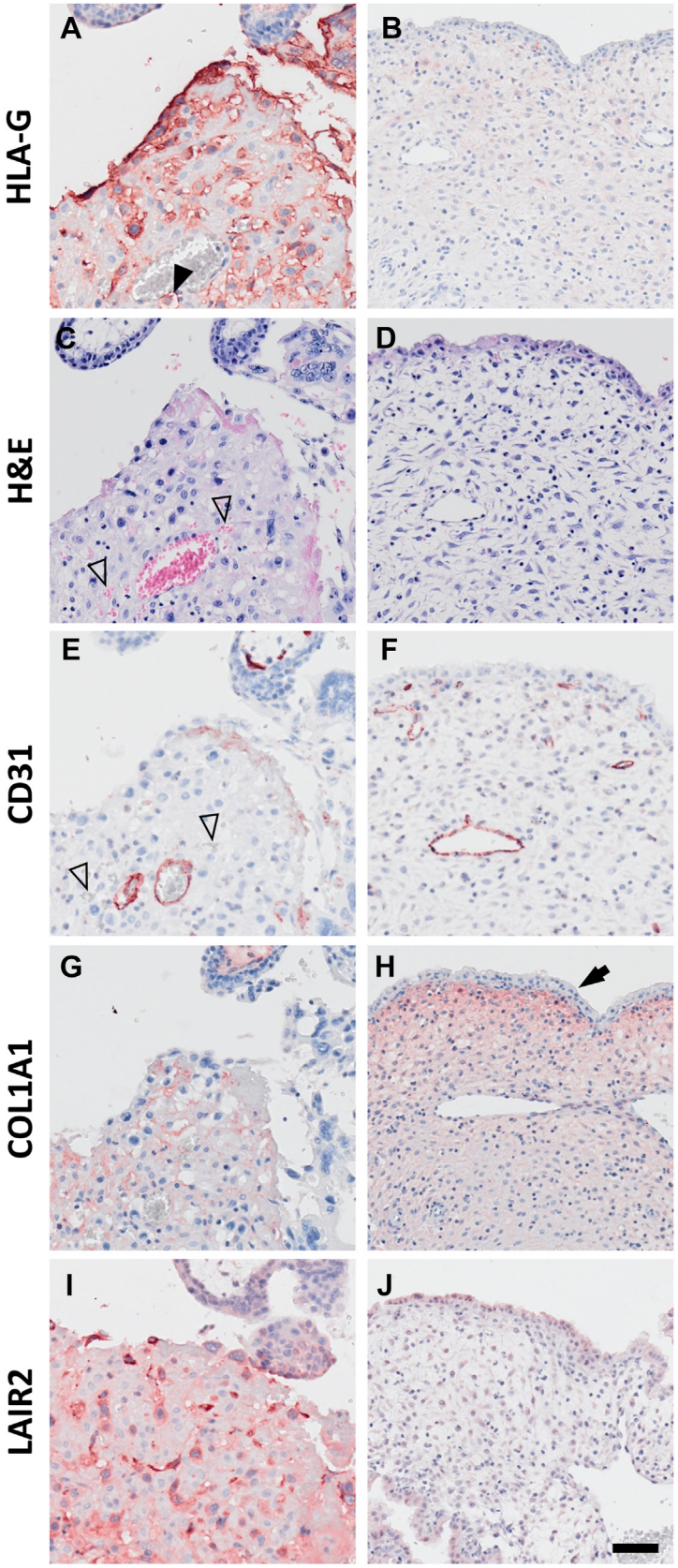

FIGURE 4 LAIR2-positive extravillous trophoblasts (EVTs) erode decidual blood vessels, leading to extravasation of maternal blood. Decidua basalis (left column) and corresponding decidua parietalis (right column) tissue sections were stained for major histocompatibility complex, class I, G (HLA-G) (A and B) and showed invasion of EVTs (arrowhead) into decidual blood vessels. Hematoxylin and eosin (H&E) staining (C and D) of consecutive sections revealed extravasated maternal erythrocytes in the invaded decidua basalis regions (C, arrowheads). This extravasation of erythrocytes (arrowheads) was confirmed by CD31 staining of the decidua basalis (E) and parietalis (F). Collagen I (COL1A1) (G and H) was detected in both decidua basalis (G) and parietalis, the latter of which showed prominent COL1A1 content underneath the uterine epithelium (H, arrow). LAIR2 staining (I and J) revealed positive cells only in the decidua basalis. Representative images were acquired from a decidua at gestational age 7+0. Scale bar represents 50 μm. LAIR2, leukocyte associated immunoglobulin like receptor 2.

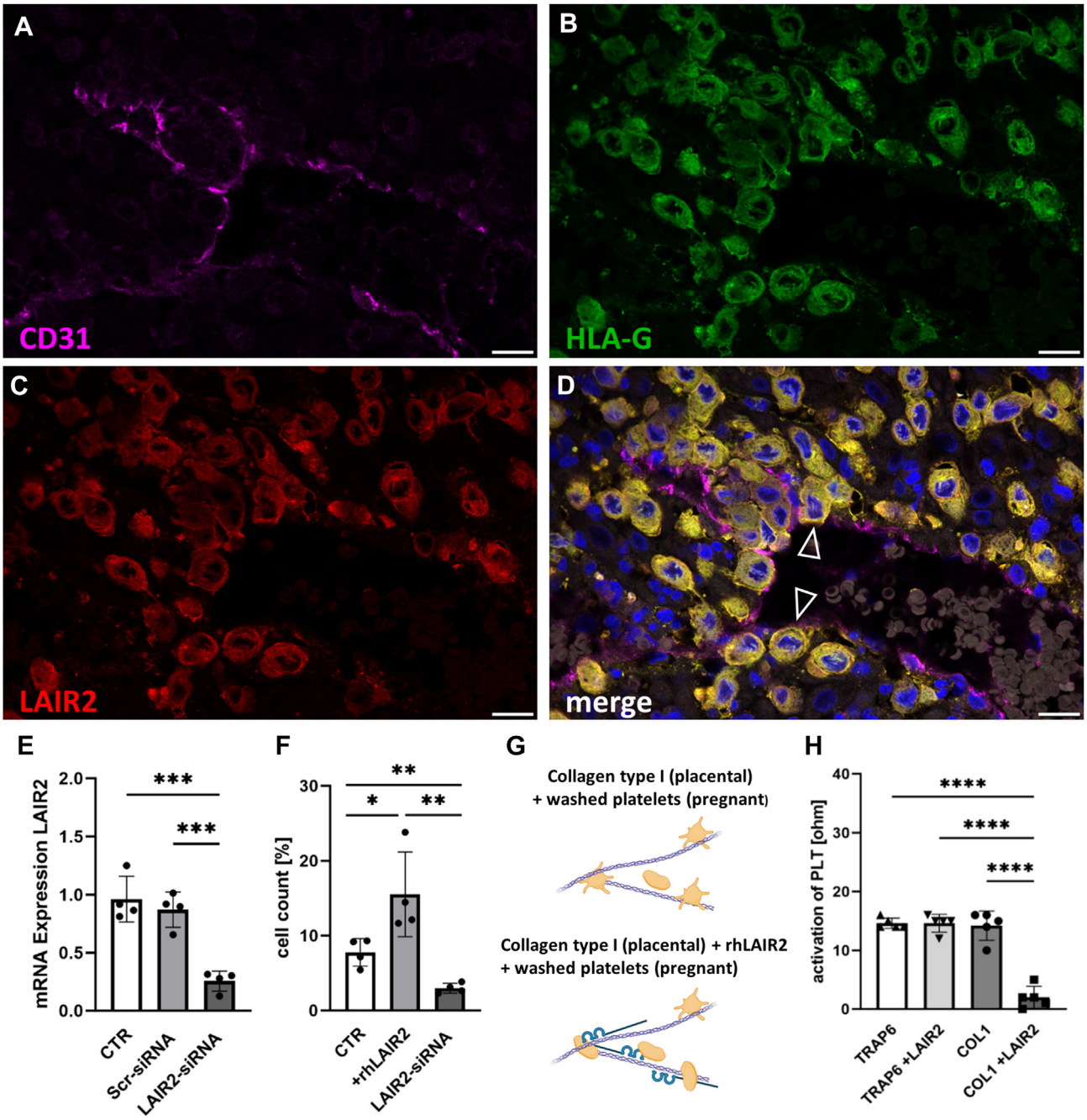

FIGURE 5 LAIR2 promotes trophoblast invasion and inhibits maternal platelet activation. Triple immunofluorescence for endothelial marker CD31 (A), HLA-G (B) and LAIR2 (C), confirmed LAIR2 expression in extravillous trophoblasts (arrowheads) that invaded in a decidual blood vessel and partly replaced the endothelial lining (D, merge). LAIR2 mRNA expression in control ACH-3P cells (CTR) was compared with that in cells treated with either scrambled siRNA (Scr-siRNA) or LAIR2-siRNA (E). Invasion of ACH-3P cells was determined by an extracellular matrix invasion assay, which showed increased invasion in the presence of rhLAIR2 and decreased invasion after siRNA-mediated LAIR2 silencing (F). To test the effect of LAIR2 on collagen-induced platelet activation, platelets from pregnant women were stimulated with either collagen type I (COL1) or TRAP6, which were either preincubated with or without rhLAIR2 (G). Subsequent aggregometry showed that preincubation with LAIR2 inhibited platelet activation induced by COL1 but not TRAP6 (H). Scale bar represents 20 μm. Data are presented as mean ± SD from 4 (E and F) and 5 (H) different experiments. CTR, control spheroids; HLA-G, major histocompatibility complex, class I, G; LAIR2, leukocyte associated immunoglobulin-like receptor 2; PLT, platelets; rhLAIR2, recombinant human LAIR2; siRNA, small interfering RNA; TRAP6, thrombin receptor activator peptide 6. $^{*}P \leq .05$, $^{**}P \leq .01$, $^{***}P \leq .0002$, $^{****}P \leq .0001$. Parts of the figure were created with BioRender.com.

nearly 2-fold, in the presence of rhLAIR2 protein, whereas it was reduced by 2.6-fold after *LAIR2* silencing, compared with the control (Figure 5F). Besides affecting invasion, LAIR2 could play a crucial role in regions where maternal blood leaks into perivascular ECM by binding and sequestering collagen, thereby possibly affecting activation of leaking maternal platelets. Aggregometry measurements using

platelet samples from pregnant women revealed that both TRAP6, a synthetic peptide that mimics the action of thrombin, as well as COL1A1 strongly activated maternal platelets. However, when both agonists were preincubated with rhLAIR2 protein, activation via collagen was almost completely blocked, while there was no interference whatsoever with TRAP6 (Figure 5G, H).

4 | DISCUSSION

Our study suggests that activation of maternal platelets and release of their cargo affect the transcriptional profile of invasive trophoblasts at the maternal-fetal interface. Bioinformatics analysis of the trophoblast transcriptome shows that cells shift toward an expression pattern associated with migration and adhesion, thereby contributing to tissue and vascular development in response to platelet-derived factors. Among the deregulated genes, *LAIR2*—a gene expressed exclusively in the extravillous lineage among trophoblast populations—is upregulated by platelet-derived factors. Importantly, bioinformatics pseudotime analysis of a snRNA-seq dataset using first trimester placenta mapped *LAIR2* expression to the CCT trajectory. This finding is substantiated not only *in situ* on mRNA and protein levels, but also *in vitro*, when primary trophoblast organoids are triggered to undergo differentiation toward the EVT phenotype. The fact that the presence of resting platelets within trophoblast spheroids did not induce *LAIR2* expression, whereas thrombin-activated platelets did, suggests that it is not the platelets themselves, but rather platelet-derived factors that play the regulatory role. In this context, we propose a novel 3D concept to study the interaction of human platelets with trophoblasts *in vitro*, mimicking the presence of platelets within the intercellular space of distal CCTs in first trimester of pregnancy [9,30]. Evidence from our previous transmission electron microscopy investigations suggests that platelets are activated in this location, further substantiating the assumption that the release of platelet-derived factors could partly influence cell column trophoblast fate and in particular induce *LAIR2* expression in this trophoblast lineage [9]. One of these factors could be platelet-derived transforming growth factor β, which has recently been suggested as a crucial driver in the differentiation of placental EVTs into decidual EVTs [31]. As expected, our data show that platelet-derived factors do not induce caspase-dependent apoptosis in trophoblast spheroids, but, in fact, increased their viability significantly. While this finding may not be surprising, given the established role of platelet-rich plasma in promoting cell viability and its increasing use as an alternative to fetal bovine serum in cell culture experiments, it nonetheless represents a noteworthy observation [32].

From the distal ends of the CCTs, invasive EVTs start to invade into the decidua basalis stroma, where they erode maternal blood vessels and replace vascular endothelial cells. Intriguingly, our histological survey revealed maternal erythrocytes within interstitial gaps of highly invaded decidua samples, suggesting extravasation of maternal blood in these areas. Leakage of blood cells usually occurs due to increased vascular permeability or compromised integrity of the vessel wall and has been described for pathological scenarios at both macroscopic and microscopic levels, including tissue trauma and within tissues characterized by leaky or immature blood vessels, such as in large atherosclerotic plaques and tumors [33]. The presence of collagen, primarily produced by decidual stromal cells, as well as EVT-derived fibronectin and laminin [34], can be expected to quickly activate leaking platelets and trigger coagulation of extravasated maternal blood. Coagulation and deposition of fibrin may contribute to the initial steps of development of the Nitabuch stria, a layer of fibrinoid located deeper in the basal plate embedding maternal and fetal cells [5]. LAIR2 is a soluble collagen receptor that can modulate immune responses by interacting with collagen. It acts as a decoy receptor, preventing the binding of LAIR1 to collagen, which can influence immune cell behavior and tumor microenvironments [35]. In the context of tumor research, *LAIR2* expression is associated with immune infiltration and can serve as a biomarker for T cell exhaustion in the tumor microenvironment [36]. Based on knowledge from tumor research, it is thus tempting to speculate about a modulating role of EVT-derived LAIR2 in the immune interactions of maternal immune cells with invading trophoblasts. However, another role of LAIR2 may be fine-tuning the coagulation of leaked maternal blood in perivascular regions of the invaded decidua (Figure 6), thereby contributing to fibrinoid deposition and the development of the Nitabuch stria. In particular, we propose that EVT invasion into decidual blood vessels and replacement of their endothelial lining is associated with maternal blood leakage into the perivascular regions of the decidual stroma, where coagulation is likely to occur in the presence of ECM components. Initial activation of platelets and the release of their cargo promotes trophoblastic *LAIR2* expression, which is subsequently secreted into the surrounding intercellular space. There, LAIR2 functions as a decoy receptor by binding to COL1A1, facilitating further trophoblast invasion while simultaneously preventing excessive maternal platelet activation.

Our results align with previous studies showing strong *LAIR2* expression mainly in CCTs as well as EVTs of first trimester placenta [27,37]. We and others have shown that LAIR2 contributes to increased invasiveness of ACH-3P cells, implicating that an upregulation of this gene might also enhance trophoblast invasiveness in an autocrine manner, potentially positively impacting placental development and function [28]. Even slightly abnormal changes in the molecular profile of trophoblasts undergoing differentiation toward the EVT lineage are proposed factors responsible for overinvasion, leading to pathologies such as abnormal invasive placenta [38]. Of note, previous publications have even discussed a potential correlation between diminished *LAIR2* expression in placental tissue and the development of preeclampsia. More specifically, it has been proposed that the downregulation of *LAIR2* expression may lead to impaired physiologic spiral artery conversion. A difference in expression levels of LAIR2 in placental tissue between women who developed preeclampsia and women who remained healthy throughout gestation

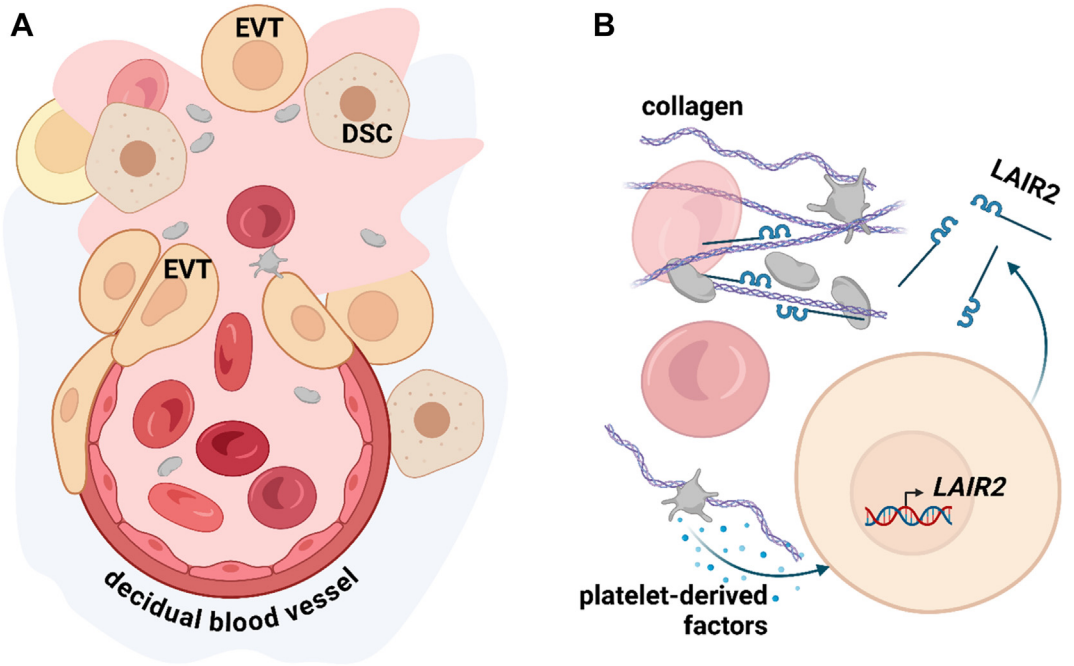

FIGURE 6 Proposed concept for LAIR2 in the maternal-fetal interface. Invaded extravillous trophoblasts (EVT) erode decidual blood vessels and partly replace the endothelial lining. Erosion of blood vessels is accompanied by leakage of maternal blood into perivascular regions of the decidual stroma (decidual stroma cells [DSC]) and can be expected to coagulate in presence of extracellular matrix components (A). Initial platelet activation and the release of their cargo induce trophoblastic LAIR2 expression, which is then secreted into the adjacent intercellular space. There, it acts as a decoy receptor by binding to collagen I, subsequently promoting further trophoblast invasion while also inhibiting excessive activation of maternal platelets (B). LAIR2, leukocyte associated immunoglobulin-like receptor 2. Figure was created with BioRender.com.

was detected by chorionic villus biopsy and has been suggested as a biomarker for preeclampsia risk prediction [27,37,39].

Bioinformatics analysis of the RNA-seq data revealed significant gene ontology terms, such as regulation of cell development and embryonic morphogenesis. Heart and neural crest derivatives expressed 1 (*HAND1*), found to be deregulated in response to platelet-derived factors, might be an important player in these processes. Here, the trophoblast cell line ACH-3P was used for functional coculture experiments with maternal platelets. This may be considered a limitation, since expression of *HAND1*, a key regulator of murine trophoblast development, is present in choriocarcinoma cells and the human trophectoderm, whereas it is absent from first trimester placenta [40]. However, the use of platelets obtained from pregnant individuals and the novel 3D coculture with trophoblasts to mimic the exposure of extravasated maternal platelets to EVTs, as described in the intercellular space of CCTs or EVT-eroded decidual blood vessels, can be considered as a strength of the current study.

In conclusion, this study suggests that maternal platelet-derived factors regulate the transcriptional profile of trophoblasts. This includes regulation of genes involved in placental development, including *LAIR2*, a gene exclusively expressed in the invasive trophoblast linage. Trophoblast-derived LAIR2 may be involved in the fine-tuning of coagulation of leaking maternal blood in the decidua and the invasiveness of EVTs into it through an autocrine manner.

ACKNOWLEDGMENTS

The authors gratefully appreciate the excellent technical assistance of Bettina Amtmann. The authors thank Dr Andreas Glasner and the staff of Auckland Medical Aid Centre for recruiting first trimester placental tissue samples for this study. Figures were partly created with BioRender (https://www.biorender.com; license granted to Martin Gauster).

AUTHOR CONTRIBUTIONS

F.L. and M.G. conceived and designed the study, analyzed data, and drafted the manuscript. F.L., D.F., J.G., N.K., K.U., L.N., C.D., D.V., J.C.K., A.L.H., and D.S.V. performed experiments and analyzed data. A.E.H., D.K., J.F., G.M., B.R., G.C., F.H., S.W., J.P., and J.L.J. provided acquisition, analysis, and interpretation of data and performed statistical analysis. All authors revised and approved the manuscript.

DECLARATION OF COMPETING INTERESTS

There are no competing interests to disclose.

DECLARATION OF GENERATIVE AI AND AI-ASSISTED TECHNOLOGIES IN THE WRITING PROCESS

During the preparation of this work the authors used ChatGPT to enhance clarity and refine complex sentence structures. After using

this tool, the authors reviewed and edited the content as needed and take full responsibility for the content of the publication.

ORCID

Julia Feichtinger https://orcid.org/0000-0002-3667-5857
Martin Gauster https://orcid.org/0000-0003-0386-6857

REFERENCES

[1] Huppertz B, Schleußner E. *The placenta: basics and clinical significance*. Heidelberg: Springer Berlin; 2023.
[2] Benirschke K, Burton GJ, Baergen RN. *Pathology of the human placenta*. 6th ed. Heidelberg: Springer-Verlag Berlin; 2012.
[3] Huppertz B, Berghold VM, Kawaguchi R, Gauster M. A variety of opportunities for immune interactions during trophoblast development and invasion. *Am J Reprod Immunol*. 2012;67:349–57.
[4] Gauster M, Moser G, Wernitznig S, Kupper N, Huppertz B. Early human trophoblast development: from morphology to function. *Cell Mol Life Sci*. 2022;79:345.
[5] Kaufmann P, Huppertz B, Frank HG. The fibrinoids of the human placenta: origin, composition and functional relevance. *Ann Anat*. 1996;178:485–501.
[6] Lackner AI, Pollheimer J, Latos P, Knöfler M, Haider S. Gene-network based analysis of human placental trophoblast subtypes identifies critical genes as potential targets of therapeutic drugs. *J Integr Bioinform*. 2023;20:20230011. https://doi.org/10.1515/jib-2023-0011
[7] Roberts VHJ, Morgan TK, Bednarek P, Morita M, Burton GJ, Lo JO, Frias AE. Early first trimester uteroplacental flow and the progressive disintegration of spiral artery plugs: new insights from contrast-enhanced ultrasound and tissue histopathology. *Hum Reprod*. 2017;32:2382–93.
[8] Sato Y, Fujiwara H, Zeng BX, Higuchi T, Yoshioka S, Fujii S. Platelet-derived soluble factors induce human extravillous trophoblast migration and differentiation: platelets are a possible regulator of trophoblast infiltration into maternal spiral arteries. *Blood*. 2005;106:428–35.
[9] Guettler J, Forstner D, Cvirn G, Maninger S, Brugger BA, Nonn O, Kupper N, Pritz E, Wernitznig S, Dohr G, Hutter H, Juch H, Isermann B, Kohli S, Gauster M. Maternal platelets pass interstices of trophoblast columns and are not activated by HLA-G in early human pregnancy. *J Reprod Immunol*. 2021;144:103280. https://doi.org/10.1016/j.jri.2021.103280
[10] Michelson AD. *Platelets*. 3rd ed. San Diego, CA: Academic Press; 2013.
[11] Boehlen F, Hohlfeld P, Extermann P, Perneger TV, de Moerloose P. Platelet count at term pregnancy: a reappraisal of the threshold. *Obstet Gynecol*. 2000;95:29–33.
[12] Forstner D, Guettler J, Gauster M. Changes in maternal platelet physiology during gestation and their interaction with trophoblasts. *Int J Mol Sci*. 2021;22:10732. https://doi.org/10.3390/ijms221910732
[13] Reese JA, Peck JD, Yu Z, Scordino TA, Deschamps DR, McIntosh JJ, Terrell DR, Vesely SK, George JN. Platelet sequestration and consumption in the placental intervillous space contribute to lower platelet counts during pregnancy. *Am J Hematol*. 2019;94:E8–11.
[14] Moser G, Guettler J, Forstner D, Gauster M. Maternal platelets—friend or foe of the human placenta? *Int J Mol Sci*. 2019;20:5639. https://doi.org/10.3390/ijms20225639
[15] Forstner D, Guettler J, Brugger BA, Lyssy F, Neuper L, Daxboeck C, Cvirn G, Fuchs J, Kraeker K, Frolova A, Valdes DS, Stern C, Hirschmugl B, Fluhr H, Wadsack C, Huppertz B, Nonn O, Herse F, Gauster M. CD39 abrogates platelet-derived factors induced IL-1β expression in the human placenta. *Front Cell Dev Biol*. 2023;11:1183793. https://doi.org/10.3389/fcell.2023.1183793
[16] Lyssy F, Guettler J, Brugger BA, Stern C, Forstner D, Nonn O, Fischer C, Herse F, Wernitznig S, Hirschmugl B, Wadsack C, Gauster M. Platelet-derived factors dysregulate placental sphingosine-1-phosphate receptor 2 in human trophoblasts. *Reprod Biomed Online*. 2023;47:103215. https://doi.org/10.1016/j.rbmo.2023.04.006
[17] Hiden U, Wadsack C, Prutsch N, Gauster M, Weiss U, Frank HG, Schmitz U, Fast-Hirsch C, Hengstschläger M, Pötgens A, Rüben A, Knöfler M, Haslinger P, Huppertz B, Bilban M, Kaufmann P, Desoye G. The first trimester human trophoblast cell line ACH-3P: a novel tool to study autocrine/paracrine regulatory loops of human trophoblast subpopulations—TNF-α stimulates MMP15 expression. *BMC Dev Biol*. 2007;7:137.
[18] Lyssy F, Forstner D, Brugger BA, Ujčič K, Guettler J, Kupper N, Wernitznig S, Daxboeck C, Neuper L, El-Heliebi A, Kloimboeck T, Kargl J, Huppertz B, Ghaffari-Tabrizi-Wizsy N, Gauster M. The chicken chorioallantoic membrane assay revisited—a face-lifted approach for new perspectives in placenta research. *Placenta*. Published online April 30, 2024. https://doi.org/10.1016/j.placenta.2024.04.013
[19] Afgan E, Baker D, Batut B, van den Beek M, Bouvier D, Cech M, Chilton J, Clements D, Coraor N, Grüning BA, Guerler A, Hillman-Jackson J, Hiltemann S, Jalili V, Rasche H, Soranzo N, Goecks J, Taylor J, Nekrutenko A, Blankenberg D. The Galaxy platform for accessible, reproducible and collaborative biomedical analyses: 2018 update. *Nucleic Acids Res*. 2018;46:W537–44.
[20] Nonn O, Debnath O, Valdes DS, Sallinger K, Secener AK, Fischer C, Tiesmeyer S, Nimo J, Kuenzer T, Ulrich J, Maxian T, Knöfler M, Karau P, Bartolomaeus H, Kroneis T, Frolova A, Neuper L, Haase N, Malt A, Müller-Bötticher N, et al. Senescent syncytiotrophoblast secretion during early onset preeclampsia. *Hypertension*. Published online October 23, 2024. https://doi.org/10.1161/HYPERTENSIONAHA.124.23362
[21] El-Heliebi A, Hille C, Laxman N, Svedlund J, Haudum C, Ercan E, Kroneis T, Chen S, Smolle M, Rossmann C, Krzywkowski T, Ahlford A, Darai E, von Amsberg G, Alsdorf W, König F, Löhr M, de Kruijff I, Riethdorf S, Gorges TM, et al. In situ detection and quantification of AR-V7, AR-FL, PSA, and *KRAS* point mutations in circulating tumor cells. *Clin Chem*. 2018;64:536–46.
[22] El-Heliebi A, Kashofer K, Fuchs J, Jahn SW, Viertler C, Matak A, Sedlmayr P, Hoefler G. Visualization of tumor heterogeneity by in situ padlock probe technology in colorectal cancer. *Histochem Cell Biol*. 2017;148:105–15.
[23] Sun C, Chamley LW, James JL. Organoid generation from trophoblast stem cells highlights distinct roles for cytotrophoblasts and stem cells in organoid formation and expansion. *Placenta*. Published online December 5, 2024. https://doi.org/10.1016/j.placenta.2024.12.003
[24] Sun C, James JL, Murthi P. Three-dimensional in vitro human placental organoids from mononuclear villous trophoblasts or trophoblast stem cells to understand trophoblast dysfunction in fetal growth restriction. *Methods Mol Biol*. 2024;2728:235–45.
[25] Siwetz M, Sundl M, Kolb D, Hiden U, Herse F, Huppertz B, Gauster M. Placental fractalkine mediates adhesion of THP-1 monocytes to villous trophoblast. *Histochem Cell Biol*. 2015;143:565–74.
[26] Blaschitz A, Siwetz M, Schlenke P, Gauster M. Adhering maternal platelets can contribute to the cytokine and chemokine cocktail released by human first trimester villous placenta. *Placenta*. 2015;36:1333–6.
[27] Founds SA, Fallert-Junecko B, Reinhart TA, Parks WT. LAIR2-expressing extravillous trophoblasts associate with maternal spiral

arterioles undergoing physiologic conversion. *Placenta*. 2013;34:248–55.

[28] Liu J, Zhao H, Zhou F, Huang Y, Chen X, Wang S, Hao J, Xu X, He B, Wang J. Human-specific LAIR2 contributes to the high invasiveness of human extravillous trophoblast cells. *Reprod Biol*. 2019;19:287–92.

[29] Lenting PJ, Westerlaken GHA, Denis CV, Akkerman JW, Meyaard L. Efficient inhibition of collagen-induced platelet activation and adhesion by LAIR-2, a soluble Ig-like receptor family member. *PLoS One*. 2010;5:e12174. https://doi.org/10.1371/journal.pone.0012174

[30] Guettler J, Forstner D, Gauster M. Maternal platelets at the first trimester maternal-placental interface - small players with great impact on placenta development. *Placenta*. 2022;125:61–7.

[31] Haider S, Lackner AI, Dietrich B, Kunihs V, Haslinger P, Meinhardt G, Maxian T, Saleh L, Fiala C, Pollheimer J, Latos PA, Knöfler M. Transforming growth factor-β signaling governs the differentiation program of extravillous trophoblasts in the developing human placenta. *Proc Natl Acad Sci U S A*. 2022;119:e2120667119. https://doi.org/10.1073/pnas.2120667119

[32] Anitua E, Zalduendo M, Troya M, Alkhraisat MH, Blanco-Antona LA. Platelet-rich plasma as an alternative to xenogeneic sera in cell-based therapies: a need for standardization. *Int J Mol Sci*. 2022;23:6552.

[33] Humar R, Schaer DJ, Vallelian F. Erythrophagocytes in hemolytic anemia, wound healing, and cancer. *Trends Mol Med*. 2022;28:906–15.

[34] Abbas Y, Carnicer-Lombarte A, Gardner L, Thomas J, Brosens JJ, Moffett A, Sharkey AM, Franze K, Burton GJ, Oyen ML. Tissue stiffness at the human maternal–fetal interface. *Hum Reprod*. 2019;34:1999–2008.

[35] Apps R, Sharkey A, Gardner L, Male V, Trotter M, Miller N, North R, Founds S, Moffett A. Genome-wide expression profile of first trimester villous and extravillous human trophoblast cells. *Placenta*. 2011;32:33–43.

[36] Chen Z, Yu M, Yan J, Guo L, Zhang B, Liu S, Lei J, Zhang W, Zhou B, Gao J, Yang Z, Li X, Zhou J, Fan J, Ye Q, Li H, Xu Y, Xiao Y. PNOC expressed by B cells in cholangiocarcinoma was survival related and LAIR2 could be a T cell exhaustion biomarker in tumor microenvironment: characterization of immune microenvironment combining single-cell and bulk sequencing technology. *Front Immunol*. 2021;12:647209. https://doi.org/10.3389/fimmu.2021.647209

[37] Founds SA, Fallert-Junecko B, Reinhart TA, Conley YP, Parks WT. LAIR2 localizes specifically to sites of extravillous trophoblast invasion. *Placenta*. 2010;31:880–5.

[38] Illsley NP, DaSilva-Arnold SC, Zamudio S, Alvarez M, Al-Khan A. Trophoblast invasion: lessons from abnormally invasive placenta (placenta accreta). *Placenta*. 2020;102:61–6.

[39] Founds SA, Conley YP, Lyons-Weiler JF, Jeyabalan A, Hogge WA, Conrad KP. Altered global gene expression in first trimester placentas of women destined to develop preeclampsia. *Placenta*. 2009;30:15–24.

[40] Dietrich B, Kunihs V, Haider S, Pollheimer J, Knöfler M. 3-Dimensional JEG-3 choriocarcinoma cell organoids as a model for trophoblast expansion and differentiation. *Placenta*. 2021;104:243–6.

SUPPLEMENTARY MATERIAL

The online version contains supplementary material available at https://doi.org/10.1016/j.jtha.2025.03.020.

Supplementary Material

Maternal platelet-derived factors induce trophoblastic LAIR2 expression to promote trophoblast invasion and inhibit platelet activation at the foetal-maternal interface

Freya Lyssy[1], Désirée Forstner[1], Jacqueline Guettler[1], Nadja Kupper[1], Kaja Ujčič[1], Lena Neuper[1], Christine Daxboeck[1], Amin El-Heliebi[1], Daniel Kummer[1], Julian C. Krappinger[1], Djenana Vejzovic[2], Beate Rinner[2], Gerhard Cvirn[3], Stefan Wernitznig[1], Gerit Moser[1], Daniela S. Valdes[4,5], Florian Herse[4,5], Anna-Lena Höbler[6], Juergen Pollheimer[6], Joanna L. James[7], Julia Feichtinger[1]*, Martin Gauster[1]*

[1]Division of Cell Biology, Histology and Embryology; Gottfried Schatz Research Center, Medical University of Graz, Austria
[2]Division of Biomedical Research, Core Facility Alternative Biomodels and Preclinical Imaging, Medical University of Graz, Austria
[3]Division of Physiological Chemistry, Otto Loewi Research Center, Medical University of Graz, Austria.
[4] Max-Delbrück-Center for Molecular Medicine in the Helmholtz Association (MDC), Berlin, Germany
[5]Experimental and Clinical Research Center, a cooperation between the Max-Delbrück-Center for Molecular Medicine in the Helmholtz Association and the Charité - Universitätsmedizin Berlin, Berlin, Germany
[6]Department of Obstetrics and Gynecology, Reproductive Biology Unit, Maternal-fetal Immunology Group, Medical University of Vienna, Vienna, Austria
[7]Department of Obstetrics, Gynaecology and Reproductive Sciences, Faculty of Medical and Health Sciences, University of Auckland; Auckland, New Zealand

*Correspondence:
Martin Gauster, https://orcid.org/0000-0003-0386-6857
Division of Cell Biology, Histology and Embryology,
Gottfried Schatz Research Center,
Medical University of Graz,
Neue Stiftingtalstraße 6, Graz 8010, Austria
Tel: +43 316 385 71896, Fax: +43 316 385 79612
E-mail: martin.gauster@medunigraz.at

Julia Feichtinger, https://orcid.org/0000-0002-3667-5857
Division of Cell Biology, Histology and Embryology,
Gottfried Schatz Research Center,
Medical University of Graz,
Neue Stiftingtalstraße 6, Graz 8010, Austria
Tel: +43 316 385 71899, Fax: +43 316 385 79612
E-mail: julia.feichtinger@medunigraz.at

Supplemental Materials and Methods

Platelet isolation and preparation of platelet releasate

The study was approved by the ethical committee of the Medical University of Graz (31-019 ex 18/19). About 15 ml citrated whole blood per patient were collected from healthy donors before caesarean section and prior any labour activity. Patients signed written informed consents. Characteristics of the different study populations are shown in Supplemental Table 1. Blood samples were centrifuged at 100 x g for 15 min at room temperature (RT) before platelet rich plasma (PRP) was gently mixed in equal volume with a platelet wash buffer consisting of distilled water containing with 128 mM NaCl (Supelco®, Merck; Darmstadt, Germany), 11 mM glucose (Sigma) 7.5 mM Na_2HPO_4 (Merck), 4.8 mM sodium citrate (Sigma-Aldrich), 4.3 mM NaH_2PO_4 (Lactan; Graz, Austria), 2.4 mM citric acid (Merck) and 0.35% bovine serum albumin (Biowest; Nuaillé, France) with addition of 2.5 ng/µl prostaglandin (Cayman Chemical Company; Ann Arbor, MI, USA). After centrifugation at 1962 x g for 15 min at RT, the pellet was resuspended in 10 ml wash buffer. After repeated centrifugation at 1962 x g for 15 min at RT, platelets were resuspended in DMEM/F12 (1:1, Gibco) supplemented with 0.1 U/ml penicillin and 0.1 µg/ml streptomycin (Gibco) and 1% (v/v) L-glutamine (Gibco; 20 mM 100X) to physiological platelet concentrations. Platelets were counted by the Sysmex KX-21NTM system (Sysmex; Horgen, Switzerland). Platelets were either directly used for co-incubation with ACH-3P spheroids, or aggregometry measurements, or further processed.

Culture of trophoblast cell line ACH-3P and spheroid formation

The human first trimester trophoblast cell line ACH-3P was kindly provided by Gernot Desoye (Department of Obstetrics and Gynecology, Medical University Graz, Austria). ACH-3P cells were cultured in DMEM/F12 (1:1, Gibco, life technologies; Paisley, UK) supplemented with 10% FCS (Gibco), 0.1 U/ml penicillin and 0.1 µg/ml streptomycin (Gibco) and 1% (v/v) L-glutamine (Gibco; 20 mM 100X) in a humidified atmosphere of 5% CO_2 at 37°C. Cells were incubated with selection medium containing 5.7 µM azaserin (Sigma-Aldrich) and 100 µM hypoxanthine (Sigma-Aldrich) every 10^{th} passage. Cells were mycoplasma free and short tandem repeat analysis was performed regularly.

RNA Sequencing and Bioinformatics analysis

Total RNA from matched PR-treated and control ACH-3P spheroids (5 per condition) was isolated with SV Total RNA Isolation System (Promega, Madison, Wi, USA) according to the manufacturer's protocol. RNA samples were then sent to Genewiz from Azenta Life Sciences and subjected to RNA quantification using Qubit 4.0 Fluorometer (Life Technologies, Carlsbad, CA, USA) and RNA integrity was checked with RNA Kit on Agilent 5300 Fragment Analyzer, RIN > 9 (Agilent Technologies, Palo Alto, CA, USA). rRNA depletion was achieved using the NEBNext® rRNA Depletion Kit (Human/Mouse/Rat Cat. No. E6310). RNA sequencing library preparation was performed using the NEBNext Ultra RNA Library Prep Kit for Illumina following the manufacturer's recommendations

(NEB, Ipswich, MA, USA). Samples were sequenced on the Illumina NovaSeq 6000 instrument in a paired-end configuration resulting in 2x250bp read pairs.

RNA-seq analysis of the 10 samples was done within Galaxy [1]: The provided FASTQ files were subjected to quality control using FASTQC (version: Galaxy Version 0.73+galaxy0) [2] as well as MultiQC (version: Galaxy Version 1,7) [3], and remaining adapter content was trimmed using Trimmomatic (version: Galaxy Version 0.38.1) [4] with recommended parameters. Reads were aligned to the basic human reference annotation available on GENCODE (GRCh38, v42) [5] using STAR (version: Galaxy Version 2.7.7a) [6] with --twopassMode Basic, --sjdbOverhang 149 (read length -1) and otherwise default parameters. The resulting BAM files were inspected using Qualimap (version: 2.2.2d+galaxy1) [7] and quantified with htseq (version: Galaxy Version 0.9.1) [8]. Resulting count data was analyzed and visualized in R (version: 4.4.1) [9]: The DESeq2 (version: 1.44.0) [10] package was used for differential expression analysis, and a gene was considered to be significantly deregulated if its absolute log2 fold change was $\geq \log2(1.5)$ and its adjusted p-value was ≤ 0.05. Plots were generated utilizing the R packages ggplot2 (version: 3.5.1) [11], EnhancedVolcano (version: 1.22.0) [12] and pheatmap (version: 1.0.12, based on relative rlog values [13]) [14]. Next, we performed gene set enrichment analysis (GSEA), applying the R packages clusterProfiler (version: 4.12.3) [15], DOSE (version: 3.30.2) [16] and org.Hs.eg.db (version: 3.19.1) [17] and used an adjusted p-value of 0.05 as significance cutoff for GSEA. All raw RNA-seq files are provided through the NCBI Short Read Archive, accession number PRJNA1194512.

qPCR analysis

Total RNA was isolated from pooled spheroid or organoid samples using the SV Total RNA Isolation System (Promega; Madison, WI, USA) according to the manufacturer´s protocol. In addition to spheroids and organoids, 100 µl of fresh culture medium supplemented with platelet releasates (PR) and 100 µl conditioned culture medium collected after cell culture were subjected to RNA isolation and subsequent qPCR analysis. NanoDrop (ND-1000, Peqlab Biotechnology GmbH; Erlangen, Germany) was used for quality check and calculation of concentrations before reverse transcription of 1 µg total RNA per reaction using High-Capacity cDNA Reverse Transcription Kit (Applied Biosystems, Foster City, CA, USA) according to manufacturer's manual. qPCR was performed with SYBR Green (Biozym, Vienna, Austria) using the Bio-Rad CFX384 Touch Real-Time PCR Detection System (Bio-Rad; Hercules, CA, USA). Primers used are shown in Supplemental Table 2. Cq values and normalised expression (ΔΔCq analysis) were automatically generated by the CFX Manager 3.1 software (Bio-Rad). The expression of YWHAZ and TBP was used as reference.

Analysis of single-nucleus RNA sequencing data

Single-nucleus RNA-sequencing (snRNA-seq) human first trimester villi datasets were accessed from Zenodo (10.5281/zenodo.8159511) and used without additional preprocessing. Matrices were loaded into R (v4.1.2) and LAIR2 expression visualized using Seurat (v4.1.0). Trophoblast nuclei (n = 58, 198

nuclei) were subsetted and used to model the differentiation trajectory of the trophoblast in-silico. Trophoblast datasets were harmonised with the 'sctransform' package (v0.3.3). Linear dimensionality reduction was performed on the 4,000 most variable genes and principal components (PCs) calculated. Using the first 30 PCs, high dimensional latent space was reduced and visualized by UMAP. Louvain clusters were computed including a random seed for reproducibility. A resolution of 0.4, yielding 11 clusters was chosen. Count matrices and associated metadata from Seurat were used to create a SingleCellExperiment object (v.1.22.0). The trajectory was modelled on the subsetted UMAP graph using the slingshot package (v2.2.1) with the starting cluster set to cluster 5 based on expression patterns of proliferation markers *TOP2A* and *MKI67*. The package identifies global structure with a cluster-based minimum spanning tree and fits simultaneous principal curves to describe each inferred lineage.
Transition genes were calculated as described in Chen et al. [18]. Genes with a $\log_2$FC ± 0.25 between the first 20% and last 20% of nuclei in the inferred pseudotime were scaled between 0 and 1. A gene-wise Spearman correlation against pseudotime values was fitted using the stats package (v4.1.2). Genes with a correlation coefficient of ± 0.4 were identified as transition genes. Endpoint DEGs per lineage were empirically calculated using a generalized linear model likelihood ratio test via the edgeR package (v3.36.0), controlling for potential outliers and variability across samples. Genes with an FDR (Benjamini-Hochberg) < 0.01 and logFC ± 0.25 were identified to demarcate start and end phenotypes.

In situ Padlock probe analysis

Sequences for padlock probe design were obtained from the National Center for Biotechnology Information (NCBI) with the GenBank accession number NM_002288.6 (LAIR2). In brief, cDNA was produced using specific reverse transcription primers. Afterwards, padlock probes were hybridized to the cDNA. After ligation, circularized padlock probes were subjected to amplification through rolling circle amplification, and visualization with fluorescently labelled detection probes in the channel TexasRed (LAIR2). As internal positive control served human actin beta (ACTB), which was detected with atto488 fluorescent detection probes. All oligonucleotide sequences are available in Supplemental Table 3. Images were analysed using Visiopharm (Version 2021.9. Visiopharm A/S, Hørsholm, Denmark). Single spheroid sections were analysed by splitting each spheroid cross section into an outer ring area with a thickness of 60 µm and an inner area covering the rest of the spheroid cross section leaving out holes without any detected nuclei. The acquired outer spheroid area was used to assess nuclei and signal counts. Nuclei were detected using the "Nuclei Detection, AI" app within Visiopharm based on a DAPI stain. Atto488 (ACTB) and TexasRed (LAIR2) signals as well as anchor signals in Cy7 were enhanced using a polynomial blob filter after which a threshold was applied on theses filtered images in order to get single signal objects. Signals below an area of 0.3 µm² were excluded. Atto488 (ACTB) and TexasRed (LAIR2) signals that did not align with an anchor signal in Cy7 were excluded as false positive signals.

Primary trophoblast isolation and organoid formation

First trimester placental tissue was obtained from Auckland Medical Aid Centre, Auckland, New Zealand, following ethical approval by the Northern X Ethics Committee (NTX/12/06/057/AM012) and written informed consent. Primary mononuclear villous trophoblasts were isolated and cultured as organoids as previously described with minor changes [19]. In brief, 1 g of placental villi from first trimester placental tissue (6+0 - 8+4 weeks of gestation, n=3) was cut into small pieces and enzymatically digested with 10 ml of Digestion Solution containing 1.5 mg/ml DNase I (Sigma-Aldrich, Burlington, MA, USA) and 0.25% Trypsin (Gibco, Auckland, New Zealand) in PBS for 10 min at 37°C. Supernatant was discarded and villi were washed with PBS until the supernatant remained clear. A second enzymatic digest was performed with 10 ml of the same Digestion Solution as before overnight at 4°C. The following day supernatant was filtered through a 70 µm mesh filter and washed 10 times with 20 ml PBS. After centrifugation at 450 x g for 8 minutes at RT cell pellets were resuspended in Trophoblast Organoid Medium (TOM) consisting of Advanced DMEM/F12 (1X, Gibco) containing B-27 supplement (50X without vitamin A, Gibco), N-2 supplement (100X, Gibco), 10 mM HEPES (1 M, Gibco), 2 mM L-glutamine (200 mM, Gibco), 0.5% penicillin-streptomycin (Gibco), 3 µM CHIR99021 (Sigma Aldrich), 100 ng/ml rhEGF (Abcam) and 1 µM A83-01 (Sigma Aldrich). After repeated centrifugation 450 x g for 8 minutes at RT, CTBs were collected in fresh TOM and counted. Cells were resuspended in the appropriate amount of TOM (40% v/v) and Cultrex® Reduced Growth Factor Basement Membrane Extract, Type R1 (60% v/v) (R&D Systems, Minneapolis, MN, USA). In each well of a 24-well plate (Multiwell 24 well, Falcon®, Corning Incorporated, Corning, NY, USA) 1.0 x 10^5 cells in 40 µl of cell/cultrex mix were placed and incubated for 1 min before turning the plate upside down to evenly distribute cells in forming domes. After 15 min plates were turned back to the right side and domes were overlaid with TOM and incubated at 37°C and 5% CO_2. Organoids formed over the next 20-30 days depending on the patient sample. When most of the organoids reached a size of 200-500 µm, organoids were either stimulated to undergo differentiation towards the EVT lineage or maintained in Trophoblast Organoid Media (TOM). To stimulate EVT differentiation TOM was exchanged for extravillous trophoblast medium 1 (EVTM1, see Supplementary Material) consisting of Advanced DMEM/F-12 supplemented with 4% KnockOut™ SR (1x, Gibco), B-27 supplement (1x, Gibco), N-2 supplement (1X, Gibco), 10 mM HEPES (1 M, Gibco), 2 mM L-glutamine (200 mM, Gibco), 0.5% penicillin-streptomycin (Gibco), 7.5 µM A83-01 (Sigma Aldrich) and 100 ng/ml NRG-1 (Abcam).

ELISA

LAIR2 levels were measured from pooled protein lysates of ACH-3P spheroids treated in presence or absence of PR. Twelve spheroids were pooled and lysed in RIPA buffer (Sigma-Aldrich) including protease inhibitor cocktail (Roche Diagnostics; Mannheim, Germany) and phosSTOP (Roche Diagnostics). Cell lysates were centrifuged at 8000 rpm at 4°C for 10 min. Total protein concentration was determined in clear supernatants using the Lowry method. Samples were diluted 1:4 and measured

in duplicates using a LAIR2 ELISA kit (ELH-LAIR2, RayBiotech Life Inc., USA), according to manufacturer's manual. Absorbance was measured using a Spark 10M Multimode Microplate Reader (Tecan; Maennedorf, Switzerland) at 450 nm wavelength. Mean absorbance was calculated and concentrations were determined via standard calibration curve and normalized to total protein concentration.

Hematoxylin and eosin staining

Placenta tissue sections were deparaffinized and incubated in acid hemalaun solution for 10 min according to Mayer (Hematoxylin monohydrate, Merck). Afterwards, sections were incubated shortly in 1 % ammonia water (Ammonia solution 25 %, Merck). Slides were transferred to 1 % aqueous eosin (Eosin Y (yellowish), Sigma-Aldrich) for 1 min and permanently mounted with Cytoseal (Glas™ Tissue Mount™, Tissue-Tek®, Sakura Finetek Germany GmbH, Umkirch, Germany) and a cover slip. Images were obtained with an Evident Olympus VS200 Slide Scanner (Evident Corporation, Tokyo, Japan).

Immunofluorescence staining

For immunofluorescence double staining, 5 µm sections were mounted on Superfrost Plus slides (Thermo Fisher Scientific), and subjected to antigen retrieval. Afterwards, slides were blocked with Ultra V block (Thermo Fisher Scientific) for 10 min at RT. Primary antibodies (Supplemental Table 4) were diluted in antibody diluent (Dako) and incubated on slides for 45 min at RT. Slides were washed three times in PBS. Secondary fluorescence-labelled antibodies (Supplemental Table 4) were diluted in PBS (1:200) and incubated on slides for 30 min at RT. After washing three times with PBS, DAPI was incubated (1:2000 in PBS) on the slides for 5 min. Slides were washed three times with PBS, left to dry and mounted with ProLong Gold Antifade reagent (Invitrogen). Images were obtained with an Evident Olympus VS200 Slide Scanner or an Evident FV3000 Confocal Laser Scanning Microscope (Evident).

Platelet aggregometry

Aggregometry of isolated platelets from pregnant women was assessed using impedance measurements with Chrono-log Model 700 Aggregometer (Chrono-Log Corporation; Havertown, PA, USA). 1 ml platelet suspension was pre-warmed to 37°C before probe with electrode was inserted. First, the baseline was established until a stable electrical current was measured. For activation either Thrombin Receptor Activator Peptide 6 (TRAP-6; HY-P0078, MedChemExpress; Monmouth Junction, NJ, USA) with a final concentration of 50 µM, or collagen type I (Col1; Chrono-Log Corporation) with a final concentration of 1 µg/ml were added to the platelet suspension. To measure the influence of LAIR2 on platelet activation, agonists were pre-incubated with or without 1 µg/ml recombinant human (rh)LAIR2 protein (ab182705, abcam) for 30 minutes at RT before measurements. The aggregation was measured by monitoring the increasing electrical resistance (ohm) in the electrodes over a period of 6 min. Experiments were repeated with platelets from five individual donors (see Supplemental Table 1).

Invasion assay

To measure the invasion ability of the ACH-3P cells through an extracellular matrix (ECM), a QCM™ 96-Well Cell Invasion Assay (ECM555, Merck) was performed according to manufacturer's protocol. In short, $1x10^5$ cells were seeded per chamber with or without 1 µg/ml rhLAIR2 protein (ab182705, abcam). Additionally, we used cells which underwent siRNA-mediated knockdown of LAIR2 expression prior to this assay. For positive controls the same number of cells was seeded and incubated simultaneously without the invasion insert. After 24 hours, cells were detached from the bottom of the chamber, lysed and stained with CyQuant GR Dye provided in the kit. Finally, samples were measured with a fluorescence plate reader CLARIOStar (BMG LABTECH GmbH, Ortenberg, Germany) 15 minutes after adding Lysis Buffer/Dye Solution to each well, preceded by shaking at 500 rpm. A settling time of 0.2 seconds and a flash mode of 40 flashes per well were used, along with top optic settings and a focal height of 5.2 mm. All measurements were performed with an emission spectrum ranging from 505-535 nm, using a gain of 1100.

Supplemental Table 1

Characteristics of the study groups

Characteristic		PR pool (n=13)	PR pool (n=11)	PR (n=3)	aggregometry (n=5)	co-culture (n=5)
Maternal age	[years]	33.5 (6.2)	32.4 (5.5)	25.0 (1.4)	31,0 (5.1)	32.2 (2.7)
Maternal BMI	[kg/m^2]	23.1 (4.2)	21.9 (2.5)	24.1 (2.1)	23.4 (1.6)	24.1 (2.0)
Gestational age	[days]	270 (8)	270 (5)	270 (2)	275 (5)	273 (6)
Platelet count	[x10^3 platelets/µl]	163 (44)		138 (62)	179 (36)	188 (32)

Data are presented as mean with SD.

Supplemental Table 2

qPCR Primer sequences

Gene	forward (5'→3')	reverse (5'→3')
HAND1	AACTCAAGAAGGCGGATGGC	CAGGGCAGGAGGAAAACCT
ITGA2	TTAGCGCTCAGTCAAGGCAT	CGGTTCTCAGGAAAGCCACT
ITGA3	GTGCTTACAACTGGAAAGGAAACA	AAGCTGCCTACCTGCATCGT
LAIR2	AGACCATCCACACGCAGG	CCTCTCCAGGCGGAATGTTT
MEST	GTTGTGCTTTTACACGGTTTT	AGTGATGTGGTCTCGGTTTG
MMP15	TACGAGTGAAAGCCAACCTG	CCGTGTAGTTCTGGATGCTAA
NLRP2	CAAGGCAATGACCAGGATGA	AACAAGACACCAACCCGAGA
NLRP7	GCTCGTGGATTGTGGATTCTC	TTCATAGGTCTTCAACCGTAGG
TBP	TGACCCAGCATCACTGTTTC	CCAGCACACTCTTCTCAGCA
TRPV6	TCAGAATGGGGGTCACTCG	GAAGGCATAGGTGATGATGAGGA
YWHAZ	GGTGGCCAATATGGGGATGT	TCCCTTTTTTCCCCGCCAG

Supplemental Table 3

Materials used for in-situ padlock probe hybridization.

The + symbol indicates that the following base is LNA (locked nucleic acid) modified. The padlock probe was 5´-phosphorylated and underlined sequences indicate the targeted complement sequence. Atto488 and CY7 are fluorescent labels.

		Sequence 5´→3´
Primer	ACTB_LNA	C+GG+GC+GG+CG+GATCGGCAAAG
	RV_LAIR2_1	GAATGTTTGAACCCC
	RV_LAIR2_2	ATCCTCCCTCTCCAG
	RV_LAIR2_3	GAGGCAGCGATAAAG
	RV_LAIR2_4	TTCACCAGCAGCTCC
	RV_LAIR2_5	GGCCTCCAGAGCTTT
	RV_LAIR2_6	TCTCCCCATTGAAGT
	RV_LAIR2_7	GCATCTGTGCATTTCT
Padlock Probe	plp_ACTB	/5Phos/AGCCTCGCCTTTGCC**TCTACGAGTTTGCA GTCACGTGCGTCTATTTAGTGGAGCC**GGTTGCT ACGATGACTCACGCCCCGCGAGCACAG
	plp_LAIR2_1	/5Phos/CGGGGCCCGGTTGGG**CAGTGAATGCGAG TCCGTCTTGCGTCTATTTAGTGGAGCC**CACCTT ACACGAAGCAATGGTGACTTTCATGTGC
	plp_LAIR2_2	/5Phos/AGGAAATGCCGGGCT**CAGTGAATGCGAG TCCGTCTTGCGTCTATTTAGTGGAGCC**CACCTT ACACGAAGCAATGTGACTCAGTAAGTGA
	plp_LAIR2_3	/5Phos/CTGAGCACAGTGACT**CAGTGAATGCGAG TCCGTCTTGCGTCTATTTAGTGGAGCC**CACCTT ACACGAAGCAATGAGCCCCCTGGATGGT
	plp_LAIR2_4	/5Phos/CCGTCTTGTGAACTT**CAGTGAATGCGAGT CCGTCTTGCGTCTATTTAGTGGAGCC**CACCTTA CACGAAGCAATGAGGAGAAATGGCCTC
Detection Oligos	D1	Atto488-TCTACGAGTTTGCAGTCACG
	D2	CY7-UGCGUCUAUUUAGUGGAGCC
	D3	TexasRed-CAGTGAATGCGAGTCCGTCT

Supplemental Table 4

Antibodies used for staining

antibody	clone / order #	company	species	AG retrieval	Dilution IHC	Dilution IF
CK7	DB 051	DB Biotech	rabbit	pH9	-	1:100
HLA-G	4H84	BD Pharmingen	mouse	pH9	1:2000	1:1000
LAIR2	319701	Invitrogen	mouse	pH9	1:500	1:200
CD42b GP1BA	12860-1-AP	Proteintech Europe	rabbit	pH9	1:1000	-
CD31	ab28364	abcam	rabbit	pH9	-	1:50
COL1A1	72026	Cell Signaling	rabbit	pH6	1:200	-
IgG1		Mouse	Dako	pH9	1:1000	-
Alexa Fluor 555		Invitrogen	mouse	-	-	1:200
Alexa Fluor 633		Invitrogen	rabbit	-	-	1:200
DAPI		Invitrogen	-	-	-	1:2000

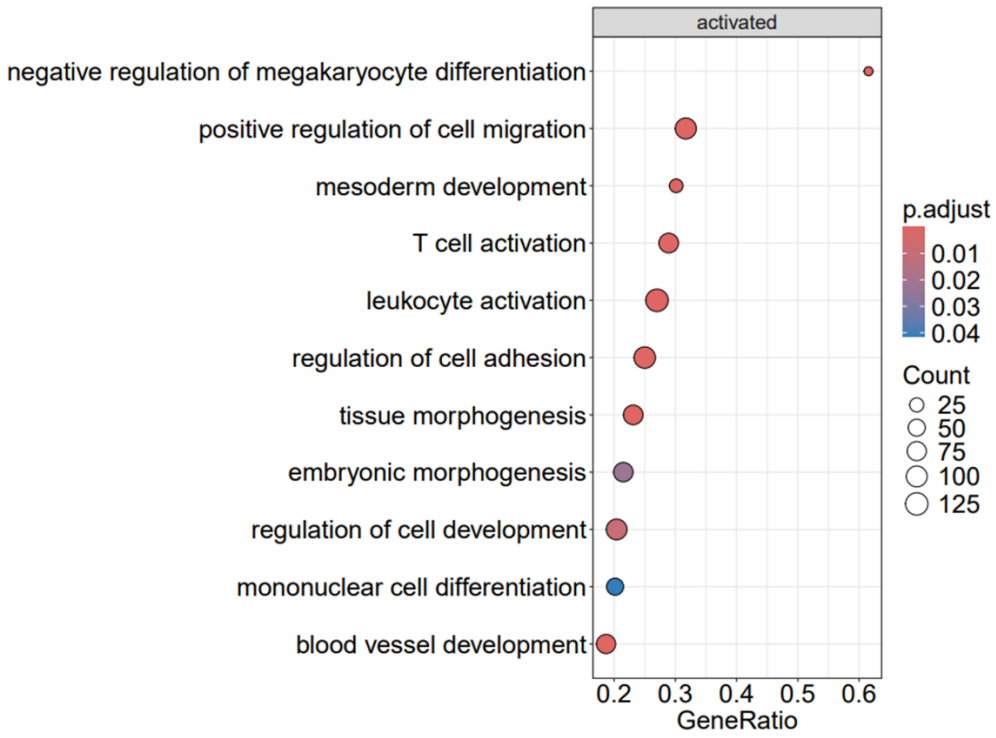

Supplemental Figure 1

Dot plot, visualizing selected GO terms from a gene set enrichment analysis comparing PR treated to control ACH-3P spheroids. The term, gene ratio signifies the number of core enriched genes compared to the total amount of genes associated with a GO term. The size of dots and their color depend on the number of core enriched genes and the adjusted p-value respectively.

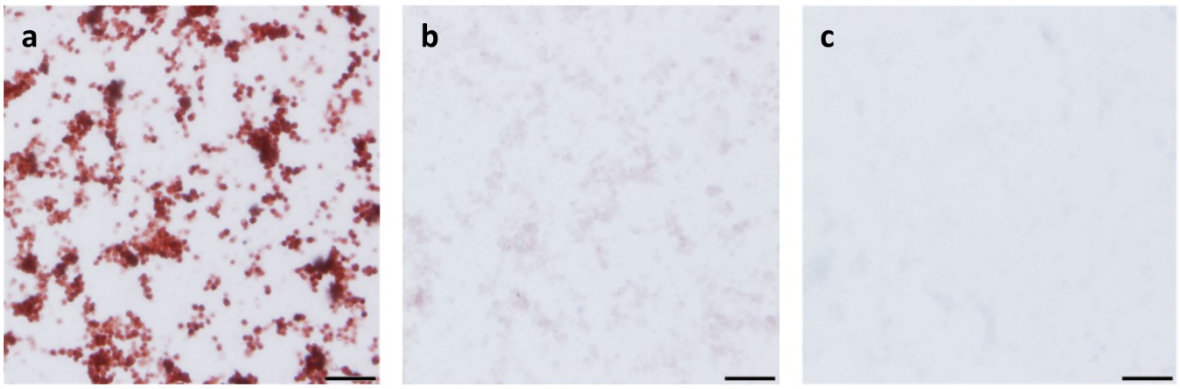

Supplemental Figure 2

Immunohistochemistry for CD42b confirmed the platelet origin of the present cells (**a**). Platelets seemed to be negative for LAIR2, showing no to very faint staining (**b**). Mouse IgG served as a negative control (**c**). Scale bars represent 20 µm

References

[1] E. Afgan, D. Baker, B. Batut, M. van den Beek, D. Bouvier, M. Čech, J. Chilton, D. Clements, N. Coraor, B.A. Grüning, A. Guerler, J. Hillman-Jackson, S. Hiltemann, V. Jalili, H. Rasche, N. Soranzo, J. Goecks, J. Taylor, A. Nekrutenko, D. Blankenberg, The Galaxy platform for accessible, reproducible and collaborative biomedical analyses: 2018 update, Nucleic Acids Res. 46 (2018) W537–W544. https://doi.org/10.1093/nar/gky379.

[2] S. Andrews, Babraham Bioinformatics - FastQC A Quality Control tool for High Throughput Sequence Data, (2010). https://www.bioinformatics.babraham.ac.uk/projects/fastqc/.

[3] P. Ewels, M. Magnusson, S. Lundin, M. Käller, MultiQC: summarize analysis results for multiple tools and samples in a single report, Bioinformatics 32 (2016) 3047–3048. https://doi.org/10.1093/bioinformatics/btw354.

[4] A.M. Bolger, M. Lohse, B. Usadel, Trimmomatic: a flexible trimmer for Illumina sequence data, Bioinforma. Oxf. Engl. 30 (2014) 2114–2120. https://doi.org/10.1093/bioinformatics/btu170.

[5] A. Frankish, M. Diekhans, A.-M. Ferreira, R. Johnson, I. Jungreis, J. Loveland, J.M. Mudge, C. Sisu, J. Wright, J. Armstrong, I. Barnes, A. Berry, A. Bignell, S. Carbonell Sala, J. Chrast, F. Cunningham, T. Di Domenico, S. Donaldson, I.T. Fiddes, C. García Girón, J.M. Gonzalez, T. Grego, M. Hardy, T. Hourlier, T. Hunt, O.G. Izuogu, J. Lagarde, F.J. Martin, L. Martínez, S. Mohanan, P. Muir, F.C.P. Navarro, A. Parker, B. Pei, F. Pozo, M. Ruffier, B.M. Schmitt, E. Stapleton, M.-M. Suner, I. Sycheva, B. Uszczynska-Ratajczak, J. Xu, A. Yates, D. Zerbino, Y. Zhang, B. Aken, J.S. Choudhary, M. Gerstein, R. Guigó, T.J.P. Hubbard, M. Kellis, B. Paten, A. Reymond, M.L. Tress, P. Flicek, GENCODE reference annotation for the human and mouse genomes, Nucleic Acids Res. 47 (2019) D766–D773. https://doi.org/10.1093/nar/gky955.

[6] A. Dobin, C.A. Davis, F. Schlesinger, J. Drenkow, C. Zaleski, S. Jha, P. Batut, M. Chaisson, T.R. Gingeras, STAR: ultrafast universal RNA-seq aligner., Bioinforma. Oxf. Engl. 29 (2013) 15–21. https://doi.org/10.1093/bioinformatics/bts635.

[7] F. García-Alcalde, K. Okonechnikov, J. Carbonell, L.M. Cruz, S. Götz, S. Tarazona, J. Dopazo, T.F. Meyer, A. Conesa, Qualimap: evaluating next-generation sequencing alignment data, Bioinforma. Oxf. Engl. 28 (2012) 2678–2679. https://doi.org/10.1093/bioinformatics/bts503.

[8] S. Anders, P.T. Pyl, W. Huber, HTSeq--a Python framework to work with high-throughput sequencing data, Bioinforma. Oxf. Engl. 31 (2015) 166–169. https://doi.org/10.1093/bioinformatics/btu638.

[9] R Core Team, R: A Language and Environment for Statistical Computing, R Foundation for Statistical Computing, Vienna, Austria, 2018.

[10] M.I. Love, W. Huber, S. Anders, Moderated estimation of fold change and dispersion for RNA-seq data with DESeq2, Genome Biol. 15 (2014) 550. https://doi.org/10.1186/s13059-014-0550-8.

[11] H. Wickham, ggplot2: Elegant Graphics for Data Analysis, 1st ed., Springer-Verlag New York, New York, 2016.

[12] K. Blighe, S. Rana, M. Lewis, EnhancedVolcano: Publication-ready volcano plots with enhanced colouring and labeling., R Package Version 1140 (2022). https://github.com/kevinblighe/EnhancedVolcano.

[13] M.I. Love, S. Anders, V. Kim, W. Huber, RNA-Seq workflow: gene-level exploratory analysis and differential expression, F1000Research 4 (2016) 1070. https://doi.org/10.12688/f1000research.7035.2.

[14] R. Kolde, pheatmap, (2019). https://cran.r-project.org/web/packages/pheatmap/index.html.

[15] T. Wu, E. Hu, S. Xu, M. Chen, P. Guo, Z. Dai, T. Feng, L. Zhou, W. Tang, L. Zhan, X. Fu, S. Liu, X. Bo, G. Yu, clusterProfiler 4.0: A universal enrichment tool for interpreting omics data, The Innovation 2 (2021) 100141. https://doi.org/10.1016/j.xinn.2021.100141.

[16] G. Yu, L.-G. Wang, G.-R. Yan, Q.-Y. He, DOSE: an R/Bioconductor package for disease ontology semantic and enrichment analysis, Bioinformatics 31 (2015) 608–609. https://doi.org/10.1093/bioinformatics/btu684.

[17] M. Carlson, org.Hs.eg.db: Genome wide annotation for Human. R package version 3.19.1., (2024). https://bioconductor.org/packages/release/data/annotation/html/org.Hs.eg.db.html.

[18] H. Chen, L. Albergante, J.Y. Hsu, C.A. Lareau, G. Lo Bosco, J. Guan, S. Zhou, A.N. Gorban, D.E. Bauer, M.J. Aryee, D.M. Langenau, A. Zinovyev, J.D. Buenrostro, G.-C. Yuan, L. Pinello, Single-cell trajectories reconstruction, exploration and mapping of omics data with STREAM, Nat. Commun. 10 (2019) 1903. https://doi.org/10.1038/s41467-019-09670-4.

[19] C. Sun, L.W. Chamley, J.L. James, Organoid generation from trophoblast stem cells highlights distinct roles for cytotrophoblasts and stem cells in organoid formation and expansion., Placenta (2024) S0143400424007914. https://doi.org/10.1016/j.placenta.2024.12.003.